THE UNIVERSITY OF MICHIGAN

COLLEGE OF ENGINEERING
Department of Atmospheric and Oceanic Science

Technical Report

AXISYMMETRIC FLOW AND STABILITY IN THE LOWER SYMMETRY REGIME OF A DIFFERENTIALLY HEATED ROTATING ANNULUS OF FLUID

Norman A. McFarlane

Aksel A. Wiin-Nielsen
Project Director

DRDA Project 002630

supported by:

NATIONAL SCIENCE FOUNDATION
GRANT NO. GA-16166
WASHINGTON, D.C.

administered through:

DIVISION OF RESEARCH DEVELOPMENT AND ADMINISTRATION ANN ARBOR

January 1974

TABLE OF CONTENTS

TABLE OF CONTENTS (concluded)

LIST OF FIGURES

ABSTRACT

AXISYMMETRIC FLOW AND STABILITY IN THE LOWER SYMMETRY REGIME OF A DIFFERENTIALLY HEATED ROTATING ANNULUS OF FLUID

by

Norman Alton McFarlane

A study is made of the axisymmetric steady state which occurs in the rotating annulus when the thermal Rossby number is small . An approximate solution of the governing equations for the axisymmetric state is obtained by the methods of singular perturbation theory.

The higher order effects of centrifugal forces and convection in the side wall boundary layers in determining the structure of the velocity and temperature fields in the interior of the fluid is discussed .

An analysis is made of the stability of the axisymmetric state also using the methods of singular perturbation theory . The first part of this analysis is concerned with the stability of wave-like disturbances with low wave numbers. It is shown that these will be stable if the thermal Rossby number is finite and sufficiently small.

The low wave-number analysis does not lead to a correct determination of the lower symmetry transition curve. It is shown that modifications of this analysis must be made for larger wave numbers. Thus the second part of the stability analysis is concerned

with the stability of disturbances with intermediate and high wave numbers. This analysis leads to a determination of the lower symmetry transition curve. The analysis is carried out far enough to account for the lowest order effects of the side wall boundary layers and centrifugal forces in determining the position and shape of the lower transition curve.

The theoretically determined transition curves are compared with the experimental ones. Good agreement is obtained as to the slope of the transition curves and fair agreement is obtained as to their position in a Rossby number vs. Taylor number diagram.

CHAPTER I

INTRODUCTION AND SURVEY OF THE LITERATURE

The history of the sciences is replete with examples of the principle that progress in the understanding of physical phenomena comes about most expeditiously through a close association of experimental and theoretical investigations. The sciences of meteorology and oceanography are not exceptions to this principle. However, by virtue of the number and complexity of phenomena which occur in them the atmosphere and oceans of the earth are not ideal laboratories. It is for this reason that, in the last two decades, considerable interest has been focused on experimental attempts to model geophysical fluid systems. While the aforementioned complexity of the atmosphere and oceans has prohibited the creation of detailed laboratory analogues it has been possible to create simplified fluid configurations which have successfully modelled some important features of large scale atmospheric and oceanic dynamics.

Fultz (1951) has described a number of early attempts to produce experimentally various fluid-dynamical phenomena of atmospheric interest. However, the modern era of laboratory simulation of the atmospheric general circulation was begun by Fultz and collaborators (Fultz et al. (1959)). The apparatus first used in these studies consisted of a cylindrical dishpan-like container which contained water. The whole apparatus was set into rotation and differentially heated by maintaining a cold source near the center of the cylindrical bottom while the outer rim of the container was heated. The motion at

the free surface of the fluid was made visible by the use of tracer particles.

These early experiments of Fultz were successful in producing free surface flow patterns which resembled closely the large-scale meanders of the middle and upper tropospheric flow in the atmosphere. Moreover Fultz was also able to produce a purely axially symmetric free-surface flow pattern and to show that this type of pattern would, under appropriate circumstances, give way to the non-symmetric pattern just described. As time progressed other features of the flow which resembled atmospheric phenomena also became apparent.

In light of the experimental work of Fultz it is not surprising that other experimentalists, as well as theoreticians, should become interested in these developments. Hide (1953) carried out experiments using an annular container rather than a dishpan. Although Hide's work was begun for a different purpose the meteorological significance of his results quickly became apparent. These experiments were of particular importance because it was possible, using the annular geometry , to produce flow patterns which contained chains of identical waves progressing around the axis of the container at a uniform rate of speed.This type of regular flow pattern had not at that time, been isolated in the open dishpan experiments.

Hide's (1953) work has influenced all of the subsequent experimental work in this field. An excellent review of the results of many of these investigations is given in Hide (1970a) . The general features of interest are illustrated in Figure 1.1. The ordinate in this

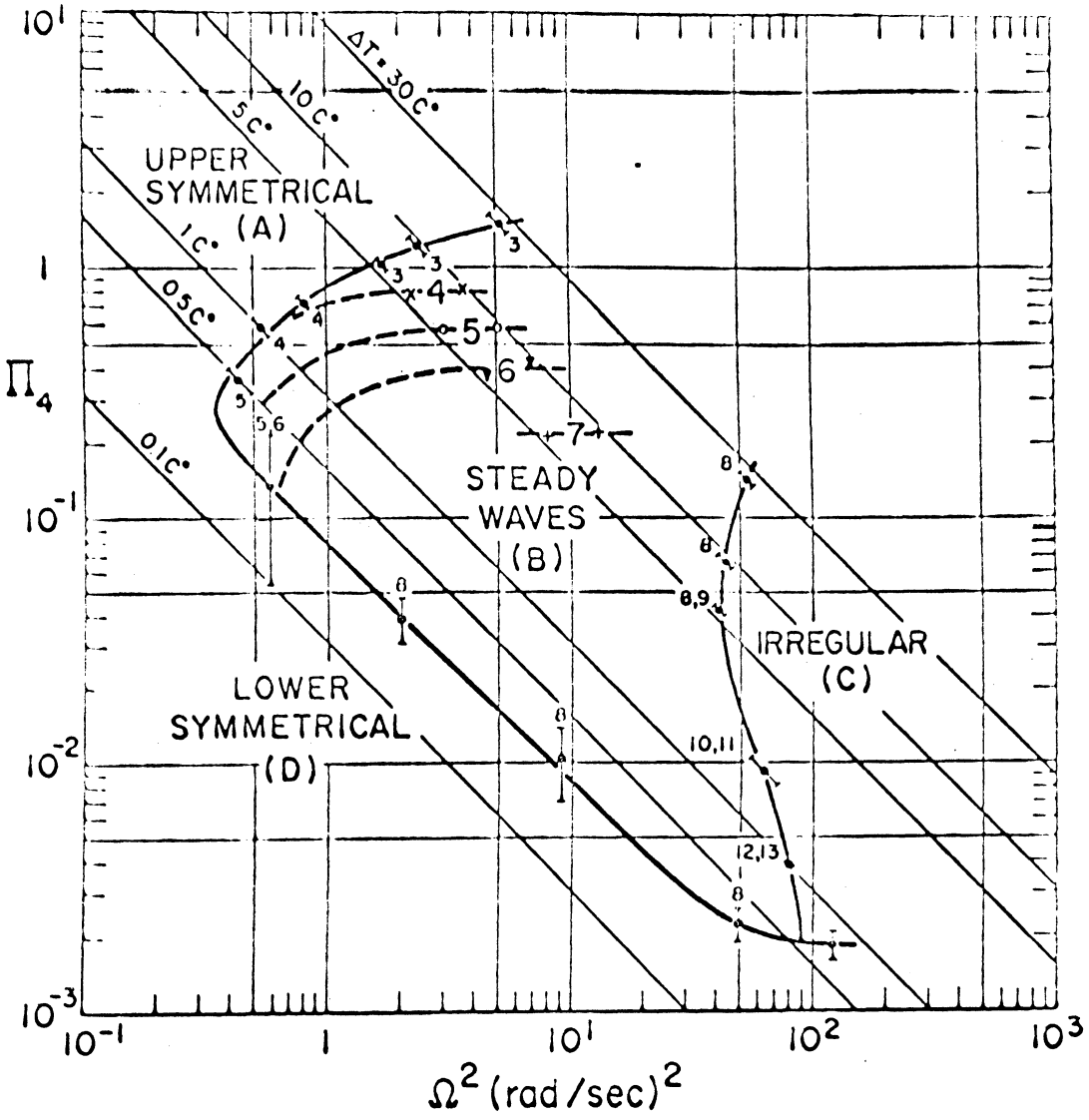

Figure 1.1. Typical experimental transition curve. (After Fowlis and Hide, 1965). $\Pi_4 = gd\Delta\rho/\bar{\rho}\,\Omega^2 L^2$. b = 6.02 cm., a = 3.48 cm., d = 10 cm., ν = 1.01 x 10^{-2}cm^{2}sec^{-1}, σ=7.19.

figure is a thermal Rossby number. This quantity is proportional to the temperature difference imposed across the annular gap and inversely proportional to the square of the rotation rate. The experimental results show that if the rotation rate is sufficiently small wave-like flow patterns will not occur. However, if this quantity is large enough to permit wave motion then this type of motion will be present only if the thermal Rossby number lies between certain limits. This amounts to saying that, for a fixed rotation rate, wave motion will not occur if the gap temperature difference is either sufficiently large or small. The symmetric flow which occurs when the larger of these two values is exceeded is usually referred to as the upper symmetry regime, while the regime which occurs if ΔT is sufficiently small is, by contrast, known as the lower symmetry regime. It was also found that if the rotation rate is sufficiently large the regular wave regime is replaced by one in which the flow pattern is irregular and turbulent in nature. Another phenomenon known as "vacillation" was also found by Hide. This phenomenon is characterized by a periodic variation in the amplitude and/or phase of a wave as it progresses around the annulus.

These experiments succeeded in producing an ideal situation : a series of fundamental physical phenomena had been isolated and studied in the laboratory. These phenomena demanded explanation. Consequently, a number of theoretical investigations followed shortly after the first experimental results became available. The earliest of these theoretical studies were concerned with the problem of explaining why more than one type of flow regime could exist in a rotating con-

tainer of fluid which was subjected to symmetric forcing in the form of differential heating. It was first suggested by Lorenz (1953) that the appearance of waves under appropriate circumstances may be a transition phenomenon in which the symmetric flow becomes unstable to non-symmetric perturbations. The possibility that a flow typical of that in the upper symmetry regime could become unstable to wave-like disturbances due to the mechanism of baroclinic instability had already been demostrated by Eady (1949).

The first studies which aimed specifically at explaining the transition from the symmetric regime to the wave regime were those of Davies (1956) and Kuo (1957). Both of these studies involved simplifying assumptions not least of which was the assumed nature of the symmetric flow. This was taken to be of a highly simplified mathematical form which, however, described the gross features which were typical of the upper symmetry regime. Despite the many simplifying assumptions which were made in the interest of mathematical tractability these studies, particularily that of Kuo, were successful in describing the gross features of the transition phenomena. Quantitative success in describing the transition curve (Figure 1.1) was lacking however.

These studies were followed by a number of others. Brindley (1960) improved on Davies (1956) study by taking better account of viscous and free surface effects and thereby obtained results which were somewhat more in line with those of Kuo.

Barcilon's (1964) study was perhaps the simplest and one of the more illustrative of these stability investigations. This

study was, again, based on a very simple type of basic state typical of the upper symmetry regime as it appears in the interior of the fluid. The annular container was taken to be bounded above and below by rigid horizontal boundaries in contact with the fluid. A further simplifying assumption was that the annular gap is much smaller than its mean radius thus making it possible to neglect curvature effects without serious error. The flow was taken to be quasi-geostrophic and inviscid in the fluid interior. Thus the basic stability problem was essentially the same as that of Eady (1949). However account was taken of the viscous effects near the upper and lower rigid boundaries via the mechanism of Ekman layer pumping in a manner similar to that of Charney and Eliassen (1949)who used it in another context. Barcilon 's analysis was successful in describing qualitatively many of the features of the curve of transition separating the symmetrical flow from the wave flow. However, again, quantitative accuracy was lacking in many respects. This was particularily true of the predicted behavior of the transition curve adjacent to the lower symmetry regime. Not only was the slope of this curve incorrectly predicted but the variation of the transition wave number and the behaviour of the transition Rossby number as a function of the vertical static stability of the basic state was incorrectly predicted. (See Kaiser (1970) for a discussion of this point).

Yet another type of study which was very illustrative of the important physical processes was that of Lorenz (1963). This study was different in many respects from those which had preceeded it and aimed mainly at elucidation of the basic physical processes in-

volved in establishment both of the symmetric regime and the wave regime. The basic model for the study was the two-level quasi - geostrophic type discussed by Lorenz (1960) . A further simplification involved expanding the dependent variables in Fourier series of spatial functions, whose amplitudes were functions of time, and retaining only a small number of terms. The result was that the governing equations were reduced to a system of eight ordinary non-linear differential equations which could in some instances be solved analytically. The effects of differential heating and boundary -layer friction were crudely parameterized.

Despite all of these simplifications Lorenz was able to obtain a curve separating the symmetric and wave flows which resembled closely the experimental curves of Fultz. In addition to this he was able to obtain curves for the transitions between consecutive wave numbers. These also resembled the experimental curves. This was the first study which attempted to theoretically deduce both the symmetric state and the wave state. However, because of all the simplifying assumptions, quantitative comparison with the experiments was virtually impossible. Moreover, the predicted slope and behavior of the transition wave number along the lower symmetry transition curve was incorrect. In this respect the results were somewhat similar to those obtained later by Barcilon in the aforementioned study.

Later studies of the transition phenomena followed along similar lines to those set out by Barcilon and Lorenz. In the latter category is that of Merilees (1968) who modified the Lorenz model to account for the annular geometry and introduced also the effects of

heat conduction and viscosity in the fluid interior. This study produced some improvement in the prediction of the behavior of the lower transition wave number but did not significantly improve predictions of the shape of the transition curve.

The recent studies of O'Neill (1968) and Warn (1973) have attacked the transition problem in a manner similar to that of Barcilon, the major modification being that the upper surface of the fluid was taken to be free rather than rigid as in Barcilon's study. These studies have produced improvement in the predicted behavior of the lower transition wave number and, also, in the predictions of the position of the "knee" of the transition curve, i.e., the critical minimum Taylor number. In addition Warn was able to produce a variation of the lower transition wave number as a function of the vertical stability of the fluid which was similar to that observed by Kaiser (1970). However, again, the position and slope of the lower transition curve was not correctly described.

All of the studies above have involved simplifying assumptions which are, in some cases, severe. All but those of Lorenz and Merilees have been based on an assumed simple symmetric flow as a basis for the analysis of stability. Yet another group of studies have been concerned with determination of the symmetric solutions to the governing equations. This problem has turned out to be much less analytically tractable. In this regard, however, some success has been achieved by numerical methods.

On the analytical side the symmetric flow in the lower symmetry regime was first investigated thoroughly by Robinson (1959),

although some work on this problem was attempted earlier by Lorenz (1953). Robinson considered the case of a rigidly bounded annulus with a narrow gap and restricted his attention to the situation in which the imposed temperature contrast was small enough that the governing equations became linear. In this case the axisymmetric flow problem is tractable by use of the techniques of singular perturbation theory. Later Hunter (1967) corrected some of the inconsistencies in Robinson's analysis and extended it to include some of the effects of permitting the upper surface to be free. The results of this study are in considerable agreement with the recent experimental results of Kaiser (1971).

McIntyre (1968) attacked the problem of determining the symmetric state for a rigidly bounded annulus when the imposed temperature contrast and fluid Prandtl number are so large that the problem of determining the temperature field is no longer linear. Although it turns out that the problem of determining the flow in the interi or of the fluid is analytically intractable in this case it is still possible to describe some of the features of the boundary layer structure. In particular strong thermal boundary layers occur on the cylindrical walls of the annulus. McIntyre was able to find similarity solutions which describe these boundary layers in qualitative agreement with the numerical results of Williams (1967). Attempts to compare McIntyre's results with experiments in which the upper surface is free must be tempered by the fact that the analysis does not, strictly speaking, apply in that case. There is also a restriction on the depth to width ratio of the annulus: it can not be much larger than unity.

The purpose of this review has been to set the stage for the present investigation. The single most prominent failure of the theoretical studies of the transition phenomena has been the lack of success in describing the position and shape of the lower transition curve. Despite this these studies all point to the likelihood that the lower symmetry regime exists mainly because the fluid is viscous and capable of conducting heat. On the other hand, by contrast with that for the lower symmetry regime, the temperature configuration in the fluid interior for the upper symmetry regime is characterized by strong gravitationally stable stratification in the vertical. Under these circumstances the purely inviscid theory of Eady (1949) predicts that symmetric flow should be stable. Despite the fact that introduction of viscous effects into a free surface version of Eady's model modifies this conclusion somewhat (Warn (1973)) the basic reason for the presence of symmetric flow is that the strong vertical stratification renders it dynamically stable to small disturbances.

There may be several reasons for the lack of success in describing the lower symmetry transition. The theoretical models depart from the experimental situation in several respects. One of the more obvious deficiencies is that the assumed symmetric states are not proper solutions of the equations governing the axisymmetric flow, even in an approximate sense. Moreover those assumed background states are not typical of the lower symmetry regime. Another shortcoming is that the effects of the sidewall boundary layers in determining the stability of the symmetric flow has been ignored in all of these studies. Yet another shorcoming is the failure to account for the

effect of centrifugal forces in the fluid.

We shall reexamine the problem of predicting the lower symmetry transition criteria. Our line of attack will be to obtain a proper approximate axisymmetric solution of the governing equations and examine the stability of this solution to small wave-like disturbances. The axisymmetric solution will be essentially that of Hunter (1967) for a free surface situation modified to account for centrifugal effects. Although Hunter's solution is available we shall nevertheless reexamine the axisymmetric problem both because we want to cast it in a form which is useful for subsequent stability analysis and also because we want to introduce the modifications which are needed to account for centrifugal effects.

The main thrust of our investigation will be contained in the results of the stability analysis. We intend to demonstrate that by starting from a proper approximate axisymmetric solution and accounting, in a consistent way, for the role of the boundary layers, heat conduction and dissipation in the interior of the fluid, and centrifugal effects, the theoretical determination of the lower symmetry transition curve can be brought into better agreement with the experimental results.

CHAPTER II

GOVERNING EQUATIONS AND BOUNDARY CONDITIONS

1. THE BOUSSINESQ EQUATIONS

We consider here motion in an annular container filled with fluid to a depth H and in rotation with angular velocity $\Omega\hat{k}$ about a central axis defined by $r=0$ in the cylindrical coordinate system (r, θ, z). The annulus is bounded below by a rigid boundary at $z=0$, above by a free surface at the mean position $z=H$, and laterally by rigid walls at $r=a$ and $r=b$, with $b > a$. Gravity acts anti-parallel to the angular velocity vector. The situation we shall examine is that which is most applicable to the experiments, i.e. we take the boundary at $z=0$ to be thermally insulated while the lateral boundaries are held at the fixed temperatures T_b and T_a, with $T_b > T_a$. The boundary condition at the free surface will be discussed later.

To simplify the analysis we assume that the fluid is incompressible. In line with this approximation, the velocity field is taken to be solenoidal, the variability of the material parameters is neglected, and density (ρ) and entropy (S) changes due to pressure changes are neglected by taking

$$\rho = \rho_0 \left[1 - \alpha (T - T_0)\right] \tag{2.1.1}$$

$$dS = \left(\partial S/\partial T\right)_p \, dT = \left(c_p/T\right) dT \tag{2.1.2}$$

where α and c_p are the coefficient of thermal expansion and the specific heat at constant pressure, and ρ_0 and T_o are reference values, with T_o the mean of T_b and T_a. The pressure P is written as

$$P = \bar{p}(r, z) + p(r, \theta, z, t) \qquad (2.1.3)$$

where $\bar{p}$ is the hydrostatic pressure for $\rho = \rho_0$, $T = T_o$. For static equilibrium in a rotating frame under the influence of gravity,

$$\frac{\partial \bar{p}}{\partial r} = \rho_o \Omega^2 r, \qquad \frac{\partial \bar{p}}{\partial z} = -\rho_o g \qquad (2.1.4)$$

Consequently, assuming that $\alpha (T-T_o)$ and p are small,

$$\frac{1}{\rho}\frac{\partial \bar{P}}{\partial r} = \frac{1}{\rho_o}\frac{\partial p}{\partial r} + \left[1 + \alpha (T-T_o)\right] \Omega^2 r \qquad (2.1.5)$$

$$\frac{1}{\rho}\frac{\partial \bar{P}}{\partial z} = \frac{1}{\rho_o}\frac{\partial p}{\partial z} - g\left[1 + \alpha (T-T_o)\right] \qquad (2.1.6)$$

to the first order in small quantities. On using these expressions in conjunction with the aforementioned assumptions the equations of motion become

$$\frac{d\vec{v}}{dt} + 2\Omega \hat{k} \times \vec{v} = -\frac{1}{\rho_o} \nabla p + \nu \nabla^2 v + \alpha (T-T_o)(g\hat{k} - \Omega^2 r \hat{r}) \qquad (2.1.7)$$

$$\nabla \cdot \vec{v} = 0 \qquad (2.1.8)$$

$$\frac{dT}{dt} = \kappa \nabla^2 T \qquad (2.1.9)$$

In writing these equations we have neglected the dissipation term in the energy equation because our subsequent scaling shows that it is small, and we are assuming that the kinematic viscosity ν and the thermal diffusivity κ can be treated as constants. Except for the inclusion of variable density when coupled with the centrifugal force, these are the conventional Boussinesq equations.

Taking the atmospheric pressure to be zero, the static pressure is

$$\bar{p} = \rho_0 g (h(r) - z) \qquad (2.1.10)$$

where

$$h(r) = H + \frac{\Omega^2}{2g} \left[r^2 - (b^2 + a^2)/2 \right] \qquad (2.1.11)$$

is the reference elevation * of the free surface. In general the sur-

---

* Although we refer to the static part of the pressure field it should be noted that a truly static state of equilibrium is not possible under the conditions imposed here. (Greenspan, 1968, p. 12). It is for this reason that we do not call h(r) the static position of the free surface. However, boundary conditions will be applied at $z = h(r)$ and hence the term "reference elevation".

face will deviate from its reference position so that a general description must be of the form

$$z = h(r) + \eta(r, \theta, t) \tag{2.1.12}$$

In what follows we will assume

$$|\eta| << h, \qquad |\nabla \eta| << |\nabla h| \tag{2.1.13}$$

and show eventually that this is consistent with the scaling assumptions which will be introduced below. In accord with (2.1.13), the free surface boundary conditions will be imposed at the reference elevation $z = h$, and the normal and tangential vectors to the free surface are approximated by the corresponding vectors for the reference elevation, i.e.

$$\hat{n} = \frac{\hat{k} - \hat{r}\,\Omega^2 r/g}{(1 + \Omega^4 r^2/g^2)^{1/2}} \tag{2.1.14}$$

$$\hat{t}^{(1)} = \frac{\hat{r} + \hat{k}\,\Omega^2 r/g}{(1 + \Omega^4 r^2/g^2)^{1/2}} \quad , \quad t^{(2)} = \hat{\theta} \tag{2.1.15}$$

Given the assumptions, the boundary conditions expressing impermeability of the surface and the absence of imposed tractions are

$$w = \frac{\partial \eta}{\partial t} + \vec{v} \cdot \nabla (h + \eta) \tag{2.1.16}$$

$$p - \rho_0 g \eta = 2 \rho_0 \nu e_{ij} n_i n_j \tag{2.1.17}$$

$$n_j e_{ij} t_i^{(n)} = 0 \quad (n = 1, 2) \tag{2.1.18}$$

where (2.1.17) and (2.1.18) are in tensor notation,

$$e_{ij} = \left(\frac{\partial v_j}{\partial x_j} + \frac{\partial v_j}{\partial x_i} \right) / 2 \tag{2.1.19}$$

is the rate of strain tensor, and where the equations are to be imposed at $z = h(r)$.

In arriving at the free surface boundary conditions we have neglected surface tension effects. This may not be entirely justifiable (Fowlis and Hide, 1965), but leads to desirable theoretical simplification.

We now need to specify a condition on the temperature field. In most of the experiments involving a free surface, a thermally insulating lid is placed a small distance above the surface to minimize heat loss by evaporation, convection, or conduction. There is still the possibility of heat transfer by radiative exchange (see Kaiser, 1969). However, under ideal circumstances this should not be significant and, in any event, a theoretical treatment requires information about heat sources or sinks which may exist external to the apparatus. We shall therefore neglect these effects and assume, as has frequently been done before, that the free surface is thermally insulated. Hence the boundary condition is

$$n \cdot \nabla T = 0 \tag{2.1.20}$$

at $z = h$. The boundary conditions at the lateral and bottom boundaries are given explicitly or implicitly in the first paragraph of this section, and the formulation is complete.

2. SCALED EQUATIONS AND THE NARROW GAP APPROXIMATION

We shall restrict our attention to the situation in which the mean radius of the annulus is much greater than its width. Denoting the mean radius, the width, and the imposed temperature difference by

$$r_o = (b + a)/2 \ , \quad L = b - a \ , \quad \Delta T = T_b - T_a \tag{2.2.1}$$

we introduce scaled variables through

$$r = r_o + L x' \ , \quad \theta = L y'/r_o \ , \quad z = L z' , \quad t = t'/2 \tag{2.2.2}$$

and

$$v = (\alpha g \Delta T / 2\Omega) \, v' \ , \quad p = (\rho_o \alpha g L \Delta T) \, p'$$

$$T = T_o + \Delta T \ T' \ , \quad \eta = R_o H \gamma \eta' \tag{2.2.3}$$

where

$$R_o = \alpha g \ T / 4\Omega^2 L \ , \quad \gamma = \Omega^2 \ L^2 / g H \tag{2.2.4}$$

the quantity R_o being the thermal Rossby number. The other dimensionless parameters which arise in the analysis are

$$\delta = L/2\, r_o \quad , \quad D = H / L \quad , \quad \epsilon = \Omega^2 r_o / g \, ,$$

$$E = \nu / 2\Omega L \quad , \quad \sigma = \nu / \kappa \tag{2.2.5}$$

where E is the Ekman number and σ is the Prandtl number. Henceforth we use $\hat{i}$ and $\hat{j}$ to denote unit vectors in the directions of increase of x' and y', and we omit the primes on the scaled variables.

The reference free surface position is given by

$$z = D + \epsilon [x + \delta (x^2 - 1/4)] \tag{2.2.6}$$

We now invoke the narrow gap approximation, valid when $\delta << 1$, by neglecting δ wherever it appears. Then (2.2.6) becomes

$$z = D + \epsilon x \tag{2.2.7}$$

and the unit vectors $\hat{n}$ and $\hat{t}^{(1)}$ defined above become

$$\hat{n} = \frac{\hat{k} - \epsilon \hat{i}}{(1+\epsilon^2)^{1/2}} \qquad t^{(1)} = \frac{\hat{i} + \epsilon \hat{k}}{(1+\epsilon^2)^{1/2}} \tag{2.2.8}$$

We now define orthogonal coordinates

$$s = \{z - (D + \epsilon x)\} / (1+\epsilon^2)^{1/2}$$

$$\bar{x} = \{x + \epsilon (z - D)\} / (1+\epsilon^2)^{1/2} \tag{2.2.9}$$

and velocity components

$$v_n = \hat{n} \cdot \vec{v} \quad , \qquad v_t = \hat{t}^{(1)} \cdot \vec{v} \tag{2.2.10}$$

and we denote the velocity components in the (x, y, z) system in the usual way . Then the free surface conditions can be written as

$$\frac{\partial v_n}{\partial \bar{x}} + \frac{\partial v_t}{\partial s} = 0 \quad , \qquad \frac{\partial v}{\partial s} + \frac{\partial v_n}{\partial y} = 0$$

$$\eta = 4 \, (p - 2 E \, \partial v_n / \partial s) \, , \qquad v_n = \gamma \left(\frac{\partial \eta}{\partial t} + R_o \, \vec{v} \cdot \nabla \eta \right) \tag{2.2.11}$$

$$\hat{n} \cdot \nabla T = 0$$

at $s = 0$, where., because of the narrow gap approximation, the gradient operator is now that for plane Cartesian coordinates .

The remaining boundary conditions are

$$\vec{v} = \partial T / \partial z = 0 \qquad \text{at} \quad z = 0 \, , \tag{2.2.12}$$

$$\vec{v} = 0 \, , \quad T = \pm 1/2 \quad , \quad \text{at} \quad x = \pm 1/2$$

and the dimensionless equations of motion are

$$\frac{\partial \vec{v}}{\partial t} + R_o (\vec{v} \cdot \nabla) \vec{v} + \hat{k} \times \vec{v} = - \nabla p + E \, \nabla^2 \vec{v} + T (\hat{k} - \epsilon \, \hat{i}) \tag{2.2.13}$$

$$\nabla \cdot \vec{v} = 0 \tag{2.2.14}$$

$$\frac{\partial T}{\partial t} + R_o \vec{v} \cdot \nabla T = \frac{E}{\sigma} \nabla^2 T \tag{2.2.15}$$

For the cases of interest $R_o \ll 1$, $\epsilon \ll 1$, $\gamma < \epsilon$, and $E \ll 1$. Thus the deviation of the free surface from its static position is small if $\eta = O(1)$.

CHAPTER III

THE AXIALLY SYMMETRIC STATE: ANALYSIS FOR THE FLUID INTERIOR AND THE EKMAN LAYERS

1. BASIC SCALING AND GOVERNING EQUATIONS

Our investigation will be restricted to situations in which the externally imposed parameters have values which are typical of those for which the lower symmetry regime is observed in the experiments. As has already been mentioned, the problem of determining the axisymmetric state has been investigated by Robinson (1959) and Hunter (1967), who also considered the free surface version of this problem . Hunter's analysis neglects all terms multiplied by ϵ and this then amounts to neglecting the mean slope of the free surface, among other things.

The analysis which follows is similar to Hunter's in many respects but does differ in the way in which the free surface conditions are treated. For the range of rotation rates which we shall consider ϵ is small enough so that the results of our analysis will differ from those of Hunter's only in terms of second or higher order corrections. However, it is useful to reexamine the axisymmetric problem not only in order to see how these modifications to Hunter's analysis arise buto also to set the stage for the stability analysis which will follow.

To be specific we shall consider the situation in which $R_o\sigma = \lambda E^{1/2}$, $\epsilon = \mu E^{1/2}$ with λ and μ being re-

garded as O(1) quantities , as are σ and D . Then the equations governing an axisymmetric steady state are obtained from (2.2.13) to (2.2.15) by setting to zero all terms involving differentiation with respect to t or y . The resulting equations are the following:

$$\frac{\lambda}{\sigma} E^{1/2}\left(u\frac{\partial u}{\partial x} + w\frac{\partial u}{\partial z}\right) - v = -\frac{\partial p}{\partial x} - \mu E^{1/2} T + E\nabla^2 u \qquad (3.1.1)$$

$$\frac{\lambda}{\sigma} E^{1/2}\left(u\frac{\partial v}{\partial x} + w\frac{\partial v}{\partial z}\right) + u = E\nabla^2 v \qquad (3.1.2)$$

$$\frac{\lambda}{\sigma} E^{1/2}\left(u\frac{\partial w}{\partial x} + w\frac{\partial w}{\partial z}\right) = -\frac{\partial p}{\partial z} + T + E\nabla^2 w \qquad (3.1.3)$$

$$\lambda\left(u\frac{\partial T}{\partial x} + w\frac{\partial T}{\partial z}\right) = E^{1/2}\nabla^2 T \qquad (3.1.4)$$

$$\frac{\partial u}{\partial x} + \frac{\partial w}{\partial z} = 0 \qquad (3.1.5)$$

We shall use the techniques of singular perturbation theory (Van Dyke (1964)) in order to obtain approximate solutions to (3.1.1) through (3.1.5).

2. THE EKMAN LAYER AT THE FREE SURFACE

Analysis of the free surface Ekman layer is most easily carried out in terms of a stretched version of the orthogonal coordinates (2.2.9). We define $\tilde{s} = -s/E^{1/2}$ and $w = E^{1/2}\hat{w}$ with $\hat{w} = O(1)$. Then the boundary conditions at the free surface are

$$\frac{\partial u}{\partial \tilde{s}} = \frac{\partial v}{\partial \tilde{s}} = \frac{\partial T}{\partial \tilde{s}} = 0 \; ; \quad \hat{w} = \mu u \,. \tag{3.2.1}$$

with errors which are $o(E^{1/2})$.

The governing equations (3.1.1) through (3.1.5) become the following:

$$v = \frac{\partial p}{\partial x} + \mu \frac{\partial p}{\partial \tilde{s}} - \frac{\partial^2 u}{\partial \tilde{s}^2} + O(E^{1/2}) \tag{3.2.2}$$

$$u = \frac{\partial^2 v}{\partial \tilde{s}^2} + O(E^{1/2}) \tag{3.2.3}$$

$$\frac{\partial u}{\partial x} + \mu \frac{\partial u}{\partial \tilde{s}} = \frac{\partial \hat{w}}{\partial \tilde{s}} + O(E) \tag{3.2.4}$$

$$\frac{\partial p}{\partial \tilde{s}} = -E^{1/2} T + O(E) \tag{3.2.5}$$

$$\frac{\partial^2 T}{\partial \tilde{s}^2} = \lambda E^{1/2} \left[u \left(\frac{\partial T}{\partial x} + \mu \frac{\partial T}{\partial \tilde{s}} \right) - \hat{w} \frac{\partial T}{\partial \tilde{s}} \right] + O(E) \tag{3.2.6}$$

The boundary condition on T in conjunction with equations (3.2.5) and (3.2.6) lead to the conclusion that p and T are independant of $\tilde{s}$ at lowest order. It then easily follows that this must also be true of u, v, and $\hat{\omega}$, again by virtue of the boundary bonditions. Thus, as is easily verified, the lowest order boundary layer solutions are, with errors which are formally O(E) or less, the following:

$$T = \theta_0(\bar{x}) + E^{1/2}\,\theta_1(\bar{x}) + E\left\{\theta_2(\bar{x}) - \theta_0''\,\tilde{s}^2/2 - \lambda(\theta_0')^2\left[\tilde{s} + e^{-\tilde{s}/\sqrt{2}}\left(\cos\frac{\tilde{s}}{\sqrt{2}} - \sin\frac{\tilde{s}}{\sqrt{2}}\right)\right]\right. \tag{3.2.7}$$

$$p = \phi_0(\bar{x}) + E^{1/2}\left(\phi_1(\bar{x}) - \tilde{s}\,\theta_0(\bar{x})\right) \tag{3.2.8}$$

$$v = \phi_0'(\bar{x}) + E^{1/2}\left\{\phi_1' - \tilde{s}\,\theta_0' - \frac{\theta_0'}{\sqrt{2}}\,e^{-\tilde{s}/\sqrt{2}}\left[\cos\frac{\tilde{s}}{\sqrt{2}} - \sin\frac{\tilde{s}}{\sqrt{2}}\right]\right\} \tag{3.2.9}$$

$$u = -E^{1/2}\,\frac{\theta_0'}{\sqrt{2}}\,e^{-\tilde{s}/\sqrt{2}}\left(\cos\tilde{s}/\sqrt{2} + \sin\tilde{s}/\sqrt{2}\right) \tag{3.2.10}$$

$$\hat{w} = -E^{1/2}\left\{\mu\frac{\theta_0'}{\sqrt{2}}\, e^{-\tilde{s}/\sqrt{2}}\left(\cos\tilde{s}/\sqrt{2} + \sin\tilde{s}/\sqrt{2}\right)\right.$$

$$\left. + \theta_0''\left[1 - e^{-\tilde{s}/\sqrt{2}}\cos\tilde{s}/\sqrt{2}\right]\right\} \qquad (3.2.11)$$

where the quantities $G_0(x)$, $G_1(x)$, $\Phi_0(x)$ and $\phi_1(x)$ are to be determined from matching requirements.

At this stage it is useful to examine the conditions for matching these solutions to those which are valid outside the boundary layer. The appropriate independant variables for these outer solutions are x and z. These may be expressed in terms of the boundary layer coordinates, i.e.,

$$x = (\bar{x} + \mu E\,\tilde{s})/(1+\mu^2 E)^{1/2} \qquad (3.2.12)$$

$$z = D + E^{1/2}(\mu\bar{x} - \tilde{s})/(1+\mu^2 E)^{1/2} \qquad (3.2.13)$$

Now let Φ denote some quantity which is known outside the boundary layer in terms of an expansion of the form

$$\Phi(x, z) = \Phi_0(x, z) + E^{1/2}\,\Phi_1(x, z) + O(E)$$

Then the "inner" expansion of this quantity near the free surface is obtained by expressing it in terms of the boundary layer coordinates

using (3.2.12) and expanding the result in powers of $E^{1/2}$ (keeping $\tilde{s}$ and $\bar{x}$ fixed) . We then get the following:

$$\Phi \sim \Phi_0(\bar{x},D) + E^{1/2}\left[\Phi_1(\bar{x},D) + \frac{\partial \Phi_0}{\partial z}(\bar{x},0)(\mu\bar{x}-\tilde{s})\right]$$

$$+E\left[\Phi_2(\bar{x},D) + \frac{1}{2}\frac{\partial^2 \Phi_0}{\partial z^2}(\bar{x},D)(\mu\bar{x}-\tilde{s})^2\right.$$

$$\left. + \frac{\partial \Phi_0}{\partial x}(\bar{x},D)\left(\mu\tilde{s} - \frac{\mu^2}{2}\bar{x}\right) + \frac{\partial \Phi_1}{\partial z}(\bar{x},D)(\mu\bar{x}-\tilde{s})\right] \qquad (3.2.13)$$

$$+ O(E^{3/2})$$

Thus, if the boundary-layer expansion of Φ is of the form

$$\tilde{\Phi} = \tilde{\Phi}_{00}(\bar{x}) + E^{1/2}\left[\tilde{\Phi}_{10}(\bar{x}) + \tilde{s}\,\tilde{\Phi}_{11}(\bar{x})\right]$$

$$+ O(E) + Exp$$

say, where Exp denotes terms which are exponentially small for large $\tilde{s}$, then matching with (3.2.13) is achieved if

$$\Phi_0(\bar{x},D) = \tilde{\Phi}_{00}(\bar{x}) \qquad (3.2.14a)$$

$$\Phi_1(\bar{x},D) = \tilde{\Phi}_{10} - \mu\bar{x}\frac{\partial \Phi_0}{\partial z}(\bar{x},D) \qquad (3.2.14b)$$

$$\frac{\partial \underline{\Phi}_0}{\partial z}(\bar{x}, D) = -\tilde{\Phi}_{11}(\bar{x}) \qquad (3.2.14c)$$

Higher order terms are matched in a similar manner by equating powers of $E^{1/2}$ and $\tilde{s}$ in the boundary layer expansion and the "inner" expansion (3.2.14).

3. ANALYSIS FOR THE INTERIOR

The requirement of matching to the upper Ekman layer suggests that in the interior v, T, and p are O(1), w = O(E) and u = O(E). This latter scaling follows from (3.1.2), (3.1.5) and the scaling of w and v. A consistent approximation scheme involves expansion in powers of $E^{1/2}$.

$$(v, p, T) = (v_0, p_0, T_0) + E^{1/2}(v_1, p_1, T_1) + O(E) \qquad (3.3.1)$$

$$(u, w) = E(u_2, w_2) + O(E^{3/2}) \qquad (3.3.2)$$

Inserting these expressions into equations (3.1.1) through (3.1.5) and equating powers of $E^{1/2}$ then leads to the following:

$$v_0 = \partial p_0 / \partial x \qquad (3.3.3)$$

$$\partial p_0 / \partial z = T_0 \qquad (3.3.4)$$

$$\nabla^2 T_0 = 0 \tag{3.3.5}$$

Matching to the upper Ekman layer requires that

$$\frac{\partial T_0}{\partial z}(\bar{x}, D) = 0 \tag{3.3.6}$$

$$\Phi_0(\bar{x}) = P_0(\bar{x}, D) \tag{3.3.7}$$

$$\Theta_0(\bar{x}) = T_0(\bar{x}, D) \tag{3.3.8}$$

Equation (3.3.6) is the upper boundary condition required for determination of T_0 .

The $O(E^{1/2})$ interior quantities are governed by the following equations:

$$\frac{\partial v_1}{\partial z} = \frac{\partial T_1}{\partial x} + \mu \frac{\partial T_0}{\partial z} \tag{3.3.9}$$

$$u_2 = \nabla^2 v_0 \tag{3.3.10}$$

$$\frac{\partial w_2}{\partial z} + \frac{\partial u_2}{\partial x} = 0 \tag{3.3.11}$$

$$\nabla^2 T_1 = \lambda \left[u_2 \frac{\partial T_0}{\partial x} + w_2 \frac{\partial T_0}{\partial z} \right] \tag{3.3.12}$$

Again matching to the upper Ekman layer provides boundary conditions.

These are

$$\frac{\partial T_1}{\partial z}(x,0) = \lambda\left(\frac{\partial T_0}{\partial x}(x,0)\right)^2 + \mu\frac{\partial T_0}{\partial x}(x,0) \qquad (3.3.13)$$

$$w_2(x,0) = -\frac{\partial^2 T_0}{\partial x^2}(x,0) \qquad (3.3.14)$$

In order to complete the determination of the zero order and $O(E^{1/2})$ interior problems boundary conditions at $z = 0$ and at the sides $x = \pm 1/2$ must be specified. These must be obtained via boundary layer analyses in these respective regions.

4. THE LOWER EKMAN LAYER

We note from (3.3.3) and (3.3.4) that v_0 can be made to satisfy the boundary condition at $z = 0$ by choosing it as follows:

$$v_0 = \int_0^z \frac{\partial T_0}{\partial x}\, dz' \qquad (3.4.1)$$

With this choice the boundary layer components of u and v in the lower Ekman layer can be taken to be $O(E^{1/2})$ and this will then imply that $w = O(E)$.

We define the stretched variable $\tilde{z} = z / E^{1/2}$. Then the relevant governing equations are the following:

$$v = \frac{\partial p}{\partial x} - \frac{\partial^2 u}{\partial \tilde{z}^2} + O(E^{1/2}) \qquad (3.4.2)$$

$$u = \frac{\partial^2 v}{\partial \tilde{z}^2} + O(E^{1/2}) \tag{3.4.3}$$

$$\frac{\partial p}{\partial \tilde{z}} = E^{1/2} T + O(E^{1/2}) \tag{3.4.4}$$

$$\frac{\partial w}{\partial \tilde{z}} + E^{1/2} \frac{\partial u}{\partial x} = 0 \tag{3.4.5}$$

$$\frac{\partial^2 T}{\partial \tilde{z}^2} = \lambda E^{1/2} \left(u \frac{\partial T}{\partial x} + E^{-1/2} w \frac{\partial T}{\partial \tilde{z}} \right) + O(E) \tag{3.4.6}$$

In line with the above discussion we take

$$p_0 = v_0 = u_0 = w_0 = w_1 = 0 \tag{3.4.7}$$

$$T_0 = \bar{\Theta}_0(x) \tag{3.4.8}$$

The $O(E^{1/2})$ solutions are then given by

$$p_1 = \bar{\Phi}_1(x) + \tilde{z}\, \bar{\Theta}_0(x) \tag{3.4.9}$$

$$T_1 = \bar{\Theta}_1(x) \tag{3.4.10}$$

$$v_1 = \bar{\Theta}_0' \tilde{z} + [\bar{\Phi}_1' + \mu \bar{\Theta}_0]\left[1 - e^{-\tilde{z}/\sqrt{2}} \cos \tilde{z}/\sqrt{2}\right] \tag{3.4.11}$$

$$u_1 = -[\bar{\Phi}_1' + \mu \bar{\Theta}_0]\, e^{-\tilde{z}/\sqrt{2}} \sin \tilde{z}/\sqrt{2} \tag{3.4.12}$$

Using these results we find the O(E) vertical velocity and temperature corrections to be

$$w_2 = \frac{1}{\sqrt{2}}\left[\bar{\Phi}_1'' + \mu\bar{\theta}_0'\right]\left[1 - e^{-\tilde{z}/\sqrt{2}}\cos\tilde{z}/\sqrt{2} + \sin\tilde{z}/\sqrt{2}\right] \qquad (3.4.13)$$

$$T_2 = -\bar{\theta}_0''\frac{\tilde{z}^2}{2} + \bar{\theta}_2(x) - \lambda\bar{\theta}_0'(\bar{\Phi}_1 + \mu\bar{\theta}_0)\left[\frac{\tilde{z}}{\sqrt{2}} + e^{-\tilde{z}/\sqrt{2}}\cos\tilde{z}/\sqrt{2}\right] \qquad (3.4.14)$$

By virtue of (3.3.6) through (3.3.8) the first terms of w_1 and T_2 match to the interior if $\bar{\theta}_0(x) = T_0(x, 0)$. Further matching requires the following to be true

$$\frac{\partial T_0}{\partial z}(x, 0) = 0 \qquad (3.4.15)$$

$$\frac{\partial T_1}{\partial z}(x, 0) = -\frac{\lambda}{\sqrt{2}}\left(\frac{\partial T_0}{\partial x}(x, 0)\right)\left(\bar{\Phi}_1' + \mu T_0(x, 0)\right) \qquad (3.4.16)$$

Now, (3.3.5), (3.3.10), (3.4.1), and (3.4.15) together imply that $u = 0$ in the interior and therefore that

$$w_2 = F(x) \tag{3.4.17}$$

$$= -\Theta_0'' \tag{3.4.18}$$

$$= \frac{1}{\sqrt{2}}\left[\bar{\Phi}_1'' + \mu\bar{\Theta}_0'\right] \tag{3.4.19}$$

where the last two equations follow from matching to the upper and lower Ekman layers respectively . Thus

$$\bar{\Phi}_1' + \mu\bar{\Theta}_0 = -\sqrt{2}\,\frac{\partial T_0}{\partial x}(\bar{x}, D) + \text{const.} \tag{3.4.20}$$

The constant in this equation must be determined by mass flux balance requirements . The continuity equation (3.1.5) shows, without approximation , that

$$\int_0^{D+\epsilon x} \frac{\partial u}{\partial x}\,dz + \epsilon u(x, D+\epsilon x) = O(\gamma\lambda E^{1/2})$$

or, alternatively,

$$\frac{d}{dx}\int_0^{D+\epsilon x} u\,dz = O(\gamma\lambda E^{1/2}) \tag{3.4.21}$$

We have used the second of the boundary conditions (3.2.1) in deriving this result. If (3.4.21) is to hold for all x the integral must be at most a constant. This constant must be zero since the alternative would imply a uniform (independant of x) horizontal mass flux .

Since $u = O(E^{1/2})$ in each of the Ekman layers and is o(E) in the interior (3.4.21) can be written approximately as

$$\int_0^\infty u_B \, d\tilde{z} + \int_0^\infty u_T \, d\tilde{s} = 0 \qquad (3.4.22)$$

which expresses the fact that the mass transports in the Ekman layers balance each other . Equation (3.4.22) can be shown to lead to the requirement that

$$\bar{\phi}_1' + \mu \bar{\Theta}_0 = -\sqrt{2}\, \Theta_0'$$

and therefore the constant in (3.4.20) is zero * . This result enables us to write the boundary condition (3.4.16) as follows :

$$\frac{\partial T_1}{\partial z}(x,0) = \lambda \left(\frac{\partial T_0}{\partial x}(x,0)\right)\left(\frac{\partial T_0}{\partial x}(x,D)\right) \qquad (3.4.23)$$

We have now specified boundary conditions on T_0 and T_1 at $z = 0$ and $z = D$. We also need conditions at $x = \pm 1/2$.

---

* Had we used a stream function to satisfy (3.1.5) from the outset the above result would have followed automatically. We have chosen to avoid the use of a stream function because we believe the results are more illustrative when the velocity components themselves are used .

These must be obtained via analysis of the side wall boundary layers. These analyses are carried out in Chapter IV . However, for convenience we anticipate the results here and state that

$$T_o \ (\pm 1/2 \ , z \ ) = \pm 1/2 \qquad (3.4.24)$$

$$T_1 \ (\pm 1/2 \ , \ z) = \lambda z \qquad (3.4.25)$$

We can now complete the zero order and $O(E^{1/2})$ interior problems . The zero order problem is defined by (3. 3. 3) through (3. 3. 6) , (3. 4. 15) , and (3. 4. 24) . The solutions which satisfy all these are

$$T_o = x \qquad (3.4.26)$$

$$v_o = z \qquad (3.4.27)$$

$$p_o = x z \qquad (3.4.28)$$

The $O(E^{1/2})$ problem is defined by (3. 3. 9) through (3. 3. 13) , (3. 4. 23) and (3. 4. 25) . On making use of the zero-order solutions (3. 3. 12) , (3. 3. 13), and (3. 4. 23) become

$$\nabla^2 T_1 = 0 \qquad (3.4.29)$$

$$\frac{\partial T_1}{\partial z}(x, \mathcal{D}) = \lambda + \mu \qquad (3.4.30)$$

$$\frac{\partial T_1}{\partial z}(x,0) = \lambda \qquad (3.4.31)$$

The solution which satisfies these equations in addition to (3.4.25) is of the form

$$T_1 = \lambda z + \sum_{n=0}^{\infty} a_n \sin[(2n+1)\pi(x+1/2)]\cosh[(2n+1)\pi z] \qquad (3.4.32)$$

where

$$a_n = 4\mu D/\{(2n+1)^2\pi^2 \sinh[(2n+1)\pi D]\} \qquad (3.4.33)$$

Finally, equations (3.4.11) and (3.4.20) show that $V_1(x,0) = -\sqrt{2}$ so that (3.3.10) and the above solution for T_1 lead to:

$$V_1 = -\sqrt{2} + \sum_{n=0}^{\infty} a_n \cos[(2n+1)\pi(x+\tfrac{1}{2})] \cdot \sinh[(2n+1)\pi z] \qquad (3.4.34)$$

These solutions complete the interior problem correct to $O(E^{1/2})$. Equations (3.4.26) and (3.4.27) are exactly the zero order solutions obtained by Hunter. The first term of (3.4.32) repre-

sents a contribution to the $O(E^{1/2})$ temperature field due to convection in the side wall boundary layers while the Fourier series represents a contribution resulting from the fact that the free surface has a mean slope of magnitude $\mu E^{1/2}$ due to the centrifugal force.

CHAPTER IV

THE SIDE WALL BOUNDARY LAYERS

We shall now verify the boundary conditions used at the sides for the interior solutions in the preceeding Chapter, restricting our attention to the cold wall (at $x = -1/2$) . The analysis of the boundary layer structure near $x = 1/2$ is similar in all respects, the only difference being that the outward normal to that wall has the opposite sign.

The results of Robinson (1959) and Hunter (1967) both indicate that there is a boundary layer near the side walls whose non-dimensional thickness is formally $O(E^{1/3})$. Hunter showed that when the interior zonal velocity is not anti-symmetric about the point $z = D/2$ a double boundary layer structure is required, the outer boundary layer having a non-dimensional thickness which is $O(E^{1/4})$. These boundary layers are thus a certain class of Stewartson-Proudman layers .

The analysis which follows differs very little from that of Hunter. We present it mainly for the sake of completeness and to illustrate the manner in which the boundary conditions (3.4.24) and (3.4.25) were obtained.

1. THE INNER LAYER

The boundary conditions which must be applied at $x = -1/2$ are the following:

$$T = -1/2 \tag{4.1.1a}$$

$$u = v = w = 0 \tag{4.1.1b}$$

For the inner boundary layer we use the stretched boundary layer coordinate $\xi = (x + 1/2) / E^{1/3}$. Bearing in mind the boundary conditions (4.1.1) and the fact that u and w are $o(E^{1/2})$ in the interior of the fluid we choose

$$T = -1/2 + E^{1/3} \hat{T} \tag{4.1.2a}$$

$$p = -z/2 + E^{1/3} \hat{p} \tag{4.1.2b}$$

$$u = E^{1/3} \hat{u} \tag{4.12c}$$

where $\hat{T}$, $\hat{p}$, $\hat{u}$ are all O (1) quantities. With this choice of scaling the governing equations take the following form:

$$\frac{\lambda}{\sigma} E^{5/6} (\hat{u} \hat{u}_\xi + w \hat{u}_z) - v = -\hat{p}_\xi + E^{1/3} \hat{u}_{\xi\xi} + O(E^{1/2}) \tag{4.1.3}$$

$$\frac{\lambda}{\sigma} E^{1/6} (\hat{u} v_\xi + w v_z) + \hat{u} = v_{\xi\xi} + O(E^{2/3}) \tag{4.1.4}$$

$$\frac{\lambda}{\sigma} E^{1/6} (\hat{u} w_\xi + w w_z) = -\hat{p}_z + \hat{T} + w_{\xi\xi} + O(E^{2/3}) \qquad (4.1.5)$$

$$\lambda E^{1/6} (\hat{u} \hat{T}_\xi + w \hat{T}_z) = \hat{T}_{\xi\xi} + O(E^{2/3}) \qquad (4.1.6)$$

$$\hat{u}_\xi + w_z = 0 \qquad (4.1.7)$$

where the subscript notation has been used to denote differentiation.

We also require boundary conditions at $z = 0$ and $z = D$. These must be obtained by analyses of the corner region solutions. Since the side wall boundary layer is thicker than the Ekman layer it may be expected that the appropriate boundary conditions would be the Ekman compatibility conditions. We shall confirm, in Chapter V, that this is indeed the case. Subject to this confirmation, we state here that the appropriate lowest order boundary conditions are the following:

$$\hat{w}(\xi, D) = 0 \qquad (4.1.8a)$$

$$\hat{w}(\xi, 0) = \frac{E^{1/6}}{\sqrt{2}} \hat{p}_{\xi\xi} \qquad (4.1.8b)$$

If we now neglect all terms multiplied by $E^{1/6}$ or higher powers of E in (4.1.3) through (4.1.8) we find that the lowest order governing equations are the following:

$$v^{(0)} = \hat{p}_{\xi}^{(0)} \tag{4.1.9}$$

$$\hat{u}^{(0)} = v_{\xi\xi}^{(0)} \tag{4.1.10}$$

$$\hat{u}_{\xi}^{(0)} + w_{z}^{(0)} = 0 \tag{4.1.11}$$

$$\hat{p}_{z}^{(0)} = \hat{T}^{(0)} + w_{\xi\xi}^{(0)} \tag{4.1.12}$$

$$\hat{T}_{\xi\xi}^{(0)} = 0 \tag{4.1.13}$$

The boundary condition on T requires that $\hat{T}^{(0)} = 0$ at $\xi = 0$ so that (4.1.13) leads to

$$\hat{T}^{(0)} = \beta_0(z)\,\xi \tag{4.1.14}$$

Then equations (4.1.12), (4.1.9) and (4.1.10) lead to the following:

$$\hat{p}^{(0)} = H_0(\xi) + \xi \int_0^z \beta_0(z')\,dz' + \int_0^z w_{\xi\xi}^{(0)}\,dz' \tag{4.1.15}$$

$$v^{(0)} = H_0' + \int_0^z \beta_0 \, dz' + \int_0^z w_{\xi\xi\xi}^{(0)} \tag{4.1.16}$$

$$\hat{u}^{(0)} = H_0''' + \int_0^z \frac{\partial^5 w^{(0)}}{\partial \xi^5} dz' \tag{4.1.17}$$

where H_0 and β_0 are to be determined.

Finally, the continuity equation (4.1.11) shows that

$$\frac{d^4 H_0}{d\xi^4} + \int_0^z \frac{\partial^6 w^{(0)}}{\partial \xi^6} dz' + w_z^{(0)} = 0 \tag{4.1.18}$$

Differentiting this with respect to z yields the governing equation for $w^{(0)}$:

$$\frac{\partial^6 w^{(0)}}{\partial \xi^6} + \frac{\partial^2 w^{(0)}}{\partial z^2} = 0 \tag{4.1.19}$$

The boundary conditions at z = 0 and z = D are, from equations (4.1.8):

$$w^{(0)}(\xi, 0) = w^{(0)}(\xi, D) = 0 \tag{4.1.20}$$

Using these we also find from (4.1.18) that

$$\frac{d^4 H_0}{d\xi^4} + \frac{1}{D}\int_0^D \int_0^z \frac{\partial^6 w^{(0)}}{\partial \xi^6} dz' dz = 0 \qquad (4.1.21)$$

so that

$$H_0 = a_0 + b_0 \xi + c_0 \xi^2 + d_0 \xi^3 - \frac{1}{D}\int_0^D \int_0^z w_{\xi\xi}^{(0)} dz' dz \qquad (4.1.22)$$

thus

$$v^{(0)} = b_0 + 2c_0 \xi + 3d_0 \xi^2 + \int_0^z \beta_0 dz'$$

$$+ \int_0^z w_{\xi\xi\xi}^{(0)} dz' - \frac{1}{D}\int_0^D \int_0^z w_{\xi\xi\xi}^{(0)} dz' dz \qquad (4.1.23)$$

$$\hat{u}^{(0)} = 6d_0 + \int_0^z \frac{\partial^5 w^{(0)}}{\partial \xi^5} dz' - \frac{1}{D}\int_0^D \int_0^z \frac{\partial^5 w^{(0)}}{\partial \xi^5} dz' dz \qquad (4.1.24)$$

The boundary conditions on $v^{(0)}$ and $\hat{u}^{(0)}$ at $\xi = 0$ now show that :

$$b_0 = -\frac{1}{D}\int_0^D \int_0^z \beta_0 dz' dz \qquad (4.1.25)$$

$$d_0 = 0 \qquad (4.1.26)$$

These conditions were obtained by simply integrating (4.1.23) and

(4.1.24) between $z = 0$ and $z = D$ and requiring the results to vanish at $\xi = 0$. They imply that

$$\left\{ \int_0^z \omega_{\xi\xi\xi}^{(\omega)} \, dz' - \frac{1}{D} \int_0^D \int_0^z \omega_{\xi\xi\xi}^{(0)} \, dz'dz \right\}_{\xi=0}$$
$$= -\int_0^z \beta_0 \, dz' + \frac{1}{D} \int_0^D \int_0^z \beta_0 \, dz'dz \qquad (4.1.27)$$

$$\frac{\partial^5 \omega^{(0)}}{\partial \xi^5}(0, z) = 0 \qquad (4.1.28)$$

Furthermore we must require that $\omega^{(0)}$ be of boundary layer type, i.e., that

$$\lim_{\xi \to \infty} \omega^{(0)} = 0 \qquad (4.1.29)$$

We now have sufficient information to determine $\omega^{(0)}$ in terms of $\beta_0(z)$. We take the solutions of (4.1.19) to be of the form:

$$\omega^{(0)} = \sum_{j=1}^{\infty} f_{0j}(\xi) \sin(j\pi z/D) \qquad (4.1.30)$$

so that the boundary conditions (4.1.20) are satisfied. Then (4.1.9) takes the form

$$\frac{d^6 f_{0j}}{d\xi^6} - \frac{j^2\pi^2}{D^2} f_{0j} = 0 \qquad (4.1.31)$$

The requirements that $\omega^{(o)}$ shall vanish at $\xi = 0$ in addition to (4.1.27), (4.1.28) and (4.1.29) imply that

$$f_{oj}(o) = \frac{d^5 f_{oj}}{d\xi^5}(o) = o \tag{4.1.32}$$

$$\frac{d^3 f_{oj}(o)}{d\xi^3} = \frac{2j\pi}{D^2}\int_o^D \cos j\pi\frac{z}{D}\left\{\int_o^z \beta_o\, dz' - \frac{1}{D}\int_o^D\int_o^{z'} \beta_o\, dz''\, dz'\right\} dz \tag{4.1.33}$$

$$\lim_{\xi\to\infty} f_{oj} = o \tag{4.1.34}$$

The solution which satisfies all of these conditions is

$$f_{oj} = -\alpha_{oj}\left\{e^{-\nu_j\xi} - e^{-\nu_j\xi/2}\left[\cos\frac{\sqrt{3}}{2}\nu_j\xi + \frac{1}{\sqrt{3}}\sin\frac{\sqrt{3}}{2}\nu_j\xi\right]\right\} \tag{4.1.35}$$

where $\nu_j = (j\pi/D)^{1/3}$ and

$$\alpha_{oj} = \frac{1}{D}\int_o^D \cos j\pi\frac{z}{D}\left\{\int_o^z \beta_o\, dz' - \frac{1}{D}\int_o^D\int_o^{z'} \beta_o\, dz''\, dz'\right\} dz \tag{4.1.36}$$

In summary we now have:

$$T \sim -\frac{1}{2} + E^{1/3}\beta_0(z)\,\xi \tag{4.1.37}$$

$$p \sim -\frac{z}{2} + E^{1/3}\left\{a_0 + \xi\left[\int_0^z \beta_0\,dz' - \frac{1}{D}\int_0^D\int_0^z \beta_0\,dz'dz\right]\right.$$
$$\left. + c_0\xi^2 + \left[\int_0^z w_{\xi\xi}^{(0)}\,dz' - \frac{1}{D}\int_0^D\int_0^z w_{\xi\xi}^{(0)}\,dz'dz\right]\right\} \tag{4.1.38}$$

$$v \sim \int_0^z \beta_0\,dz' - \frac{1}{D}\int_0^D\int_0^z \beta_0\,dz'dz + 2c_0\xi$$
$$+ \left[\int_0^z w_{\xi\xi\xi}^{(0)}\,dz' - \frac{1}{D}\int_0^D\int_0^z w_{\xi\xi\xi}^{(0)}\,dz'dz\right] \tag{4.1.39}$$

$$u \sim E^{1/3}\left[\int_0^z \frac{\partial^5 w^{(0)}}{\partial\xi^5}\,dz' - \frac{1}{D}\int_0^D\int_0^z \frac{\partial^5 w^{(0)}}{\partial\xi^5}\,dz'dz\right] \tag{4.1.40}$$

The errors in these solutions are formally $O(E^{1/6})$. We can now see why it is that an additional outer boundary layer is required. The expression (4.1.37) matches to the interior temperature field if $\beta_0(z) = 1$. However, this then implies that the leading two terms of (4.1.39) are $z - D/2$ and it is clear that this expression does not match to the interior expression for v_0 since that quantity does not vanish on integration from $z = 0$ to $z = D$. Thus, an outer boundary layer is required to bring the mean value

of the difference between the interior V_0 and the inner boundary layer $V^{(0)}$ to zero at $x = -1/2$.

Having found $\hat{u}^{(0)}$, $w^{(0)}$ and $T^{(0)}$ it is now easy, using (4.1.6), to obtain the $O(E^{1/6})$ correction to the temperature field. We find from (4.1.6) that

$$\hat{T}^{(1)}_{\xi\xi} = \lambda \hat{u}^{(0)} \beta_0(z) = \lambda \beta_0 \frac{\partial^2 V^{(0)}}{\partial \xi^2} \qquad (4.1.41)$$

Thus

$$\hat{T}^{(1)} = \beta_1(z)\,\xi + \lambda \beta_0 V^{(0)} \qquad (4.1.42)$$

and this clearly satisfies the boundary condition at $\xi = 0$. The full expression, correct to $O(E^{1/2})$ for the temperature field is now:

$$T \sim -\tfrac{1}{2} + E^{1/3}\beta_0 \xi + E^{1/2}\left[\beta_1 \xi + \lambda \beta_0 V^{(0)}(z,\xi)\right] \qquad (4.1.43)$$

The quantities $\beta_0(z)$ and $\beta_1(z)$ as well as a_0 and c_0 must be determined from matching conditions.

2. THE OUTER LAYER

The characteristic non-dimensional thickness of the outer layer is $E^{1/4}$. This can be demonstrated by an argument which amounts to showing that this is the characteristic thickness which is

required if the side wall layer is to be capable of accepting the Ekman layer flux near $z = 0$ (cf. Jacobs (1964)) . Thus, if we take $\zeta = (x + 1/2) / E^{\alpha}$ where α is to be determined , and anticipate that all velocity components are no greater than $O(1)$ we then have

$$u \sim E^{1-2\alpha} v_{\zeta\zeta}$$

or , $u = O(E^{1-2\alpha})$. Then continuity implies that $w = O(E^{1-3\alpha})$. However the Ekman layer thickness is $E^{1/2}$ and if $u = O(1)$ and is of boundary layer type in the lower Ekman extension to the side wall layer then continuity also shows that the flux from the Ekman layer is $O(E^{1/2-\alpha})$, i.e. it is formally the order of magnitude of the ratio of the Ekman layer thickness to the side wall layer thickness. Thus our postulate that the side wall layer should be capable of accepting the lowest order Ekman layer flux leads to $O(E^{1-3\alpha}) = O(E^{1/2-\alpha})$. This is the case if $\alpha = 1/4$, as was previously stated.

This argument suggests the following scaling

$$\zeta = (x+1/2)/E^{1/4} \qquad (4.2.1)$$

$$u = E^{1/2}\hat{u} \qquad (4.2.2)$$

$$w = E^{1/4}\hat{w} \qquad (4.2.3)$$

Also we shall scale T and p so as to make them consistent with this and the inner side wall layer:

$$T = -1/2 + E^{1/4}\,\hat{T} \tag{4.2.4a}$$

$$p = -z/2 + E^{1/4}\,\hat{p} \tag{4.2.4b}$$

The lowest order governing equations are now the following :

$$v = \hat{p}_\zeta + O(E^{1/2}) \tag{4.2.5}$$

$$\hat{u} = v_{\zeta\zeta} + O(E^{1/4}) \tag{4.2.6}$$

$$\hat{p}_z = \hat{T} + O(E^{1/2}) \tag{4.2.7}$$

$$\hat{u}_\zeta + \hat{w}_z = 0 \tag{4.2.8}$$

$$\hat{T}_{\zeta\zeta} = \lambda E^{1/4}(\hat{u}\hat{T}_\zeta + \hat{w}\hat{T}_z) + O(E^{1/2}) \tag{4.2.9}$$

Again, subject to later confirmation, we state the boundary conditions at z = 0 and z = D :

$$\hat{w}(\zeta, D) = 0 \tag{4.2.10}$$

$$\hat{w}(\zeta,0) = \frac{1}{\sqrt{2}}\,\hat{P}_{\zeta\zeta}(\zeta,0) \tag{4.2.11}$$

The lowest order approximation to $\hat{T}$ is given by

$$\hat{T}^{(0)} = \beta_0(z)\,\zeta \tag{4.2.12}$$

and this matches to the corresponding quantity in the inner side layer. Then, (4.2.7), (4.2.5) and (4.2.6) lead to the following :

$$\hat{p}^{(0)} = h_0(\zeta) + \zeta \int_0^z \beta_0\, dz' \tag{4.2.13}$$

$$v^{(0)} = h_0' + \int_0^z \beta_0\, dz' \tag{4.2.14}$$

$$\hat{u}^{(0)} = h_0''' \tag{4.2.15}$$

Finally (4.2.8) leads to

$$\hat{w}^{(0)} = g_0(\zeta) - z\,\frac{d^4 h_0}{d\zeta^4} \tag{4.2.16}$$

Applying the boundary conditions (4.2.10) and (4.2.11) then shows that

$$g_0(\tau) = D\frac{d^4 h_0}{d\tau^4} \tag{4.2.17}$$

$$= \frac{1}{\sqrt{2}} h_0'' \tag{4.2.18}$$

Thus we can take h_0 to be of the form

$$h_0 = \alpha_0 + \delta_0 \tau + \kappa_0 e^{-\tau/2^{1/4}\sqrt{D}} \tag{4.2.19}$$

Then

$$\hat{p}^{(0)} = \alpha_0 + \tau\left(\delta_0 + \int_0^\tau \beta_0 d\tau'\right) + \kappa_0 e^{-\tau/2^{1/4}\sqrt{D}} \tag{4.2.20}$$

In order to match this to (4.1.28) we write the "inner" expansion of (4.2.20) by replacing τ by $E^{1/12}\xi$ and expanding in powers of $E^{1/12}$ for fixed ξ. The result must match to those terms of (4.1.28) which are not exponentially small for large ξ. Thus, using (4.2.20), the full inner expansion of p becomes :

$$p \sim -\frac{z}{2} + E^{1/4}\left\{\alpha_0 + \kappa_0 + E^{1/12}\xi\left[\delta_0 - \frac{\kappa_0}{2^{1/4}\sqrt{D}} + \int_0^\tau \beta_0 d\tau'\right] + E^{1/6}\frac{\xi^2}{2}\frac{\kappa_0}{\sqrt{2}D} + O(E^{1/4})\right\} \tag{4.2.21}$$

This matches to (4.1.28) if the following are true :

$$a_0 = 0 = \alpha_0 + \kappa_0 \tag{4.2.22}$$

$$\delta_0 - \frac{\kappa_0}{2^{1/4}\sqrt{D}} = -\frac{1}{D}\int_0^D \int_0^z \beta_0 \, dz' dz \tag{4.2.23}$$

$$c_0 = E^{1/12} \kappa_0 / 2\sqrt{2}\, D \tag{4.2.24}$$

These conditions also ensure that $v^{(0)}$ will match to (4.1.29).

When ζ becomes large the boundary layer quantities must match to the corresponding values of the interior solutions near $x = -1/2$. The inner expansions of the interior zero order temperature and pressure fields are the following:

$$\begin{aligned} T &\sim -1/2 + E^{1/4}\zeta \\ p &\sim -z/2 + E^{1/4}\zeta z \end{aligned} \tag{4.2.25}$$

These match to the corresponding boundary layer quantities if $\beta_0 = 1$ and $\delta_0 = 0$. We then have from (4.2.23) that $\kappa_0 = D^{3/2} / 2^{3/4}$ and therefore:

$$\hat{p}^{(0)} = -\frac{D^{3/2}}{2^{3/4}}\left[1 - e^{-\zeta/2^{1/4}\sqrt{D}}\right] + z\zeta \tag{4.2.26}$$

$$v^{(0)} = z - \frac{D}{2}\, e^{-z/2^{1/4}\sqrt{D}} \tag{4.2.27}$$

$$\hat{u}^{(0)} = \frac{1}{2\sqrt{2}}\, e^{-z/2^{1/4}\sqrt{D}} \tag{4.2.28}$$

$$\hat{w}^{(0)} = \frac{(D-z)}{2D^2}\, e^{-z/2^{1/4}\sqrt{D}} \tag{4.2.29}$$

Note that the first term of (4.2.26) generates an $O(E^{1/4})$ constant term as a correction to the interior pressure field . If a similar analysis is carried out for the boundary layers near $x = 1/2$ exactly the same term arises and therefore it is necessary to add this constant to the interior pressure field. However this does not in any way affect the interior results since it is possible to add any arbitrary constant to the pressure field without affecting any of the other dependent variables.

Having obtained $\hat{T}^{(0)}$ and $\hat{u}^{(0)}$ we can now find $\hat{T}^{(1)}$, which is given by

$$\hat{T}^{(1)}_{zz} = \lambda \beta_0\, \hat{u}^{(0)} = \lambda \beta_0\, v^{(0)}_{zz} \tag{4.2.30}$$

Thus

$$T^{(1)} = \beta_1(z)z + \lambda \beta_0 v^{(0)} \tag{4.2.31}$$

and this clearly matches to (4.1.32) . Thus we have :

$$T \sim -\frac{1}{2} + E^{1/4}\zeta + E^{1/2}\left[\beta_1 \zeta + \lambda\left(\zeta - \frac{D}{2}\right) e^{-\zeta/2^{1/4}\sqrt{D}}\right] \quad (4.2.32)$$

This expression matches, correct to $O(E^{1/2})$ with the interior temperature field if we take

$$\beta_1 (z) = 0 \quad (4.2.33)$$

This analysis has verified the boundary conditions used for determining the interior temperature fields .

3. DISCUSSION OF THE BOUNDARY LAYER SOLUTIONS

The side wall boundary layer solutions have a number of interesting features. First of all , the lowest order inner layer contains a closed meridional circulation cell . This is most easily seen by noting that:

$$\int_0^\infty w^{(0)}(\xi, \zeta)\, d\xi = 0 \quad (4.3.1)$$

and

$$\int_0^D \hat{u}^{(0)}(\xi, \zeta)\, d\zeta = 0 \quad (4.3.2)$$

Thus there is no net horizontal or vertical mass transport in a me-

ridional plane.

Now , although we have not computed all the $O(E^{1/6})$ corrections in the inner layer it is still possible to obtain information about the nature of the results. The boundary condition at $z = D$ ensures that there will be no net mass flux out of (into) the boundary layer near the free surface. This is true also for the outer layer. Now the net flux at the bottom of the inner layer is proportional to the integral , over the width of the boundary layer, of the side wall vertical velocity at $z = 0$. The same is true for the outer layer. The Ekman pumping conditions then show that the total net flux into the side wall layers at $z = 0$ is proportional to

$$\frac{1}{\sqrt{2}} \left\{ \int_0^\infty \frac{\partial v^{(0)}}{\partial \tau}(\tau, 0)\, d\tau + \int_0^\infty \frac{\partial v^{(0)}}{\partial \xi}(\xi, 0)\, d\xi \right\} \qquad (4.3.3)$$

where, of course , $v^{(0)}$ takes on the appropriate representation in each of these two integrals . Now $v_0 = 0$ at $z = 0$ in the interior and it is easily seen that by virtue of the matching conditions connecting the side wall layers (4. 3. 3) must vanish . Thus there is no net flux into , or out of, the side wall boundary layers. This is simply because there is a net mass flux out of the Ekman layer into the inner side wall layer which is balanced by a net flux into the Ekman layer from the outer boundary layer. This is the case near the cold wall. The situation is exactly reversed near the hot wall.

These conclusions are consistent with the fact that the meridional mass transport in those parts of the Ekman layers which

are adjacent to the interior is very small ($O(E^{1/2})$ in non - dimensional terms) . Thus the picture which results is that the closed circulations in the inner side layer extend , at the next higher order of approximation, into the lower Ekman layer and the outer side layer. Near the cold wall this circulation consists of downward motion directly adjacent to the wall and corresponding upward motion in the outer portions of the boundary layer. The circulation is in the opposite sense in the boundary layers near the hot wall.

The zonal velocities in both side wall layers consist of a positive (in the direction of rotation) flow in the upper part of the annulus and a negative return flow in the lower portion of the annulus. The return flow becomes exponentially small in the outer limits of the boundary layers and is very small ($O(E^{1/2})$) in the interior .

This zonal flow structure has some effect on the structure of the temperature field . At lowest order the temperature field is simply that which would result from heat conduction alone. The modifications to this state are $O(E^{1/2})$. In the interior they result in a weak vertical stratification, due to convection in the side wall layers, as well as a contribution due to the fact that the upper surface has a mean slope owing to the presence of centrifugal forces. This latter contribution is confined entirely to the interior at lowest order.

The side wall boundary layer structure of the temperature field reflects the behaviour of the zonal flow . This is illustrated in part by equation (4.2.32)* which shows that the $O(E^{1/2})$ correction to the conductive state is positive above the curve defined by

$$z - \frac{D}{2}\, e^{-t/2^{1/4}\sqrt{D}} = 0$$

and negative below it . Thus, due to convection near the cold wall, the isotherms have equilibrium positions which are on the wall side of the conductive state above the curve and the opposite of this below the curve. The hot wall boundary layer temperature field is also cooled from the conductive state in the lower part of the layer and warmed in the upper part. This has the opposite effect on the displacement of the isotherms relative to the wall however. The overall effect of convection is thus to provide the fluid with a weak gravitationally stable stratification.

CHAPTER V

ANALYSIS OF THE CORNER REGIONS

1. THE UPPER EKMAN EXTENSIONS OF THE SIDE WALL LAYERS

This chapter is devoted to verification of the upper and lower boundary conditions which were used in the preceeding chapter. We begin with a consideration of the free surface Ekman extension to the inner side wall layer , The analysis being facilitated by use of a set of orthogonal coordinates based on those used in Chapter II . We define

$$s = \frac{D - z + \mu E^{1/2} x}{E^{1/2} (1+\mu^2 E)^{1/2}} \qquad (5.1.1a)$$

$$\bar{\xi} = \frac{x + 1/2 + \mu E^{1/2} (z - D)}{E^{1/3} (1+\mu^2 E)^{1/2}} \qquad (5.1.1b)$$

The side wall independant variables, expressed in terms of these coordinates, are

$$z = D - \frac{E^{1/2}}{1+\mu^2 E} \left\{ (s - \mu E^{1/3} \bar{\xi})(1+\mu^2 E)^{1/2} + \frac{\mu}{2} \right\} \qquad (5.1.2a)$$

$$\xi = \frac{1}{1+\mu^2 E} \left\{ (\bar{\xi} + \mu E^{2/3} s)(1+\mu^2 E)^{1/2} + \frac{\mu^2 E^{2/3}}{2} \right\} \qquad (5.1.2b)$$

Expressing the solutions for the inner side wall layer in terms of and s using these relationships and expanding for small values of E leads to the following:

$$T \sim E^{1/3}\bar{\xi} + E^{1/2}\lambda V^{(0)}(\bar{\xi}, D) \qquad (5.1.3a)$$

$$V \sim V(\bar{\xi}, D) + E^{1/2}\frac{\partial V}{\partial z}(\bar{\xi}, D)(s + \tfrac{\mu}{2}) \qquad (5.1.3b)$$

$$p \sim -\frac{D}{2} + E^{1/3}\hat{p}(\bar{\xi}, D) - \frac{E^{1/2}}{2}(s + \tfrac{\mu}{2}) \qquad (5.1.3c)$$

$$u \sim E^{1/3}\left[\hat{u}(\bar{\xi}, D) + E^{1/2}\frac{\partial \hat{u}}{\partial z}(\bar{\xi}, D)(s + \tfrac{\mu}{2})\right] \qquad (5.1.3d)$$

$$w \sim E^{1/2}\frac{\partial w}{\partial z}(\bar{\xi}, D)(s + \tfrac{\mu}{2}) \qquad (5.1.3e)$$

with errors which are $o(E^{1/2})$.

Now the boundary conditions which apply at $s = 0$ are, as in Chapter III,

$$\frac{\partial u}{\partial s} = \frac{\partial V}{\partial s} = \frac{\partial T}{\partial s} = 0; \quad W = \mu E^{1/2} u \qquad (5.1.4)$$

It is readily seen that these conditions are satisfied by the expressions (5.1.3) with errors whcih are $O(E^{1/2})$ or less. Thus it

may be expected that , just as for the analysis of Chapter III, the Ekman layer is not required at lowest order. This conclusion can be verified by formal analysis of the Ekman layer equations as they apply in the present case. Similar considerations apply to the free surface Ekman layer extension to the outer side wall layer. The analysis for these Ekman layer extensions is relatively straight forward and little would be gained by presenting them here. It is sufficient to say that the absence of an Ekman layer at lowest order ensures that w must be $O(E^{1/2})$ or less near $z = D$ and this implies the upper boundary conditions used in the preceeding chapter.

2. THE LOWER EKMAN EXTENSIONS

The appropriate stretched independant variables for the lower Ekman extension to the inner side layer are $\eta = z / E^{1/2}$ and $\xi = (x + 1/2) E^{-1/3}$. The boundary conditions which must be satisfied at $\eta = 0$ are

$$u = v = w = \frac{\partial T}{\partial \eta} = 0 \qquad (5.2.1)$$

We scale T , p , and w to facilitate matching to the side wall layer solutions. This is achieved by choosing

$$w = E^{1/6} \hat{w}; \quad p = E^{1/3} \hat{p}; \quad T = -1/2 + E^{1/3} \hat{T}$$

with $\hat{\omega}$, $\hat{p}$ and $\hat{T}$ being regarded as O(1) quantities. The lowest order governing equations are then the Ekman layer equations:

$$v = -\hat{p}_\xi - u_{\eta\eta} + O(E^{1/6}) \tag{5.2.2}$$

$$u = v_{\eta\eta} + O(E^{1/6}) \tag{5.2.3}$$

$$\hat{p}_\eta = -E^{1/6}/2 + O(E^{1/3}) \tag{5.2.4}$$

$$u_\xi + \hat{\omega}_\eta = 0 \tag{5.2.5}$$

$$\hat{T}_{\eta\eta} = \lambda E^{1/6}(u\hat{T}_\xi + \hat{\omega}\hat{T}_\eta) + O(E^{1/3}) \tag{5.2.6}$$

The first approximations to $\hat{p}$, v, u, and $\hat{\omega}$ are the usual Ekman layer solutions:

$$\hat{p}_0 = \bar{\Phi}_0(\xi) \tag{5.2.7}$$

$$v_0 = \bar{\phi}_0'[1 - e^{-\eta/\sqrt{2}}\cos\eta/\sqrt{2}] \tag{5.2.8}$$

$$u_0 = -\bar{\phi}_0' e^{-\eta/\sqrt{2}}\sin\eta/\sqrt{2} \tag{5.2.9}$$

$$\hat{\omega}_0 = \frac{\bar{\phi}_0''}{\sqrt{2}}\left[1 - e^{-\eta/\sqrt{2}}(\cos\eta/\sqrt{2} + \sin\eta/\sqrt{2})\right] \qquad (5.2.10)$$

Equations (5.2.6), (5.2.9), and (5.2.10) can be used to obtain the first two terms in an expansion for T. We find that

$$\hat{T} \sim \bar{\Theta}_0(\xi) + E^{1/6}\{\bar{\Theta}_1(\xi) - \lambda\bar{\Theta}_0'\bar{\phi}_0'[\eta/\sqrt{2} + e^{-\eta/\sqrt{2}}\cos\eta/\sqrt{2}]\} \qquad (5.2.11)$$

Matching with the side layer solutions is achieved at lowest order by choosing $\bar{\phi}_0(\xi) = \hat{p}_0(\xi, 0)$, $\bar{\Theta}_0(\xi) = \xi$. Equation (5.2.10) then implies the Ekman pumping condition. However, the full outer expansion of (5.2.11) now takes the form

$$\hat{T} \sim \xi + E^{-1/3}\frac{\lambda}{\sqrt{2}}\frac{\partial\hat{p}_0}{\partial\xi}(\xi, 0)z + O(E^{1/6}) \qquad (5.2.12)$$

Since $\frac{\partial\hat{p}_0}{\partial\xi}(\xi, 0) \neq 0$ it is clear that the second term of this expression will not match to the side wall temperature field. This inconsistency is removed by considering a thicker corner region near $z = 0$. However before doing this we may note that the solutions for the lower Ekman extension to the outer side layer are obtained by taking $p = E^{1/4}\hat{p}$; $T = -1/2 + E^{1/4}\hat{T}$, $\omega = E^{1/4}\hat{\omega}$ to ensure matching

to the side layer. Then at lowest order $\hat{p}_o = F_o(\tau)$ with v_o, u_o, and $\hat{\omega}_o$ being identical in form to the expressions (5.2.8) through (5.2.10) with $\bar{\Phi}_o$ replaced by F_o. The expansion for T correct to $O(E^{1/2})$ is then given by

$$T \sim -\tfrac{1}{2} + E^{1/4}\,\Theta_o(\tau) + E^{1/2}\left[\Theta_1(\tau) - \lambda\,\Theta_o' F_o'\left(\eta/\sqrt{2}\right.\right.$$

$$\left.\left. + e^{-\eta/\sqrt{2}} \cos \eta/\sqrt{2}\right)\right] \qquad (5.2.13)$$

where, of course, $\tau = (x + 1/2)\,E^{-1/4}$. Again matching of the pressure and velocity fields is achieved by choosing $F_o(\tau) = h_o(\tau)$ where this latter quantity was determined in Chapter IV, i.e.,

$$F_o(\tau) = -\frac{D^{3/2}}{2^{3/4}}\left[1 - e^{-\tau/2^{1/4}\sqrt{D}}\right] \qquad (5.2.14)$$

Again, the choice $\Theta_o(\tau) = \tau$ ensures matching of the first two terms of (5.2.13) but the third term can not be matched directly and a thicker boundary layer is required to remove the inconsistency.

3. THE LOWER SQUARE CORNER REGIONS

The inconsistency which arises in attempting to match the expressions for the temperature field, as they appear in the Ekman extensions, to those for the side wall layers can be removed

by considering the square corner regions adjacent to the side wall layers. To illustrate this we consider the $E^{1/4} \times E^{1/4}$ region where the appropriate independent variables are now τ and $y = z / E^{1/4}$. Rather than go to great detail we shall simply sketch the results. It is easily shown that, at lowest order the appropriate expressions for p, u, v, and w are just the outer expansions of the Ekman layer solutions. Then, if we choose the scaling $T = -1/2 + E^{1/4} T^*(\tau, y)$, it is easily shown that at lowest order T^* must be a solution of the partial differential equation

$$\frac{\partial^2 T_o^*}{\partial \tau^2} + \frac{\partial^2 T_o^*}{\partial y^2} = \frac{\lambda}{\sqrt{2}} F_o'' \frac{\partial T_o^*}{\partial y} \qquad (5.3.1)$$

where $F_o(\tau)$ is the expression appearing in (5.2.14).

The lower boundary condition on T_o^* is obtained by matching to the Ekman layer expression (5.2.13) and is

$$\frac{\partial T_o^*}{\partial y}(\tau, 0) = -\frac{\lambda}{\sqrt{2}} F_o' \frac{\partial T_o^*}{\partial \tau}(\tau, 0) \qquad (5.3.2)$$

We also need a condition at $\tau = 0$ and this is obtained by matching directly to the inner side wall which leads to the requirement that T_o^* be continous at $\tau = 0$ and that

$$T_o^*(0, y) = 0 \qquad (5.3.3)$$

For large ζ and y the solution must merge with the side wall solution ($y \to \infty$, ζ fixed) and/or the interior solution ($\zeta \to \infty$, y fixed) . This is achieved by requiring that $T_o^* \sim \zeta$ for both large y and large ζ .

Now , the problem of solving (5. 3. 1) subject to all these conditions is not separable and because of this we have not been able to find an appropriate analytical solution. The $E^{1/3} \times E^{1/3}$ corner region poses similar difficulties. Thus, at this stage we choose to proceed on the assumption that appropriate solutions exist and therefore we shall not pursue the matter further. Our main purpose in this chapter was to verify the boundary conditions which were used in Chapter IV and we have done this subject to the presumption that the appropriate corner region solutions exist.

CHAPTER VI

THE STABILITY OF THE AXIALLY SYMMETRIC FLOW TO PERTURBATIONS WITH LOW WAVE NUMBERS

1. A PRELIMINARY DISCUSSION OF THE STABILITY PROBLEM

The analysis in the preceding chapters has led to an approximate solution of the equations governing an axisymmetric steady state when the imposed parameters are typical of those for which the lower symmetric regime has been observed in experiments. The experiments (Kaiser, 1970) also support the suggestion that a lower transition occurs when the axially symmetric flow becomes unstable to small disturbances. If this is so the conditions under which the symmetric state described in the preceding chapters becomes just unstable should approximate those for which the experiments indicate that the lower symmetry transition occurs. The remainder of the present study will be devoted to the analysis of this stability problem. Before doing so, however , we shall anticipate some of the results in order to clarify our subsequent discussion.

The symmetrical steady temperature field of our basic state is characterized by being nearly conductive throughout the fluid, i.e., it is only weakly stably stratified in the vertical . Thus, when in this state , the fluid is very nearly neutrally bouyant and it may be expected that the absence of the gravitational restoring force which would exist if the fluid were strongly stably stratified would favour the development of non-symmetrical disturbances. This is in marked contrast to the situation for the upper symmetric state where the

experiments show that strong stable stratification exists throughout most of the fluid. In fact, as most of the previous theoretical studies have shown, the presence of stable stratification in the basic state is crucial in ensuring the stability of the upper symmetry regime. Its absence in our analysis will thus place a limitation on the results. We can not expect them to be accurate for thermal Rossby numbers which are too large.

An inviscid theoretical model of baroclinic instability of the type studied by Eady (1949) can be used, with qualitative success, to explain the upper symmetry transition. On the other hand, it is incapable of describing the lower transition because of the fact that viscous and heat conduction effects are neglected. (It predicts that the wave regime will persist to vanishingly small Rossby numbers). On the other hand all those stability studies which have been qualitatively successful in predicting a lower symmetry transition have included, in some form, mechanisms which describe viscous and/or heat conductive effects. The accumulated theoretical and experimental findings to date point to these mechanisms as the ones of major importance in determining the lower symmetry transition criteria. (See Hide (1970) for a discussion of this point). Our subsequent analysis will show not only that heat conduction and viscous effects are important in the fluid interior near the lower symmetry transition, but also that centrifugal effects play a role in determining the slope of the transition curve as plotted on a Rossby number vs. Taylor number diagram. We will assume, throughout the analysis, that the non-symmetric perturbations have wave-like character, in agreement with experi-

mental observations . The first part of the analysis will proceed on the assumption that the wave number of the disturbance , defined in non-dimensional form as follows

$$k = LN/r_o \quad ; \quad N = 1, 2, 3 \ldots,$$

is an O (1) parameter . We shall refer to this as the "low" wave number analysis because it will turn out that , near the transition curve the quantity $k\, E^{1/8}$ is approximately O (1) .

The low wave number analysis will proceed in two stages. The first of these will show that instability will always occur if the Rossby number is sufficiently large. This is mainly because the aforementioned mechanism of gravitational stabilization due to the presence of the stable vertical stratification is absent at lowest order. The second stage will show that as the Rossby number becomes small heat conduction becomes important in the interior of the fluid. When this is the case there is a critical Rossby number such that for values less than the critical one a disturbance will be stable.

It will turn out, however , that the low wave number analysis does not properly define the curve of transition since it implies that the limiting minimum value of the critical Rossby number is reached only as the wave number of the disturbance becomes indefinitely large. However, as the wave number increases the viscous terms, which are neglected in the fluid interior for the low wave number analysis , become increasingly large. Thus we will be led to discuss what happens when the wave number is so large that the viscous terms play a role in the zero-order interior dynamics . We shall re-

fer to this discussion as the "high" wave number analysis. This analysis will show, in contrast to that for low wave numbers , that the limiting minimum value of the Rossby number is approached as the wave number becomes vanishingly small. (The same limiting Rossby number is predicted in both cases).

The apparent conflict between the predictions of the low and the high wave number analyses is resolved by considering the manner in which the limiting value of the Rossby number is approached for each . A comparison of the limiting expressions for the critical Rossby number as obtained from each analysis leads to a determination of the order of magnitude of the wave number near the point where they overlap. This "intermediate" wave number scaling leads to an analysis which results in determination of the minimum critical Rossby number and the corresponding wave number. These are the values which should compare with experimental results.

2. FORMULATION OF THE STABILITY PROBLEM

The equations governing the stability problem are those which are obtained by linearization with respect to a time independent axisymmetric state given in general terms by $\vec{V} = \underline{V}(x, z)$, $T = \underline{T}(x, z)$. The equations governing infinitesimal perturbations imposed on this state are the following:

$$\frac{\partial \vec{V}}{\partial t} + R_o\left(\underline{V}\cdot\nabla\vec{V} + \vec{V}\cdot\nabla\underline{V}\right) + \hat{k}\times\vec{V} = -\nabla p$$

$$+T\left(\hat{k} - \epsilon\hat{i}\right) + E\nabla^2\vec{V} \qquad (6.2.1)$$

$$\nabla \cdot \vec{V} = 0 \qquad (6.2.2)$$

$$\frac{\partial T}{\partial t} + R_o (\underline{V} \cdot \nabla T + \vec{V} \cdot \nabla \underline{T}) = \frac{E}{\sigma} \nabla^2 T \qquad (6.2.3)$$

where $\vec{V}$, p , and T are perturbation quantities.

As before, we are interested in those cases where $R_o \leq O(E^{1/2})$, $\epsilon = O(E^{1/2})$, $0 < E << 1$. Under these circumstances a number of time scales may be important . In general an arbitrary initial disturbance will excite all of the permisisible gravity-inertial oscillations as well as a mode of motion whose evolution is so slow that it is, in the first approximation, steady and geostrophic in the interior of the fluid. As time progresses however the geostrophic mode * will eventually begin to deviate from its initial values. This will happen when $t E^{1/2} \simeq O(1)$ since this is the amount of time which must elapse before the boundary layers have a noticeable effect on the interior motion. If $R_o = O(E^{1/2})$ the advective terms in equations (6.2.1) and (6.2.3) will also have an effect on the evolution of the geostrophic mode. Since these are the terms which will may give rise to instability, it could be expected that this

---

* The geostrophic mode as referred to here has that character only in the interior of the fluid. Geostrophic balance does not exist in the boundary layers.

instability , if possible , should become apparent in the evolution of the geostrophic mode.

On the other hand, the higher frequency gravity-inertial modes of motion will still be present at these longer times . At this stage their further evolution will also be affected by the boundary layers and advective terms. However experimental evidence indicates that the wave speeds of the observed annulus waves are small when R_o is small (see Kaiser (1972)) while theoretical considerations suggest that the stability properties of the higher frequency modes will not be affected by the advective terms (correct to $O(E^{1/2})$) while the effect of the boundary layers is to cause them to be damped with time. (Greenspan (1968)). Thus , since our main purpose here is to examine the stability problem, we shall bypass the initial-value problem and consider the behavior of the geostrophic mode explicitly.

We look for wave solutions of the form

$$(V, p, T) = (V, p, T)\, e^{ik(y - R_o c t)} \qquad (6.2.4)$$

where k is the $O(1)$ wave number defined above, c is an $O(1)$ phase speed, and V , p , T are functions of x and z . Inserting (6.2.4) into (6.2.1) to (6.2.3) and dropping the superhats gives the following governing equations:

$$\frac{\lambda}{\sigma} E^{1/2}\{ik(\hat{j}\cdot\underline{V}-c)\vec{V} + \underline{V}\cdot\nabla_2\vec{V} + \vec{V}\cdot\nabla_2\underline{V}\}$$

$$+\hat{k}\times\vec{V} = -\nabla p + T(\hat{k}-\epsilon\hat{i}) + E\nabla^2\vec{V} \qquad (6.2.5)$$

$$\nabla\cdot\vec{V} = 0 \qquad (6.2.6)$$

$$\lambda\{ik(\hat{j}\cdot\underline{V}-c)T + \underline{V}\cdot\nabla_2 T + \vec{V}\cdot\nabla_2\underline{T}\} = E^{1/2}\nabla^2 T \qquad (6.2.7)$$

where we have used the definitions:

$$\nabla_2 = \hat{i}\frac{\partial}{\partial x} + \hat{k}\frac{\partial}{\partial z}$$

$$\nabla = \nabla_2 + ik\hat{j}$$

3. THE INTERIOR FLOW

The analysis of the axisymmetric flow problem has established that the basic velocity and temperature fields in the interior of the fluid are given, correct to $O(E^{1/2})$, by the following:

$$\underline{V} = (0,\ z + E^{1/2}\mathcal{V},\ 0) \qquad (6.3.1)$$

$$\underline{T} = x + E^{1/2} \tau \qquad (6.3.2)$$

where τ and V are given by equations (3.4.32) and (3.4.34) respectively.

We take $\omega = E^{1/2} \hat{\omega}$ with $\hat{\omega} = O(1)$ to insure the possiblity of satisfying the compatibility conditions which will arise from analysis of the Ekman layers. Equations (6.2.5) to (6.2.7) now take the following form:

$$ik\frac{\Delta}{\sigma} E^{1/2}(z + E^{1/2} V - c)u - v = -p_x - \mu E^{1/2} T + E\nabla^2 u \qquad (6.3.3)$$

$$\frac{\Delta}{\sigma} E^{1/2}[ik(z + E^{1/2} V - c)v + E^{1/2}\hat{\omega}] + u = -ikp + E\nabla^2 v \qquad (6.3.4)$$

$$ik\frac{\Delta}{\sigma} E(z + E^{1/2} V - c)\hat{\omega} = -p_z + T + E^{3/2}\nabla^2 \hat{\omega} \qquad (6.3.5)$$

$$u_x + ik v + E^{1/2} \hat{\omega}_z = 0 \qquad (6.3.6)$$

$$\lambda [ik(z + E^{1/2} V - c)T + u + E^{1/2} u T_x + E \hat{w} T_z$$

$$= E^{1/2} \nabla^2 T \qquad (6.3.7)$$

A vorticity equation can be obtained from (6.3.3), (6.3.4) and (6.3.6) :

$$\hat{\omega}_z = -ik\mu T + ik \frac{\Lambda}{\sigma} [(z-c)(v_x - iku) + O(E^{1/2})]$$

$$- E^{1/2} \nabla^2 (v_x - iku) \qquad (6.3.8)$$

If we now neglect all terms multiplied by $E^{1/2}$ or E we obtain the following zero order results :

$$v^{(0)} = p_x^{(0)} \qquad (6.3.9a)$$

$$u^{(0)} = -ik p^{(0)} \qquad (6.3.9b)$$

$$p_z^{(0)} = T^{(0)} \tag{6.3.9c}$$

$$ik(z-c)T^{(0)} + u^{(0)} = 0 \tag{6.3.9d}$$

From (6.3.9b, c, d) we have:

$$(z-c)p_z^{(0)} - p^{(0)} = 0 \tag{6.3.10}$$

This has a solution of the form

$$p^{(0)} = (z-c)A_0(x) \tag{6.3.11}$$

so that

$$T^{(0)} = A_0(x) \tag{6.3.12}$$

The function $A_0(x)$ must be determined. Equation (6.3.8) enables the calculation of the zero order values of $\hat{w}$:

$$\hat{w}_z^{(0)} = -ik\mu A_0 + ik\frac{\Lambda}{\sigma}(z-c)^2 \mathcal{L} A_0 \qquad (6.3.13)$$

where

$$\mathcal{L} A_0 = \frac{d^2 A_0}{dx^2} - k^2 A_0$$

Integrating (6.3.13) between $z = 0$ and $z = D$ provides the governing equation for A_0 when the boundary conditions on $\hat{w}^{(0)}$ are known, i.e.,

$$[\hat{w}^{(0)}(D,x) - \hat{w}^{(0)}(0,x)] = -ik\mu D A_0$$

$$+ ik\frac{\Lambda}{\sigma} D^3\left[\frac{1}{3} - \frac{c}{D} + \frac{c^2}{D^2}\right] \mathcal{L} A_0 \qquad (6.3.14)$$

The values of $\hat{w}^{(0)}$ at $z = 0$ and $z = D$ are to be determined via analysis of the Ekman layers.

We have not formally considered here what effect, if any, may arise from the presence of a critical level (where $|z - c| \ll 1$) in the interior of the fluid. It may be expected that the viscous and heat conduction terms in the governing equations would play a more important role in a small region surrounding the critical level than they do else where in the interior. For instance equation (6.3.7) shows that within a vertical distance of dimensionless magnitude $O(E^{1/6})$ of the point where $|z - c| \ll 1$ the term involving $(z-c)\,T$ is of the same order of magnitude as the term involving $E^{1/2}\partial^2 T/\partial z^2$

if T is a sufficiently rapidly varying function of $z.(\partial T/\partial z = O(E^{-1/6}))$. The same consideration would apply to equation (6.3.8).

A formal analysis of the critical layer can in fact be carried out using (6.3.3) through (6.3.8) and a stretched variable defined by $\xi = (z-c)\, E^{-1/6}$. However , rather than present the details of such an analysis we shall simply state that the lowest order equations which we have just presented are unchanged provided we bear in mind the additional condition that $-7\pi/6 < \arg(z-c) < \pi/6$. This condition is one which ensures that the critical layer solutions will have the asymptotic behavior which ensures the possibility of matching them to those which are valid outside that layer. Exactly the same condition was presented by Lin (1966) , for the same reason. Moreover, it is automatically satisfied for self excited waves.

4. THE EKMAN LAYER NEAR THE FREE SURFACE

The analysis here is very similar to that which was carried out for the axisymmetric flow. As in that case we use the orthogonal boundary layer coordinates defined in Chapter III . We also scale the vertical velocity so that $w = E^{1/2}\hat{w}$; $\hat{w} = O(1)$.

The boundary conditions which must be satisfied at the static position of the free surface ($\tilde{s} = 0$) are the following:

$$\frac{\partial u}{\partial \tilde{s}} = \frac{\partial v}{\partial \tilde{s}} = \frac{\partial T}{\partial \tilde{s}} = 0; \quad \hat{w} = \mu u \tag{6.4.1}$$

with errors which are $O(E^{1/2})$ or less.

The relevant basic state quantities are the axisymmetric solutions displayed in equations (3.2.8) through (3.2.12). Using these and (6.3.1) and (6.3.2) the governing equations for the perturbations are the following:

$$ik\frac{\Lambda}{\sigma}E^{1/2}(D-c)u - v = -(p_{\tilde{x}} + \mu p_{\tilde{\zeta}}) - \mu E^{1/2}T + u_{\tilde{\zeta}\tilde{\zeta}} + O(E) \qquad (6.4.6)$$

$$ik\frac{\Lambda}{\sigma}E^{1/2}(D-c)v + u = -ikp + v_{\tilde{\zeta}\tilde{\zeta}} + O(E) \qquad (6.4.7)$$

$$-E^{-1/2}(p_{\tilde{\zeta}} - \mu E p_{\tilde{x}}) = T + O(E) \qquad (6.4.8)$$

$$(u_{\tilde{x}} + \mu u_{\tilde{\zeta}}) + ikv - (\hat{w}_{\tilde{\zeta}} - \mu E \hat{w}_{\tilde{x}}) = 0 \qquad (6.4.9)$$

$$\lambda E^{1/2}[ik(D-c)T + u] = T_{\tilde{\zeta}\tilde{\zeta}} + O(E) \qquad (6.4.10)$$

The solutions, correct to $O(E^{1/2})$, which satisfy the boundary conditions (6.4.1) are given by the following expressions:

$$T = \Theta_0(\bar{x}) + E^{1/2}\left[\Theta_1(\bar{x}) + \frac{ik\Lambda}{2}\tilde{s}^2((D-c)\Theta_0 - \phi_0(\bar{x}))\right] \qquad (6.4.11)$$

$$p = \phi_0(\bar{x}) + E^{1/2}(\phi_1(\bar{x}) - \tilde{s}\,\Theta_0(\bar{x})) \qquad (6.4.12)$$

$$v = \phi_0' + E^{1/2}\left\{\phi_1' - \tilde{s}\,\Theta_0' + \frac{k^2\Lambda}{\sigma}(D-c)\phi_0 - \frac{1}{\sqrt{2}}e^{-\tilde{s}/\sqrt{2}}\left[(\Theta_0' + ik\Theta_0)\cos\tilde{s}/\sqrt{2} - (\Theta_0' - ik\Theta_0)\sin\tilde{s}/\sqrt{2}\right]\right\} \qquad (6.4.13)$$

$$u = -ik\phi_0 + E^{1/2}\left\{-ik(\phi_1 - \tilde{s}\,\Theta_0) - \frac{ik\Lambda}{\sigma}(D-c)\phi_0' - \frac{1}{\sqrt{2}}e^{-\tilde{s}/\sqrt{2}}\left[(\Theta_0' + ik\Theta_0)\sin\tilde{s}/\sqrt{2} + (\Theta_0' - ik\Theta_0)\cos\frac{\tilde{s}}{\sqrt{2}}\right]\right\} \qquad (6.4.14)$$

$$\hat{\omega} = \mu u + E^{1/2}\left\{-ik\frac{\Lambda}{\sigma}\tilde{s}(D-c)(\phi_0'' - k^2\phi_0) - (\Theta_0'' - k^2\Theta_0)\left[1 - e^{-\tilde{s}/\sqrt{2}}\cos\tilde{s}/\sqrt{2}\right]\right\} \qquad (6.4.15)$$

Thus, just as in the axisymmetric case, the lowest order solutions are all independent of $\tilde{s}$. These quantities will match to the interior solutions if

$$\phi_0(\bar{x}) = (D-c) A_0(\bar{x}) \qquad (6.4.16)$$

$$\theta_0(\bar{x}) = A_0(\bar{x}) \qquad (6.4.17)$$

$$\hat{w}^{(0)}(D,\bar{x}) = -ik\mu (D-c) A_0(\bar{x}) \qquad (6.4.18)$$

By virtue of (6.4.16) and (6.4.17) the term multiplied by $\tilde{s}^2$ in (6.4.11) vanishes so that the boundary layer corrections to the interior temperature field are at most $O(E^{1/2})$. The interior temperature field satisfies the upper boundary condition at lowest order.

5. THE LOWER EKMAN LAYER

The equations governing the perturbations in the lower Ekman layer are, with $w = E^{1/2}\hat{w}$ and $\eta = z / E^{1/2}$, the following:

$$u = v = \hat{w} = \frac{\partial T}{\partial \eta} = 0 \qquad \text{at } \eta = 0 \qquad (6.5.1)$$

$$-ik\frac{\Lambda}{\sigma} E^{1/2} c\, u - v = -p_x - \mu E^{1/2} T + u_{\eta\eta} + O(E) \qquad (6.5.2)$$

$$-ik\frac{\Lambda}{\sigma}E^{1/2}cv+u=-ikp+v_{\eta}\eta+O(E) \tag{6.5.3}$$

$$\lambda E^{1/2}(-ikcT+u)=T_{\eta}\eta+O(E) \tag{6.5.4}$$

$$u_x+ikv+\hat{\omega}_{\eta}=0 \tag{6.5.5}$$

The zero-order solutions for $(p, v, u, \hat{\omega})$ are the following

$$p^{(0)}=\Phi_0(x)$$

$$v^{(0)}=\Phi_0'\left[1-e^{-\eta/\sqrt{2}}\cos\eta/\sqrt{2}\right]$$

$$-ik\Phi_0 e^{-\eta/\sqrt{2}}\sin\eta/\sqrt{2} \tag{6.5.6}$$

$$u^{(0)}=-ik\Phi_0\left[1-e^{-\eta/\sqrt{2}}\cos\eta/\sqrt{2}\right]$$

$$-\Phi_0' e^{-\eta/\sqrt{2}}\sin\eta/\sqrt{2} \tag{6.5.7}$$

$$\hat{w}^{(0)} = \frac{1}{\sqrt{2}} (\Phi_0'' - k^2 \Phi_0) \left[1 - e^{-\eta/\sqrt{2}} (\cos \eta/\sqrt{2} + \sin \eta/\sqrt{2}) \right] \qquad (6.5.8)$$

while T is, correct to $O(E^{1/2})$, given by :

$$T = \bar{\theta}_0(x) + E^{1/2} \bar{\theta}_1(x) - \lambda E^{1/2} \left\{ \frac{\eta^2}{2} ik (c\bar{\theta}_0 + \Phi_0) + \frac{\eta}{\sqrt{2}} (\bar{\Phi}_0' - ik\Phi_0) + e^{-\eta/\sqrt{2}} (\Phi_0' \cos \eta/\sqrt{2} - ik\Phi_0 \sin \eta/\sqrt{2}) \right\} \qquad (6.5.9)$$

Matching of the zero-order pressure, temperature and velocity components to the corresponding interior quantities is accomplished if:

$$\Phi_0 = -c A_0(x) \qquad (6.5.10)$$

$$\bar{\theta}_0 = A_0(x) \qquad (6.5.11)$$

$$\hat{w}^{(0)}(0,x) = -\frac{c}{\sqrt{2}} (A_0'' - k^2 A_0) \qquad (6.5.12)$$

The conditions (6.5.10) and (6.5.11) ensure that the term multiplied by η^2 in (6.5.9) must vanish . However the term multiplied by η can only match the interior temperature field if that quantity satisfies the following condition:

$$\frac{\partial T^{(0)}}{\partial z}(0,x) = \frac{\lambda}{\sqrt{2}} c\,(A_0' - ikA_0) \qquad (6.5.13)$$

Clearly this condition is not consistent with the fact that the zero order interior temperature field is independent of z unless the right side of (6.5.13) is small. In fact , since the terms which have been neglected in arriving at the zero order interior solutions are at most $O(E^{1/2})$, this means that the right side of (6.5.13) must be at most $O(E^{1/2})$ if matching is to be possible. We do not anticipate that this will be the case and therefore note that the inconsistency can be remove by considering a thicker boundary layer which connects the Ekman layer to the interior.

We shall defer the discussion of this boundary layer to the stage at which the analysis for intermediate wave numbers is carried out. It will turn out that the results of the boundary layer analysis have a direct bearing on the nature of the interior solutions at one of the orders of approximation which we shall consider there. For the present it will suffice to state that it can be shown, via analysis of the intervening boundary layer, that the Ekman pumping condition (6.5.12) is the appropriate lowest order boundary condition for the interior.

6. DETERMINATION OF $A_o(x)$ AND THE FIRST APPROXIMATION TO c

Equation (6.3.14) in combination with (6.4.18) and (6.5.12) provides the governing equation for $A_o(x)$:

$$\frac{c}{\sqrt{2}}\left(\alpha+\sqrt{2}\,ik\mu\right)A_o-ik\frac{\lambda}{\sigma}D^3\left(\frac{1}{3}-\frac{c}{D}+\frac{c^2}{D^2}\right)\alpha A_o=0 \qquad (6.6.1)$$

Boundary conditions at $x = \pm 1/2$ are required . The side wall boundary layer analysis in the Appendix can be used to show that

$$A_o(\pm 1/2) = 0 \qquad (6.6.2)$$

Equations (6.6.1) and (6.6.2) have solutions of the form

$$A_o = \text{const . } \sin\, m\pi(x-1/2)\ ;\quad m=\pm 1\ ,\ \pm 2\ ,\ \ldots \qquad (6.6.3)$$

provided c is given by:

$$c^2-D\left[1-\frac{i\sigma}{\sqrt{2}\,k\lambda D^2}-\frac{\mu\sigma}{\lambda\kappa^2D^2}\right]c+\frac{D^3}{3}=0 \qquad (6.6.4)$$

where $\kappa^2 = k^2 + m^2\pi^2$. This characteristic equation has the solutions

$$c = -\frac{D}{2}\left\{\left[1 - \frac{i\sigma}{\sqrt{2}\,k\lambda D^2} - \frac{\mu\sigma}{\kappa^2\lambda D^2}\right]\right.$$

$$\pm\left[\left(1-\frac{\mu\sigma}{\kappa^2\lambda D^2}\right)^2 - \frac{\sqrt{2}\,i\sigma}{k\lambda D^2}\left(1-\frac{\mu\sigma}{\kappa^2\lambda D^2}\right)\right.$$

$$\left.\left.-\frac{\sigma^2}{2k^2\lambda^2 D^4} - \frac{4}{3}\right]^{1/2}\right\} \qquad (6.6.5)$$

The condition that Im (c) $\geq$ 0 for one of these two roots is that

$$\frac{\sigma}{k\lambda D^2} \leq \left[\sqrt{a^2+b^2} - a\right]^{1/2} \qquad (6.6.6)$$

where

$$a = \left(1 - \frac{\mu\sigma}{\lambda\kappa^2 D^2}\right)^2 - \frac{\sigma^2}{2k^2\lambda^2 D^4} - \frac{4}{3} \qquad (6.6.7)$$

$$b = \frac{\sqrt{2}\,\sigma}{k\lambda D^2}\left(1 - \frac{\mu\sigma}{\kappa^2\lambda D^2}\right) \qquad (6.6.8)$$

Some simple algebra shows that (6.6.6) reduces to

$$\frac{\sigma^2}{k^2\lambda^2 D^4} \geq 0 \qquad (6.6.9)$$

This is clearly true for all finite values of σ, k, λ and D. Therefore we conclude that there is always one root of (6.6.5) which corresponds to a self excited (unstable) wave solution.

The solutions obtained here correspond to unstable Rossby waves . The quantity $\sigma\mu/\lambda D^2$ plays the same role as the local latitudinal gradient of the Coriolis parameter in the well known Rossby formula for the phase speed of large scale atmospheric waves. We may also note that if we had considered an inviscid system, i.e. if the Ekman pumping condition were replaced by the requirement that $\hat{w}$ should vanish at $z = 0$, equation (6.6.5) would then take the form :

$$c = \frac{D}{2}\left[1 - \frac{\sigma\mu}{k^2\lambda D^2}\right] \pm \frac{D}{2}\left[\left(1 - \frac{\sigma\mu}{k^2\lambda D^2}\right)^2 - \frac{4}{3}\right]^{1/2} \qquad (6.6.10)$$

This equation is exactly analogous to one obtained by Fjortoft (1951) for the stability of large scale disturbances in an atmosphere with neutrally stable vertical stratification. Equation (6.6.10) admits neutrally stable solutions if

$$\left(1 - \frac{\mu\sigma}{k^2\lambda D^2}\right)^2 > 4/3 \qquad (6.6.11)$$

or

$$\lambda < (\sqrt{3}\,\mu\sigma)/[(2+\sqrt{3})\,k^2D^2] \qquad (6.6.12)$$

That is for fixed λ , μ , σ , D there is a long wave cut off wave number , k_c, such that for $k < k_c$ disturbances are stable. This is directly analogous to Fjortoft's aforementioned results, and illustrates that, due to the fact that the upper surface of the fluid is sloping because of the centrifugal effect, Rossby waves are possible because vortex line stretching permits the vertical component of the fluid vorticity to vary with time.

The Ekman pumping destabilizes those waves which would be stable under the condition (6.6.12) . Thus, that stability condition is not relevant here. A similar effect of the Ekman layer has been found by Holopainen (1961) for baroclinic atmospheric Rossby waves.

Since the experiments show that axisymmetric flow exists if λ is sufficiently small (but finite) we must conclude that the above results do not apply near the stability boundary . We expect that stabilization may result if heat conduction and/or viscous terms should happen to play a role , additional to that of the Ekman pumping condition , in the interior dynamics of the fluid. In order to gain some insight into how this may come about we shall first examine the behaviour of the solutions to (6.6.4) as λ becomes small (with all other parameters fixed). Our purpose in doing this to obtain a relationship between c and λ which we shall subsequently use in determining the order of magnitude of λ in the situation in which heat conduction may be of importance in the fluid interior . This procedure will ensure that the solutions which will subsequently be obtained for the situation in which λ is formally small (how small is yet to be determined) will merge asymptotically with those which have just been obtained (but do

not apply if λ is too small) .

When λ is small there is one root of (6.6.4) which is $O(\lambda)$. We denote this by $c = \lambda c_1$, with

$$c_1 \sim -\frac{D^3\sqrt{2}}{3\sigma} \frac{k\kappa^2[\sqrt{2}\mu k - i\kappa^2]}{2\mu k^2 + \kappa^4} \qquad (6.6.13)$$

This is evidently an approximation to the eigenvalue for the unstable mode. The other root is $O(\lambda^{-1})$, i.e., $c = c_2/\lambda$ with

$$c_2 \sim -\frac{\sigma}{\sqrt{2}k\kappa^2 D}(\sqrt{2}\mu k + i\kappa^2) \qquad (6.6.14)$$

and this corresponds to the damped mode.

We are interested in the behavior of the unstable solutions and this discussion has shown that $c = O(\lambda)$ as λ becomes small for these solutions. We can now use this information to establish the appropriate scaling for small λ .

7. THE DYNAMICS FOR SMALL λ WITH $k = O(1)$

The mechanisms which are available for stabilization of the growing mode for small values of λ are heat conduction and viscous dissipation of perturbation kinetic energy. We would like to isolate that situation in which either or both of these plays a role in the zero-order interior dynamics. To achieve this we assume that

$E^{1/2} << \lambda << 1$ and take $c = \lambda \hat{c}$ with $\hat{c} = O(1)$ in line with the conclusions of our recent discussion. With these assumptions we may again proceed to obtain asymptotic solutions to equations (6.3.3) through (6.3.8). Equations (6.3.9a, b, c) are again true for the zero-order horizontal velocity and pressure fields. Since $\lambda << 1$ the term involving c is absent in equations (6.3.9), (6.3.10) and (6.3.11) i.e.

$$p^{(0)} = z A_0(x) \tag{6.7.1}$$

while (6.3.12) is still correct. Equation (6.3.13) now becomes :

$$\hat{w}_z^{(0)} = -ik\mu A_0 \tag{6.7.2}$$

while the boundary condition at $z = 0$ is that $\hat{w}^{(0)}(0, x) = 0$. (The Ekman pumping vanished because of the functional form (6.7.1) of $p^{(0)}$). Thus

$$\hat{w}^{(0)} = -ik\mu A_0(x) \tag{6.7.3}$$

and this automatically satisfies the upper boundary condition. Thus, in order to determine $A_0(x)$ we must proceed to the next order of approximation.

The terms which are $O(\lambda)$ (in a perturbation expansion in powers of λ) give rise to the following:

$$v^{(1)} = p_x^{(1)} \tag{6.7.4}$$

$$u^{(1)} = -ik\,p^{(1)} \tag{6.7.5}$$

$$p_z^{(1)} = T^{(1)} \tag{6.7.6}$$

$$\hat{w}_z^{(1)} = -ik\mu T^{(1)} + ik\frac{z^2}{\sigma}\,\mathcal{L}A_o \tag{6.7.7}$$

where $\mathcal{L}A_o = d^2A_o/dx^2 - k^2A_o$.

We can find solutions in the following form:

$$p^{(1)} = z\,A_1(x) - \hat{c}\,A_o + \frac{i}{k}\left(\frac{E}{\lambda^2}\right)^{1/2}\mathcal{L}A_o \tag{6.7.9}$$

$$T^{(1)} = A_1(x) \tag{6.7.10}$$

The boundary conditions at $z = 0$ and $z = D$ thus become:

$$\hat{w}^{(1)}(D,x) = -ik\mu\left\{DA_1 - \hat{c}A_o + \frac{i}{k}\left(\frac{E}{\lambda^2}\right)^{1/2}\mathcal{L}A_o\right\} \tag{6.7.11}$$

$$\hat{\omega}^{(1)}(0,x) = \frac{\mathcal{L}}{\sqrt{2}}\left\{ -\hat{c} A_0 + \frac{i}{k}\mathcal{L} A_0 \right\} \qquad (6.7.12)$$

Integrating (6.7.7) between $z = 0$ and $z = D$, making use of these conditions, leads to an equation for A_0:

$$(\mathcal{L} + \sqrt{2}\, i k \mu)(\mathcal{L} A_0 + i k \hat{c} \frac{\lambda^2}{E^{1/2}} A_0)$$

$$+ \frac{\sqrt{2}\, D^3}{3\sigma} \frac{\lambda^2 k^2}{E^{1/2}} \mathcal{L} A_0 = 0 \qquad (6.7.13)$$

We now note that if $\lambda^2 >> E^{1/2}$ this equation becomes, as a first approximation, the same as (6.6.1) for small values of λ (with $c = O(\lambda)$). This is true away from possible boundary layer regions in which $\mathcal{L} A_0 = O(\lambda^2 E^{-1/2})$. However if $\lambda = O(E^{1/4})$ all the terms in (6.7.13) are formally of the same order of magnitude in the interior, that is, heat conduction plays a role, in the interior of the fluid, at the lowest order of approximation. This is the situation which we wished to isolate. Therefore we take $\lambda = \gamma E^{1/4}$ with γ being formally O (1).

Equations (6.7.13) is fourth order in A_0 and therefore sufficient boundary conditions are required in order to obtain a solution. These are obtained by matching to the solutions determined from analysis of the side wall boundary layers. It is shown in the Appendix that the correct boundary conditions are the following:

$$A_o(\pm 1/2) = 0 \qquad (6.7.14)$$

$$\frac{d^2 A_o}{dx^2}(\pm 1/2) = \mp \frac{ik\gamma D^{3/2}}{2^{3/4}} \frac{dA_o}{dx}(\pm 1/2) \qquad (6.7.15)$$

8. SOLUTION OF THE STABILITY PROBLEM

Solutions of (6.7.13) exist in the form $A_o \propto e^{rx}$ with r satisfying the following indicial equation:

$$(r^2-k^2)^2 + \left[ik(\bar{\mu}+\bar{c}) + \sqrt{2}\frac{k^2 D^3 \gamma^2}{3\sigma}\right](r^2-k^2)$$

$$-\bar{\mu}\,\bar{c}\,k^2 = 0 \qquad (6.8.1)$$

where $\bar{\mu} = \sqrt{2}\,\mu$ and $\bar{c} = \gamma^2 \hat{c}$. The roots of this equation are $\pm r_1$, and $\pm r_2$ where r_1 and r_2 are given by:

$$r_1 = \text{P. V. } (k^2 + \kappa_1)^{1/2} \qquad (6.8.2a)$$

$$r_2 = \text{P. V. } (k^2 + \kappa_2)^{1/2} \qquad (6.8.2b)$$

where "P. V." denotes the principal value of the (complex) square roots and

$$(K_1, K_2) = -\frac{1}{2}\left[ik(\bar{\mu}+\bar{c}) + \sqrt{2}\frac{k^2\gamma^2 D^3}{3\sigma}\right] \pm \frac{b}{2} \qquad (6.8.3)$$

$$b = P.V.\left\{\left[ik(\bar{\mu}+\bar{c}) + \sqrt{2}\frac{k^2\gamma^2 D^3}{3\sigma}\right]^2 + 4\bar{\mu}\bar{c}k^2\right\}^{1/2} \qquad (6.8.4)$$

where the negative sign in the second term of (6.8.3) corresponds to K_2.

We consider first the case in which $r_1 \neq r_2$. In this case the boundary conditions (6.6.14) and (6.6.15) permit two types of solutions. One of these is a function which is odd on the interval $-1/2 \leq x \leq 1/2$ but has even first derivatives in that same interval. The other type is even with odd first derivatives. We shall consider each of these in turn.

(i) The Odd Modes

In this case we take a solution of the form

$$A_o = a_1 \sinh r_1 x + b_1 \sinh r_2 x \qquad (6.8.5)$$

Then the boundary conditions (for <u>both</u> boundaries) require the following to be true:

$$a_1 \sinh r_1/2 + b_1 \sinh r_2/2 \qquad (6.8.6)$$

$$a_1\left\{r_1^2 \sinh r_1/2 + \frac{i k \gamma D^{3/2}}{2^{3/4}} r_1 \cosh r_1/2\right\}$$

$$+ b_1\left\{r_2^2 \sinh r_2/2 + \frac{i k \gamma D^{3/2}}{2^{3/4}} r_2 \cosh r_2/2\right\} = 0 \qquad (6.8.7)$$

The requirement that the determinant of the coefficients of a_1 and b_1 shall vanish leads to the following characteristic equation:

$$(r_2^2 - r_1^2) \sinh \frac{r_2}{2} \sinh \frac{r_1}{2} +$$

$$+ \frac{i k \gamma D^{3/2}}{2^{3/4}}\left[r_2 \cosh \frac{r_2}{2} \sinh \frac{r_1}{2} - r_1 \cosh \frac{r_1}{2} \sinh \frac{r_2}{2}\right] = 0 \qquad (6.8.8)$$

The quantity which we want to determine from (6.8.8) is the value of $\bar{c}$ when all the other parameters of the problem are specified. Equation (6.8.8) is transcendental in $\bar{c}$ and must be solved numerically. In order to do this we must know the solution for at least one particular parameter specification. The case $\gamma = 0$ can be solved and is ideal for this purpose. When $\gamma = 0$ we have:

$$\kappa_1 = -i k c \qquad (6.8.9)$$

$$\kappa_2 = -i k \bar{\mu} \qquad (6.8.10)$$

$$r_1 = (k^2 - ik\bar{c})^{1/2} \qquad (6.8.11)$$

$$r_2 = (k^2 - ik\bar{\mu})^{1/2} \qquad (6.8.12)$$

Assuming that $r_1 \neq r_2$ equation (6.8.8) reduces to

$$\sinh \frac{r_1}{2} \sinh \frac{r_2}{2} = 0 \qquad (6.8.13)$$

For real values of $\bar{\mu}$ the only acceptable solution is

$$r_1 = 2 i n \pi \quad ; \quad n = 0, 1, 2, \ldots \qquad (6.8.14)$$

whence

$$\bar{c} = - i (k^2 + 4 n^2 \pi^2) / k \qquad (6.8.15)$$

The case n= 0 corresponds to the trivial solution so that the least stable mode is the gravest one (n = 1) .

(ii) The Even Modes

The even modes correspond to a solution of the form

$$A_o = a_2 \cosh r_1 x + b_2 \cosh r_2 x \qquad (6.8.16)$$

Application of the boundary conditions leads to the characteristic equation for this case:

$$(r_2^2 - r_1^2)\cosh\frac{r_1}{2}\cosh\frac{r_2}{2} + \frac{ikrD^{3/2}}{2^{3/4}}\left[r_2\sinh\frac{r_2}{2}\cosh\frac{r_1}{2} - r_1\sinh\frac{r_1}{2}\cosh\frac{r_2}{2}\right] = 0 \qquad (6.8.17)$$

when $\gamma = 0$ this is solved by :

$$r_1 = (2n+1)i\pi \quad ; \quad n = 0, 1, 2\ldots \qquad (6.8.18)$$

$$\bar{c} = -i\left[k^2 + (2n+1)^2\pi^2\right] / k \qquad (6.8.19)$$

The gravest mode (n = 0) is less stable that corresponding to the odd solutions. This would suggest that the even modes may become unstable, as γ is increased, before the odd ones do. The numerical results verify this conclusion and we will not , therefore, concern ourselves further with the odd modes.

(iii) Equal Roots

We now consider the case $r_1 = r_2 = r$. In this case we must have $\kappa_1 = \kappa_2$ and equation (6.8.3) then shows that b = 0. This in turn implies that

$$\bar{c} = \left[\bar{\mu} + \sqrt{2}\, i \frac{k^2 \gamma^2 D^3}{3\sigma}\right] \pm \left[4\sqrt{2}\, i k \bar{\mu} \frac{D^3 \gamma^2}{3\sigma}\right]^{1/2} \qquad (6.8.20)$$

The solutions are now given by the following:

Odd Modes: $A_0 = a_1 \sinh rx + b_1 x \cosh rx$ (6.8.21a)

Even Modes: $A_0 = a_2 \cosh rx + b_2 x \sinh rx$ (6.8.21b)

The characteristic equations corresponding to these are the following:

Odd Modes: $r(\cosh r - 1) + \frac{i k \gamma D^{3/2}}{2^{7/4}} (\sinh r - r) = 0$ (6.8.22a)

Even Modes: $r(\cosh r + 1) + \frac{i k \gamma D^{3/2}}{2^{7/4}} (\sinh r + r) = 0$ (6.8.22b)

These must be satisfied subject to the constraint on $\bar{c}$ given by (6.8.20). Since this defines r in terms of the specified parameters it is clear that either or both of the equations (6.8.22) can not be satisfied for arbitrary values of these parameters. Moreover, in the limit $\gamma \to 0$ there are no solutions, for real $\bar{\mu}$, which satisfy all of the constraints. Also, when $\bar{\mu} = 0$, $r = k$ and there are no solutions for real values of γ. It can be verified by direct calculation that this is also true if $\bar{\mu} > 0$ and in the range of interest to us here. We conclude that there are no relevant solutions such that $r_1 = r_2$.

9. NUMERICAL SOLUTIONS OF THE CHARACTERISTIC EQUATION AND RESULTS

The characteristic equation (6.8.19) for the even modes is of the general form

$$\mathcal{F}(\bar{c}; \bar{\mu}, \gamma, k, D, \sigma) = 0 \qquad (6.9.1)$$

We must solve this for $\bar{c}$ when the physical parameters ($\bar{\mu}$, γ, k, D, r) are specified. As shown above solutions can be found analytically when $\gamma = 0$. Then, for small values of γ these solutions can be used as a basis for Newton's method. The simplest form of this involves computing the limit of the sequence

$$\bar{c}_{j+1} = \bar{c}_j - \mathcal{F}(\bar{c}_j) \Big/ \frac{\partial \mathcal{F}}{\partial \bar{c}}(\bar{c}_j) \qquad (6.9.2)$$

(We have suppressed the other arguments of $\mathcal{F}$ for notational convenience).

The numerical procedure involves first setting γ equal to a small positive number (in practice we started with $\gamma = 0.1$) and using the value of $\bar{c}$ for $\gamma = 0$ as the starting member of the sequence (6.9.2). If the sequence converges the limiting value is the required solution. Once this has been found γ is incremented again by a small amount and the value of $\bar{c}$ just found is used to start the sequence for this new value of γ. The calculations are continued in

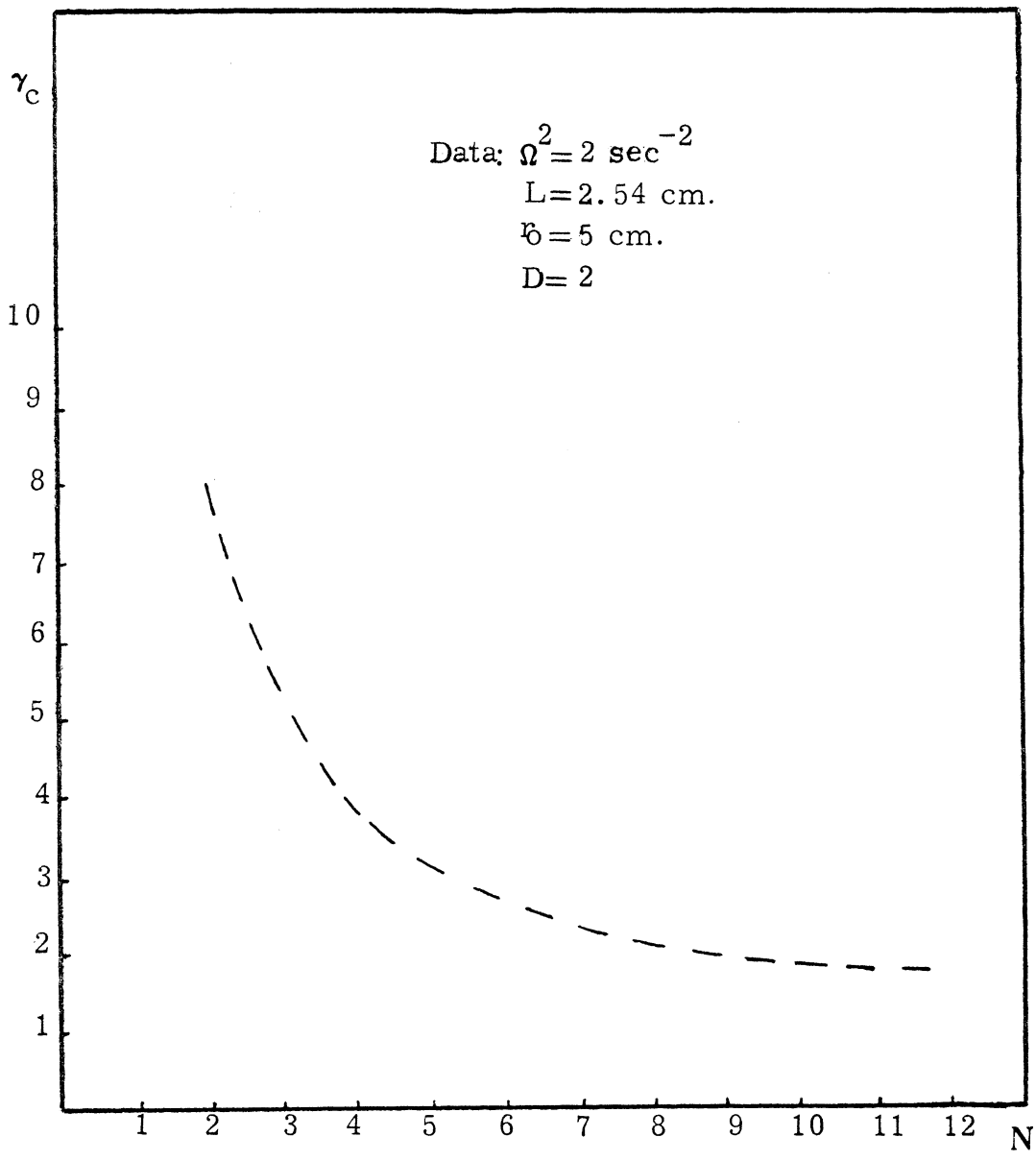

Figure 6.1. The behavior of γ_c as a function of wave number from the low wave number results. Data: L = 2.54 cm., r_o = 5 cm., D = 2, σ = 7.19, ν = 1.01 x 10^{-2}cm^{2}sec^{-1}.

this manner until $\gamma > \gamma_c$ where γ_c is that value of γ such that $\mathrm{Im}(\bar{c}) = 0$. In practice we always used an increment of 0.1 for γ. Convergence was very rapid in all cases.

Some results are shown in figures 6.1 and 6.2. The first of these (Fig. 6.1) illustrates the behavior of γ_c as a function of wave number.* This figure illustrates a point mentioned earlier, i.e., that γ_c approaches limiting minimum only as the wave number becomes indefinitely large. This behaviour is at variance with experimental results which indicate that the lower transition occurs for finite values of the wave number and, moreover, that the transition wave number varies slowly.

Figure 6.2 illustrates the behavior of γ_c as a function of Ω^2 (note that the Taylor number is proportional to Ω^2/ν^2) for wave number $N = 8$. There is a tendency for γ_c to increase as Ω^2 becomes large due to the effect of the centrifugal force. This feature becomes very pronounced for $\Omega^2 > 10$. However, for $\Omega^2 \leq 10$, γ_c is almost independent of the rotation rate.** This means that the thermal Rossby number at the transition varies as $E^{3/4}$ ($R_{oc} = \gamma_c E^{3/4}/\sigma$) or, as $T_a^{-3/8}$. The experiments indicate that $R_{oc} \propto T_a^{-.86}$ approximately (see Fowlis and Hide (1965)) so that the observed "slope" of the lower transition curve on a R_o vs. T_a diagram is significantly

---

* Note that the actual wave number, N, the number of troughs and ridges in one mean annular circumference, is plotted. The wave number used in our analysis is given by $k = N L/r_o$.

** If the centrifugal effects had been neglected, i.e. $\mu \equiv 0$, γ_c would be strictly independent of Ω.

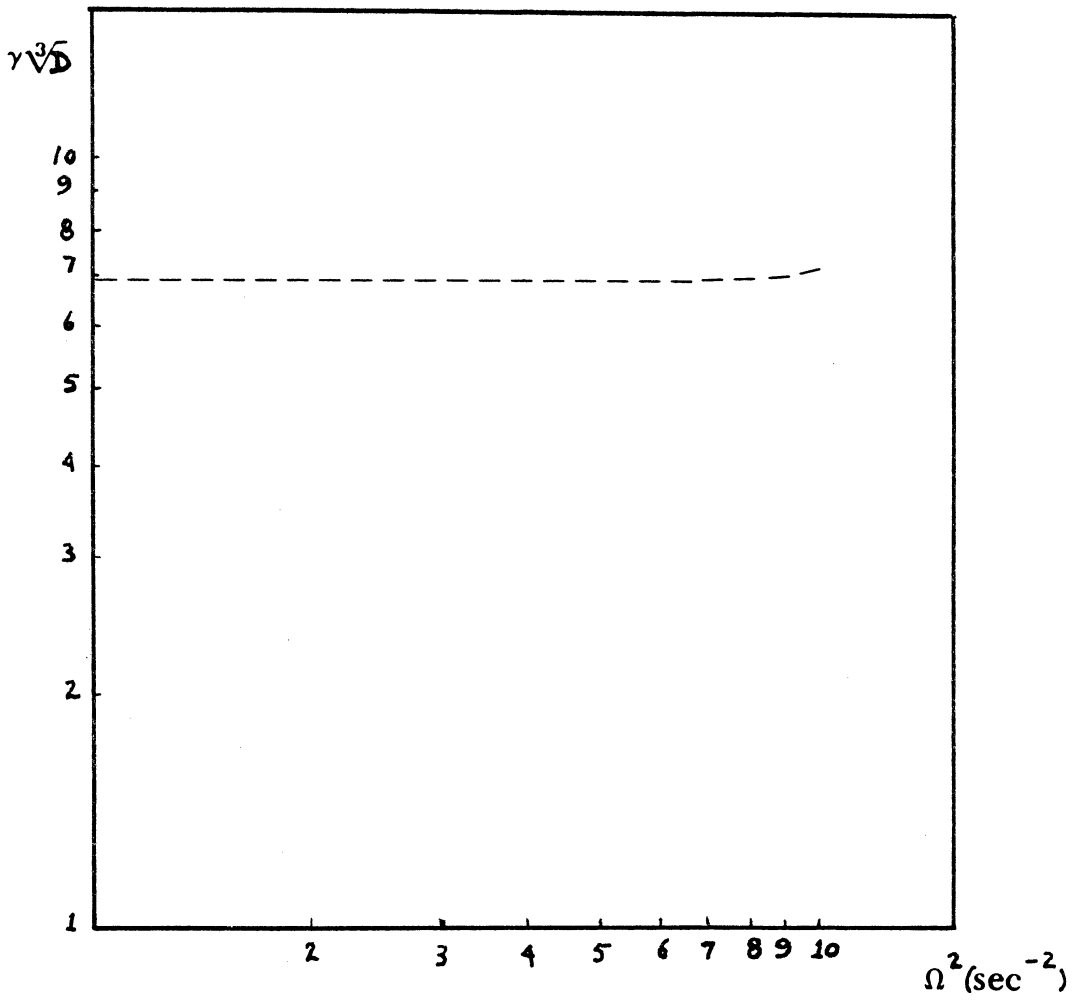

Figure 6.2. The behavior of γ_c as a function of the rotation rate. Other data as in Figure 6.1.

steeper than our predicted one.

Finally, in Figure 6.3, we have plotted transition curves for several wave numbers in terms of $R_0\sigma$ in order to facilitate comparison with experimental results. These curves illustrate further the points mentioned above.

These results illustrate the deficiencies of the theory presented in this chapter. The main difficulty here is that the theory is not valid as the wave number becomes too large. For instance, for the physical parameters used in plotting Figure 6.1, $k E^{1/4} \simeq 0.6$ when $N = 8$ and 0.9 when $N = 12$. Thus some of the terms which have been neglected in the analysis of this chapter are in fact not negligible, when compared with those which have been retained, if k is sufficiently large. This leads us to consider what modifications must be made to account for this situation.

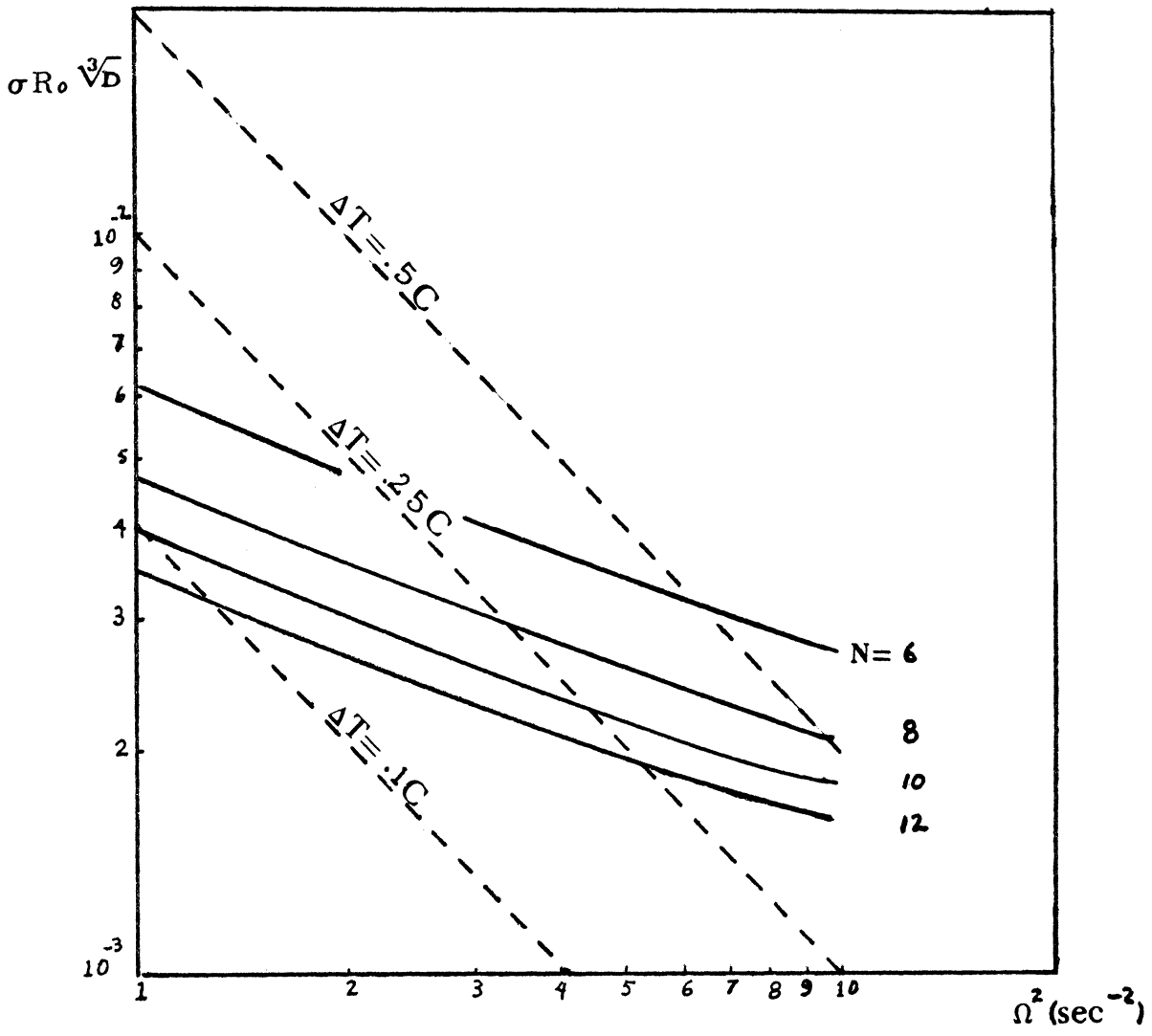

Figure 6.3. Transition curves from the low wave number analysis. Other data as in Figure 6.1.

CHAPTER VII

STABILITY ANALYSIS FOR INTERMEDIATE AND HIGH WAVE NUMBERS

1. THE LIMITING BEHAVIOR OF THE LOW WAVE NUMBER SOLUTIONS : DEVELOPMENT OF A "THERMAL" BOUNDARY LAYER

Before proceeding directly to a discussion of the modifications which must be made to our previous analysis when k becomes large it is of interest to explore the asymptotic behavior of the solutions for the low wave number analysis under these circumstances. Equations (6.7.13), (6.7.15) may be written in the following form:

$$\left(k^{-2}\frac{d^2}{dx^2} - 1 + i\mu k^{-1}\right)\left(k^{-2}\frac{d^2A}{dx^2} + (i\bar{c}-1)A\right)$$

$$+ \sqrt{2}\,\frac{D^3\gamma^2}{3\sigma}\left(k^{-2}\frac{d^2A}{dx^2} - A\right) = 0 \qquad (6.7.13a)$$

$$A\left(\pm 1/2\right) = 0 \qquad (6.7.14a)$$

$$k^{-1}\frac{d^2A}{dx^2}\left(\pm\tfrac{1}{2}\right) = \mp\, i\gamma\frac{D^{3/2}}{2^{3/4}}\frac{dA}{dx}\left(\pm 1/2\right) \qquad (6.7.15a)$$

where $\bar{c} = \gamma^2 \hat{c}\, k^{-1}$.

A rational approximation scheme for large k involves

expansion in powers of k^{-1} . However this involves loss of the most highly differentiated terms in (6. 7. 13a) and (6. 7. 15a). Consequently it will not be possible to satisfy both of the sets of boundary conditions (6. 7. 14a) and (6. 7. 15a) for the lowest order determination of A . Thus we must expect boundary layers near $x = \pm 1/2$. The non-dimensional thickness of these boundary layers is $O(k^{-1})$ and therefore if $k = O(E^{-1/4})$ they merge with the outer Stewartson layers. However , if $1 \ll k \ll E^{-1/4}$ they are thicker than the outer Stewartson layers and the analysis in the Appendix indicates that the boundary conditions (6. 7. 14) and (6. 7. 15) are still compatible with matching to the Stewartson layer solutions with errors, however, which are $O(k E^{1/4})$. We shall proceed on the assumption that $k \ll E^{-1/4}$.

Considering first the solutions for the interior, away from the boundary layers , the lowest approximation is the following:

$$\left(i \bar{c}_0 - 1 + \sqrt{2}\, \frac{\gamma^2 D^3}{3\sigma} \right) A_0 = 0 \qquad (7.1.1)$$

If A_0 is non trivial the quantity in square brackets must vanish and this shows that the first approximation to the stability boundary is such that

$$\gamma_0^2 = 3\sigma / \sqrt{2}\, D^3 \qquad (7.1.2)$$

and this , of course, implies that $\bar{c}_0 = 0$. At higher orders of approximation the stability boundary is not given by (7.1.2) and we therefore regard this as the first erm of an approximation in which

we shall determine corrections to γ_0 in powers of k^{-1}. These corrections are to be chosen at each order in such a way as to ensure that $\mathrm{Im}(\bar{c}) = 0$ for all orders of approximation. Thus we write :

$$(A, \bar{c}, \gamma_c) = (A_0, \bar{c}_0, \gamma_0) + \sum_{j=1}^{\infty} k^{-j} (A_j, \bar{c}_j, \gamma_j) \qquad (7.1.3)$$

where γ_c is such that $\mathrm{Im}(\bar{c}) = 0$ and therefore, at each stage, γ_j is such that $\mathrm{Im}(\bar{c}_j) = 0$.

The leading terms in this approximation scheme give rise to (7.1.1) and (7.1.2). The $O(k^{-1})$ approximations leads to the following :

$$\left[-(\bar{\mu} + \bar{c}_1) - 2\sqrt{2}\, \frac{\gamma_0 \gamma_1 D^3}{3\sigma} \right] A_0 = 0 \qquad (7.1.4)$$

The bracketed terms must vanish and therefore we choose

$$\gamma_1 = 0 \qquad (7.1.5)$$

$$\bar{c}_1 = -\bar{\mu} \qquad (7.1.6)$$

The $O(k^{-2})$ terms lead to a determination of A_0. Using the above results we get the following :

$$\frac{d^2 A_0}{dx^2} + \left(i\bar{c}_2 - 2\bar{\mu}^2 + 2\sqrt{2}\, \frac{\gamma_0 \gamma_2 D^3}{3\sigma} \right) A_0 = 0 \qquad (7.1.7)$$

In order to solve this equation we must determine the boundary conditions for A_o. This requires examination of the boundary layers mentioned above. We shall consider the one near $x = -1/2$. The lowest order boundary layer equations are (bearing in mind that $\bar{c}_o = 0$ and γ_o is given by (7.1.2) the following:

$$\frac{d^2}{d\rho^2}\left(\frac{d^2A}{d\rho^2} - A\right) = 0 \qquad (7.1.8)$$

$$A(0) = 0 \qquad (7.1.9)$$

$$\frac{d^2A}{d\rho^2}(0) = \frac{i\gamma_o D^{3/2}}{2^{3/4}}\frac{dA}{d\rho}(0) \qquad (7.1.10)$$

where $\rho = k(x + 1/2)$ is the boundary layer coordinate.

In order to facilitate matching to the solution outside the boundary layer we take A to be of the following form:

$$A \sim k^{-1} b_o \left\{\rho - \frac{i\gamma_o D^{3/2}}{2^{3/4} + i\gamma_o D^{3/2}}(1 - e^{-\rho})\right\} \qquad (7.1.11)$$

It can be verified that this solution satisfies the boundary conditions (7.1.9) and (7.1.10). Matching to the solution outside the boundary layer is accomplished if

$$A_o(-1/2) = 0 \qquad (7.1.12)$$

$$b_0 = \frac{dA_0}{dx}(-1/2) \qquad (7.1.13)$$

and therefore

$$A_1(-1/2) = -\frac{i\gamma_0 D^{3/2}}{2^{3/4} + i\gamma_0 D^{3/2}} \frac{dA_0}{dx}(-1/2) \qquad (7.1.14)$$

A similar analysis of the boundary layer near $x = 1/2$ will show that

$$A_0(1/2) = 0 \qquad (7.1.15)$$

$$A_1(1/2) = \frac{+i\gamma_0 D^{3/2}}{2^{3/4} + i\gamma_0 D^{3/2}} \frac{dA_0}{dx}(1/2) \qquad (7.1.16)$$

Equations (7.1.12) and (7.1.15) are the required boundary conditions for $A_0(x)$ while (7.1.14) and (7.1.15) are those for $A_1(x)$.

The solution of (7.1.7) which satisfies the boundary conditions is of the form

$$A_0 = \text{const.} \sin m\pi(x-1/2) \; ; \; m = \pm 1, \pm 2, \ldots \qquad (7.1.7)$$

provided that

$$\bar{c}_2 = 0 \qquad (7.1.18)$$

$$\gamma_2 = \frac{3\sigma}{2\sqrt{2}\,\gamma_0 D^3}\,(m^2\pi^2 + 2\bar{\mu}^2) \qquad (7.1.19)$$

Obviously the minimum value of γ_2 is for the gravest non-trivial mode (m=1) . Thus we have shown that

$$\gamma_c \sim \gamma_0\left[1 + \tfrac{1}{2}(\pi^2 + 2\bar{\mu}^2)/k^2\right] + O(k^{-3}) \qquad (7.1.20)$$

We shall not proceed to the $O(k^{-3})$ approximation since (7.1.20) is sufficient for our purpose.

2. HIGH WAVE NUMBERS: THE LOWEST ORDER CHARACTERISTIC EQUATIONS

We shall now carry out a brief analysis of the situation in which $k = O(E^{-1/4})$. Our purpose in doing this is to show that , for these large values of k, γ_c is an increasing function of k , in contrast to the behavior exhibited in (7.1.20) . We anticipate that there is an intermediate range where , say , $k = \delta E^{-\alpha}$ and $\delta = O(1)$, $0 < \alpha < 1/4$, such that for some value δ_c, γ_c behaves asymptotically as (7.1.20) for $\delta < \delta_c$ and as the high wave number expansion (to be found here) when $\delta > \delta_c$. We will determine α by comparing the low and high wave number expansions "asymptotically". These ideas will be made more precise as we proceed.

We begin by taking $k_* = k E^{1/4} = O(1)$, $\lambda = \gamma E^{1/4}$. We refer back to equations (6.3.3) through (6.3.8) . A comparison of terms in these equations will show that the following re-scaling of

dependent variables is appropriate to this situation:

$$P = \frac{E^{1/4}}{k_*} \bar{P} \tag{7.2.1a}$$

$$v = \frac{E^{1/4}}{k_*} \bar{v} \tag{7.2.1b}$$

$$T = \frac{E^{1/4}}{k_*} \bar{T} \tag{7.2.1c}$$

$$\hat{\omega} = \frac{k_*}{E^{1/4}} \bar{\omega} \tag{7.2.1d}$$

where ($\bar{p}$, $\bar{v}$, $\bar{T}$, $\bar{\omega}$) are all formally O (1) and u is left unchanged from its original scaling.

On substituting the quantities (7.2.1) into (6.3.6) through (6.3.8) we obtain the following lowest order approximations:

$$\bar{v}^{(0)} = \bar{P}_x^{(0)} \tag{7.2.2}$$

$$u^{(0)} = -i \bar{P}^{(0)} \tag{7.2.3}$$

$$\bar{P}_z^{(0)} = \bar{T}^{(0)} \tag{7.2.4}$$

$$\bar{\omega}_z^{(0)} = \frac{\gamma k_*}{\sigma} \left(z - c - \frac{i\sigma}{\gamma} k_* \right) u^{(0)} \tag{7.2.5}$$

$$\gamma\left[i\left(z-c-i\frac{k_*}{\gamma}\right)\bar{T}^{(0)}+u^{(0)}\right]=0 \qquad (7.2.6)$$

The upper and lower boundary conditions on $\bar{w}^{(0)}$ can be shown by Ekman layer analysis * to be :

$$\bar{w}^{(0)}(D,x)=0 \qquad (7.2.7)$$

$$\bar{w}^{(0)}(0,x)=-\frac{1}{\sqrt{2}}\,\bar{p}^{(0)}(0,x) \qquad (7.2.8)$$

Equations (7.2.2), (7.2.3), (7.2.4), and (7.2.6) are solved by taking

$$\bar{p}^{(0)}=\left(z-c-i\frac{k_*}{\gamma}\right)A_0(x) \qquad (7.2.9)$$

where $A_0(x)$ has yet to be determined.

Substituting (7.2.9) into (7.2.5) and integrating between $z = 0$ and $z = D$ using (7.2.7) and (7.2.8) shows that :

---

* Note that an intervening boundary layer analysis is needed, as in the low wave number case, in order to verify the validity of (7.2.8).

$$\left\{ \bar{c}^2 + \frac{\gamma}{k_*}\left[D - \frac{i k_*}{\gamma}(\sigma+1) + \frac{i\sigma}{\sqrt{2}\,D\gamma k_*} \right] \bar{c} \right.$$

$$\left. - \left[\frac{\sigma}{\sqrt{2}\,D k_*^2}\left(1 - \sqrt{2}\,\frac{\gamma^2 D^3}{3\sigma}\right) + i\,\frac{D(\sigma+1)}{2}\,\frac{\gamma}{k_*} \right.\right.$$

$$\left.\left. + \sigma \right] \right\} A_0 = 0 \qquad (7.2.10)$$

where $\bar{c} = \gamma c / k_*$.

If A_0 is to be non-trivial the quantity in curly brackets must vanish and this provides the zero-order characteristic equation. As in the previous section, A_0 must be determined by proceeding to higher orders of approximation. However, our main purpose here is to explore the solutions of the lowest order characteristic equation and therefore we will not proceed beyond this point.

The characteristic equation is easily solved for $\bar{c}$ and the value γ_c such that $\mathrm{Im}(\bar{c}) = 0$ is obtained by calculation of the roots. Figure 7.1 illustrates the behavior of γ_c for both the "low" and "high" wave number analyses. Neither of these analyses is valid at the point of intersection of the two γ_c curves in the diagram, the low wave number analysis being asymptotically valid to the left of this point and the high wave number analysis to the right of it. However the magnitude of k at the point of intersection should indicate the appropriate intermediate wave number scaling. In order to make this

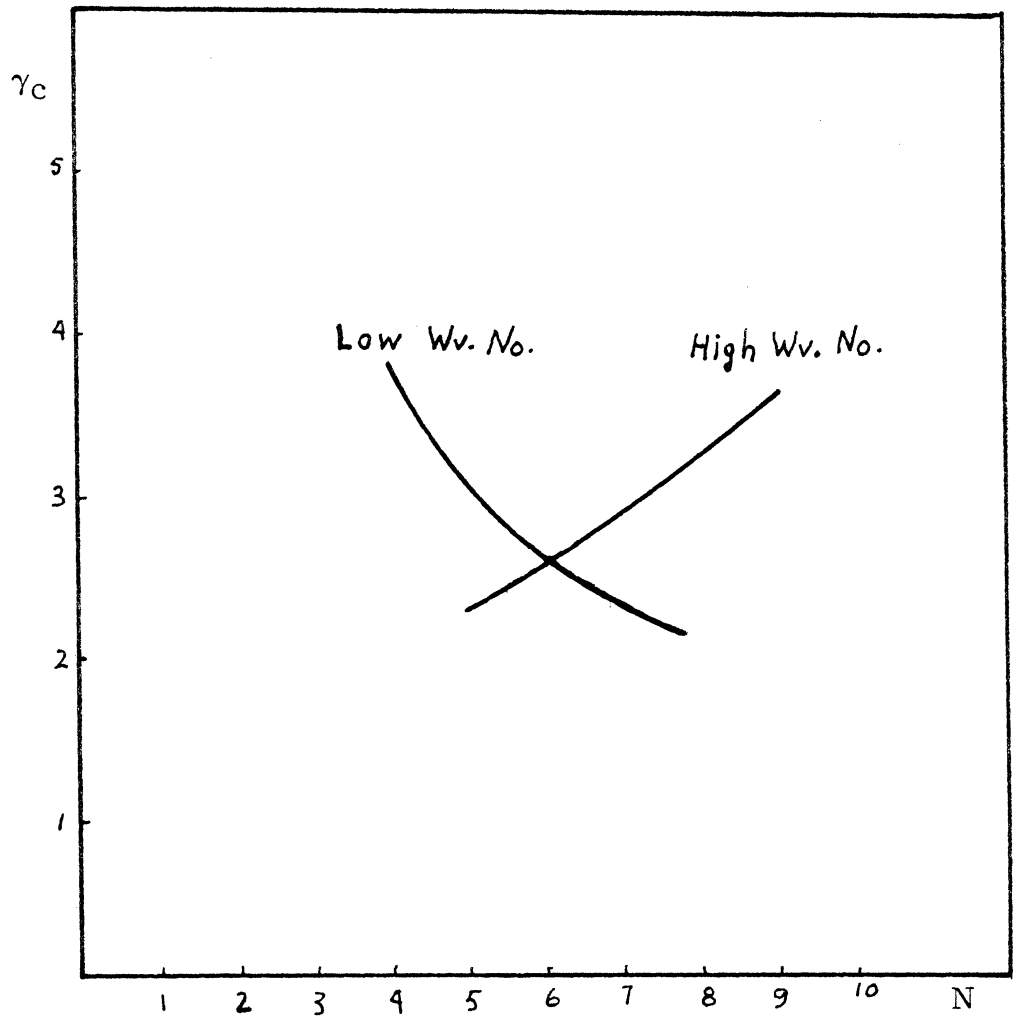

Figure 7.1. Comparison of the low and high wave number curves for γ_c as a function of wave number. Other data as in Figure 6.1.

more precise we consider the behavior of the solutions to the characteristic equation (7.2.10) when k_* is small (but greater than $O(E^{1/4})$) .

When k_* is small one of the roots of (7.2.10) is $O(1)$ while the other is $O(k_*^{-2})$. This latter root corresponds to a solution which decays with time (stable) . The other root corresponds to a solution which can become unstable . We shall proceed, as in Section 7.1 , in such a way as to determine an approximation to the stability boundary for this case. The appropriate expansion parameter is k_* and therefore we take:

$$\bar{c} = \bar{c}_o + k_* \bar{c}_1 + \ldots \qquad (7.2.11)$$

$$\gamma_c = \gamma_o + k_* \gamma_1 + \ldots \qquad (7.2.12)$$

where , as before, $(\gamma_o , \gamma_1 , \ldots)$ are chosen so that $\mathrm{Im}(\bar{c}_o , \bar{c}_1 , \ldots) = 0$. The first three terms in this scheme lead to the following :

$$\bar{c}_o = 0 \qquad (7.2.13a)$$

$$\gamma_o^2 = 3\sigma / \sqrt{2}\, D^3 \qquad (7.2.13b)$$

$$\gamma_1 = 0 \qquad (7.2.14a)$$

$$\bar{c}_1 = D^2 (\sigma + 1) \quad / \sqrt{2}\,\sigma \qquad (7.2.14b)$$

$$\gamma_1 = \gamma_0 \, D (3 + 5\sigma) / 2\sqrt{2}\,\sigma \qquad (7.2.15)$$

Thus we have

$$\gamma_c \sim \gamma_0 \left[1 + k_*^2 \, \frac{D(3+5\sigma)}{2\sqrt{2}\,\sigma} \right] \qquad (7.2.16)$$

It is interesting to note that the limiting minimum value of this expression, γ_0 , is the same as that obtained from (7.1.20). That expression is comparable in magnitude to (7.2.16) when $k^{-2} = O(k^2 E^{1/2})$, or , $k = O(E^{-1/8})$. In that case the error in both expressions is formally $O(E^{3/8})$. Thus we have that $\alpha = 1/8$, i.e., the intermediate wave number scaling is $k = \delta E^{-1/8}$, $\delta = O(1)$.

3. INTERMEDIATE WAVE NUMBERS: THE GOVERNING EQUATIONS

Having found the scaling which is appropriate for intermediate wave numbers we may now proceed to analyse this situation formally. In doing so we can make use of some of the features of the high and low wave number expansions. Firstly we re-scale u , p , and T as follows

$$(u, p, T) = (\hat{u}, \hat{p}, \hat{T}) \, E^{1/8} / \delta \qquad (7.3.1)$$

This is similar to the high wave number scaling. We do not re-scale $\hat{w}$ since subsequent analysis will show that it is not necessary to do so . Now the low wave number analysis showed that:

$$c = \frac{kE^{1/4}}{\gamma^2}\,\bar{c} = O(E^{1/4}/\gamma^2)$$

so that $c = O(E^{1/4})$. The high wave number analysis showed that $c = k_* \bar{c}\,/\gamma \propto k_*^2 = O(E^{1/4})$ when $k_* = \delta E^{1/8}$, $\delta = O(1)$.

Thus it seems appropriate to take $c = E^{1/4}\hat{c}$, $\hat{c} = O(1)$. As before we take $\lambda = \gamma E^{1/4}$, $\gamma = O(1)$. When these quantities are inserted into equations (6. 3. 3) to (6. 3. 8) we obtain the following governing equations:

$$\hat{v} = \hat{p}_x + O(E^{1/2}) \tag{7. 3. 2}$$

$$u = -i\hat{p} + O(E^{3/4}) \tag{7. 3. 3}$$

$$\hat{p}_z = \hat{T} + O(E^{3/4}) \tag{7. 3. 4}$$

$$\hat{\omega}_z = -i\mu\hat{T} + i\frac{\delta^2\gamma}{\sigma}\left[(z - E^{1/4}\hat{c})\left(\frac{E^{1/4}}{\delta^2}\hat{v}_x - iu\right)\right]$$

$$- \delta^3 E^{1/8}\left[\frac{E^{1/4}}{\delta^2}\left(\frac{\partial^2}{\partial x^2} + \frac{\partial^2}{\partial z^2}\right) - 1\right]\left[\frac{E^{1/4}}{\delta^2}\hat{v}_x\right.$$

$$\left. - iu\right] + O(E^{1/2}) \tag{7. 3. 5}$$

$$\gamma\left[\lambda(z-E^{1/4}\hat{c})\hat{T}+u+E^{1/2}(\lambda V\hat{T}+T_x u)\right]$$

$$=\delta E^{1/8}\left[\frac{E^{1/4}}{\delta^2}\left(\frac{\partial^2}{\partial x^2}+\frac{\partial^2}{\partial z^2}\right)\hat{T}-\hat{T}\right] \qquad (7.3.6)$$

Ekman layer analysis shows that

$$\hat{w}(D,x)=\mu u(D,x)-E^{3/8}\delta\left[\frac{E^{1/4}}{\delta^2}\hat{T}_{xx}-\hat{T}\right]$$

$$+O(E^{1/2}) \qquad (7.3.7)$$

$$\frac{\partial\hat{T}}{\partial z}(D,x)=0+O(E^{1/2})$$

$$\hat{w}(0,x)=\frac{\delta}{\sqrt{2}E^{1/8}}\left[\frac{E^{1/4}}{\delta^2}\hat{P}_{xx}-\hat{P}\right]+O(E^{1/2}) \qquad (7.3.8)$$

$$\frac{\partial\hat{T}}{\partial z}(0,x)=-\frac{\gamma\delta}{\sqrt{2}}E^{1/8}\left[\frac{E^{1/8}}{\delta}\hat{P}_x-\lambda\hat{P}\right] \qquad (7.3.9)$$

Equation (7.3.9) can, again, only be satisfied via an intermediate boundary layer analysis which connects the Ekman layer near $z = 0$ to the interior. It is appropriate at this stage to sketch

briefly this intermediate boundary layer analysis. The appropriate boundary layer variable in this case is $\eta = z / E^{1/8}$. Using this and the following scaling of dependent variables:

$$(u, v, w, p, T) =$$

$$\left(E^{1/8}\tilde{u},\ \frac{E^{1/4}}{\delta}\tilde{v},\ \delta E^{1/2}\tilde{w},\ \frac{E^{1/4}}{\delta}\tilde{p},\ \frac{E^{1/4}}{\delta}\tilde{T}\right) \qquad (7.3.10)$$

leads to the following governing equations and boundary conditions, correct to $O(E^{3/8})$:

$$\tilde{v} = \tilde{p}_x + \mu E^{3/8}\tilde{T} \qquad (7.3.11)$$

$$\tilde{u} = -i\tilde{p} \qquad (7.3.12)$$

$$\tilde{p}_\eta = \tilde{T} \qquad (7.3.13)$$

$$\tilde{w}_\eta = \frac{E^{1/8}}{\delta}\left\{-i\mu\tilde{T} - \delta E^{1/4}\left[\frac{\partial^2}{\partial\eta^2} - \delta(\delta + \frac{i\gamma}{\sigma}(\eta - E^{1/8}\hat{c}))\right]\tilde{p}\right. \qquad (7.3.14)$$

$$\tilde{P}_{\eta\eta\eta} - i\delta\gamma\left[(\eta - E^{1/8}\hat{c}) - \frac{i\delta}{\gamma}\right]\tilde{P}_{\eta} + i\delta\gamma\tilde{P}$$

$$= E^{1/4}\left[\tilde{P}_{\eta xx} + i\delta\gamma E^{1/8} V(0)\tilde{P}_{\eta}\right] \qquad (7.3.15)$$

$$\tilde{\omega}(0,x) = \frac{1}{\sqrt{2}}\,\mathcal{L}\,\tilde{p}(0,x) \qquad (7.3.16)$$

$$\tilde{P}_{\eta\eta}(0,x) = -\frac{\gamma\delta}{\sqrt{2}}\,E^{3/8}\left(\frac{E^{1/8}}{\delta}\,\tilde{P}_x - i\,\tilde{P}\right)(0,x) \qquad (7.3.17)$$

where $\mathcal{L} = E^{1/4}\,\delta^{-2}\,\partial^2/\partial x^2 - 1$.

A solution , correct to $O(E^{3/8})$ can be found in the form

$$\tilde{p} = (\eta - E^{1/8}\hat{c})\,A(x) + \frac{i\delta}{\gamma}\,\mathcal{L}\,A(x)$$

$$+ E^{3/8}\left[\frac{\delta^2}{\sqrt{2}}\,\chi(\eta)/\frac{d^2\chi(0)}{d\eta^2} + V(0)\right]A(x) \qquad (7.3.18)$$

where

$$\chi(\eta) = (\eta - \tfrac{i\delta}{\gamma}) \int_{\eta}^{\infty} \frac{1}{(\eta' - \tfrac{i\delta}{\gamma})} H_{2/3}^{(1)}(y)\, d\eta'$$

$$(-\pi/2 \leq \arg(\eta - i\delta/\gamma) \leq \pi/6) \quad (7.3.19)$$

and

$$y = \frac{2i}{3} (i\delta\gamma)^{1/2} (\eta' - i\delta/\gamma)^{3/2} \quad (7.3.20)$$

and $H_{2/3}^{(1)}(y)$ is the Hankel function of the first kind of order $2/3$, the arguments of $(\eta - i\delta/\gamma)$ having been chosen to ensure the appropriate exponentially decreasing behavior for large positive η. It should be noted that $\chi(\eta)$ as given by (7.3.19) is a solution of

$$\chi_{\eta\eta\eta} - i\delta\gamma(\eta - i\delta/\gamma)\chi_{\eta} + i\delta\gamma\chi = 0$$

the other independent solution which we have used being simply given by the linear quantity $\eta - i\delta/\gamma$. The third independent solution of this equation involves the Hankel function of the second kind. However this solution can not be used because it does not have the appropriate behavior for large positive values of η.

The solution (7.3.18) satisfies the boundary condition (7.3.17). We now obtain from equation (7.3.14) the following:

$$\tilde{w} = \tilde{w}(0,X) + \frac{E^{1/8}}{\delta}\left\{-i\mu\eta A + \frac{\delta^2\gamma E^{1/4}}{\sigma}\left[\frac{\eta^3}{3} - \frac{i\delta}{2\gamma}(\sigma+1)\eta^2 - \frac{\delta^2\sigma}{\gamma}\eta\right]A\right\} + O(E^{1/2}) \qquad (7.3.21)$$

where

$$\tilde{w}(0,X) = -\frac{1}{\sqrt{2}}\left\{\left(\frac{i\delta}{\gamma} + E^{1/8}\hat{c}\right)\mathcal{L}A - \frac{iE^{1/4}}{\delta\gamma}\frac{d^2A}{dX^2}\right\} - E^{3/8}\left\{\frac{\delta^2}{2}\frac{\chi(0)}{\chi''(0)} + \frac{V(0)}{\sqrt{2}}\right\}A + O(E^{1/2}) \qquad (7.3.22)$$

Equation (7.3.22) is the Ekman pumping condition modified by the effects of the intervening boundary layer. We shall show shortly that the interior solutions match to those obtained above if this condition is satisfied by the interior vertical velocity, i.e.,

$$\hat{w}(0,X) = \frac{\delta}{\sqrt{2}}\left\{\left(\frac{i\delta}{\gamma} + E^{1/8}\hat{c}\right)\mathcal{L}A + \frac{i}{\delta\gamma}A''\right\} - E^{3/8}\delta\left\{\frac{\delta^2}{2}\frac{\chi(0)}{\chi''(0)} - 1\right\}A \qquad (7.3.23)$$

where we have used the fact that $V(0) = -\sqrt{2}$.

4. THE INTERIOR SOLUTIONS

We are now ready to solve (7.3.2) to (7.3.6) subject to (7.3.23). We can simplify the analysis considerably by noticing that if $\hat{p}$ is of the form

$$\hat{p} = (z - E^{1/4}\hat{c})\,A(x) + \frac{i\delta}{\gamma} E^{1/8}\,\mathcal{L}A \tag{7.4.1}$$

then (7.3.3), (7.3.4), and (7.3.6) will be solved with an error which is formally $O(E^{1/2})$. Moreover, this expression matches with (7.3.18).

If we now insert (7.4.1) into (7.3.5), integrate from $z = 0$ to $z = D$ using (7.3.7) and (7.3.23) and retaining only those terms which are formally $O(E^{3/8})$ or greater we obtain, after some algebra, the following equation for $A(x)$:

$$\left(1 - \sqrt{2}\,\frac{\gamma^2 D^3}{3\sigma}\right) A - \frac{i}{\delta} E^{1/8}\left\{\sqrt{2}\,\mu + \gamma\hat{c} - \delta^2\frac{(\sigma+1)}{\sqrt{2}\,\sigma} D^2\gamma\right\} A$$

$$+ E^{1/4}\left\{\frac{1}{\delta^2}\left(\frac{\sqrt{2}\,\gamma^2 D^3}{3\sigma} - 2\right)\frac{d^2A}{dx^2} - \sqrt{2}\left[\frac{\mu\gamma\hat{c}}{\delta^2}\right.\right.$$

$$\left.\left. - D\left(\frac{\gamma^2\hat{c}D}{\sigma} + \delta^2\right)\right] A\right\} + E^{3/8}\left\{\frac{i}{\delta^3}\left[\sqrt{2}\,\mu + \gamma\hat{c}\right.\right.$$

$$\left.\left. - \sqrt{2}\,\delta^2\frac{(\sigma+1)}{\sigma} D^2\gamma\right]\frac{d^2A}{dx^2} - \sqrt{2}\,i D\gamma\left[\delta\hat{c}\frac{(\sigma+1)}{\sigma}\right.\right. \tag{7.4.2}$$

$$\left.\left. - \frac{\delta}{2D}\,\frac{\chi(0)}{\chi''(0)}\right] A\right\} = 0$$

We shall now solve this by looking for solutions of the form:

$$A = A_o + E^{1/8} A_1 + \dots$$

$$\gamma_c = \gamma_o + E^{1/8} \gamma_1 + \dots$$

$$\hat{c} = \hat{c}_o + E^{1/8} \hat{c}_1 + \dots$$

where, as before, γ_c is that value of γ for which $\mathrm{Im}(\hat{c}) = 0$. This scheme then leads to the following results for the first three orders of approximation:

$$O(E^o): \qquad \gamma_o^2 = 3\sigma/\sqrt{2}D^3 \tag{7.4.3}$$

$$O(E^{1/8}): \qquad \gamma_1 = 0;\ \hat{c}_o = -\frac{\sqrt{2}\mu}{\gamma_o} + \frac{\delta^2(\sigma+1)D^2}{\sqrt{2}\sigma} \tag{7.4.4}$$

$$O(E^{1/4}): \qquad \frac{1}{\delta^2}\frac{d^2A_o}{dx^2} + \left\{ \frac{i\gamma_o\hat{c}_1}{\delta} + 2\frac{\sqrt{2}\gamma_o\gamma_2 D^3}{3\sigma} - \frac{2\mu^2}{\delta^2} \right.$$

$$\left. + \mu\gamma_o D^2\frac{(3+\sigma)}{\sigma} - \frac{D\delta^2(3+5\sigma)}{\sqrt{2}\sigma} \right\} A_o = 0 \tag{7.4.5}$$

This is the governing equation for $A_o(x)$. In order to solve it we

must determine the boundary conditions which must be applied at $x = \pm 1/2$. In order to do this we must carry out an analysis of the thermal boundary layers near $x = \pm 1/2$. This analysis leads to exactly the same results as those found in Section 7.1 above . We shall verify this in the section which follows this and state here that:

$$A_o(\pm 1/2) = 0 \qquad (7.4.6)$$

$$A_1(\pm 1/2) = \pm \frac{[2^{3/4}\gamma_o D^{3/2}\lambda + \gamma_o^2 D^3]}{\delta[2^{3/2} + \gamma_o^2 D^3]} \frac{dA_o}{dx}(\pm \tfrac{1}{2}) \qquad (7.4.7)$$

The solutions of (7.4.5) which satisfies (7.4.6) are of the form

$$A_o = a \,.\, \sin m\pi (x - 1/2) \; ; \; m = \pm 1 \, , \pm 2 \, , \ldots \qquad (7.4.8)$$

and this leads to

$$\hat{c}_1 = 0 \qquad (7.4.9)$$

$$\gamma_2 = \frac{\gamma_o}{2}\left\{ \frac{m^2\pi^2 + 2\mu^2}{\delta^2} + \frac{\delta^2 D}{\sqrt{2}}\frac{(3+5\sigma)}{\sigma} - \mu\gamma_o D^2 \frac{(3+\sigma)}{\sigma} \right\} \qquad (7.4.10)$$

Thus, at this order of approximation we have:

$$\gamma \sim \gamma_0 \left\{ 1 + \frac{E^{1/4}}{2} \left[\frac{m^2\pi^2 + 2\mu^2}{\delta^2} + \delta^2 D \frac{(3+5\sigma)}{12\sigma} \right.\right.$$

$$\left.\left. - \mu \gamma_0 D^2 \frac{(3+\sigma)}{\sigma} \right] + O(E^{3/8}) \right\}$$

(7.4.11)

Comparison with (7.1.20) and (7.2.16) shows that this expression does indeed behave asymptotically as the low wave number result when $\delta << 1$ and as the high wave number result when $\delta >> 1$. In fact the first three terms of (7.4.11) are what we would have obtained had we formed a "composite" expansion from (7.1.20) and (7.2.16) by adding these two together and subtracting from the result the part which is common to both (γ_0).

We shall refer to (7.4.11) as the "two term" expansion for the transition thermal Rossby number (since $R_o = (\gamma/\sigma) E^{3/4}$). Before discussing (7.4.11) further we shall obtain the $O(E^{3/8})$ corrections to it since these involve the lowest order contributions from the side wall boundary layers and the intermediate boundary layer near $z = 0$. The $O(E^{3/8})$ terms lead to the following:

$$\frac{d^2 A_1}{dx^2} + m^2\pi^2 A_1 + \delta^2 H A_0 = 0 \qquad (7.4.12)$$

$$A_1(\pm 1/2) = \pm G \frac{dA_0}{dx}(\pm 1/2) \qquad (7.4.13)$$

where

$$H = 2\sqrt{2}\,\frac{\gamma_0\gamma_3}{3\sigma}\,D^3 + \frac{i}{\delta}\,(\gamma_0\hat{c}_2 + \gamma_2\hat{c}_0)$$

$$+ i\,\frac{m^2\pi^2}{\delta^3}\,\left[\sqrt{2}\,\mu + \hat{c}_0 - \sqrt{2}\,\delta^2\,\frac{(\tau+1)}{\sigma}\,D^2\gamma_0\right]$$

$$- i\sqrt{2}\,\delta\,D\,\gamma_0\,\frac{(\tau+1)}{\sigma}\left(\frac{\gamma_2 D}{2} - \gamma_0\hat{c}_0\right)$$

$$- \frac{i\delta\gamma_0}{\sqrt{2}}\,\frac{\chi(0)}{\chi''(0)} \qquad (7.4.14)$$

$$G = \frac{2^{3/4}\gamma_0 D^{3/2} i + \gamma_0^2 D^3}{2\left[2^{3/4} + \gamma_0^2 D^3\right]} \qquad (7.4.15)$$

Now, since A_o is a solution of the homogenous part of (7.4.12) and (7.4.13), a solution of these equations exists only if a certain solubility condition is satisfied. This condition is

$$H = \frac{1}{\delta^2}\,\frac{\left[A_0' A_1\right]_{-1/2}^{1/2}}{\int_{-1/2}^{1/2} A_0^2\,dx} \qquad (7.4.16)$$

or, taking A_o to be given (in normalized form) by

$$A_o = \sqrt{2}\,\sin\, m\pi\,(x - 1/2)$$

and, using (7.4.13),

$$H = 4 m^2 \pi^2 G / \delta^2 \qquad (7.4.17)$$

This condition enables us to obtain a solution to (7.4.12) and (7.4.13). It is easily verified that a particular solution exists in the form

$$A_{1p} = \frac{\delta^2 H}{\sqrt{2}\, m\pi} \times \cos m\pi (x - 1/2) \qquad (7.4.18)$$

However this solution is not unique since it is possible to add an arbitrary multiple of the solution of the homogenous problem corresponding to (7.4.12) and (7.4.13), i.e. $A_1 = \alpha A_0 + A_{1p}$. To ensure uniqueness we shall choose α so as to minimize the norm of A_1, i.e. we want

$$\int_{-1/2}^{1/2} |A_1|^2 dx$$

to be minimized with respect to α. Bearing in mind that A_0 is real we have that

$$\int_{-1/2}^{1/2} |A_1|^2 dx = \int_{-1/2}^{1/2} [|\alpha|^2 A_0^2 + \alpha A_0 A_{1p}^* + \alpha^* A_0 A_{1p} + |A_{1p}|^2] dx \qquad (7.4.19)$$

where α^* is the complex conjugate of α. It is easily verified that this expression is minimized if

$$\alpha = -\int_{-1/2}^{1/2} A_0 A_{1p}\, dx \qquad (7.4.20)$$

(Note that A_0 has been normalized) . This is equivalent to the statement that A_0 and A_1 are orthogonal to each other .

Equation (7.4.20) then leads to

$$A_1 = \frac{\delta^2 H}{\sqrt{2}\, m\pi}\left[\frac{1}{4m\pi}\sin m\pi(x-1/2) + x\cos m\pi(x-1/2)\right] \qquad (7.4.21)$$

Equation (7.4.17) enables the determination of $\hat{c}_2$ and γ_3 . Using the results from previous orders we find that the latter is given by

$$\gamma_3 = \frac{\gamma_0}{2}\left\{\frac{4\sqrt{2}\, m^2\pi^2\gamma_0^2}{\delta^3(4+3\sigma)} - \frac{\delta\gamma_0}{\sqrt{2}}\,\mathrm{Im}\left(\frac{\chi(0)}{\chi''(0)}\right)\right\} \qquad (7.4.22)$$

or ,

$$\gamma \sim \gamma_0\left\{1 + \frac{E}{2}^{1/4}\left[\frac{m^2\pi^2+2m^2}{\delta^2} + \delta^2 D\frac{(3+5\sigma)}{\sqrt{2}\,\sigma} - \mu\gamma_0 D^2\frac{(3+\sigma)}{\sigma}\right]\right.$$

$$\left. + \frac{E}{2}^{3/8}\left[\frac{4\sqrt{2}\, m^2\pi^2\gamma_0^2}{\delta^3(4+3\sigma)} - \frac{\delta\gamma_0}{\sqrt{2}}\,\mathrm{Im}\left(\frac{\chi(0)}{\chi''(0)}\right)\right]\right\} \qquad (7.4.23)$$

This is our final approximation to γ . It is interesting to note that γ_3 is non-zero solely because we have included the effects of the side wall boundary layers and the critical layer near $z = 0$. On the other hand , the two term expansion (7.4.11) contains no boundary layer contributions other than those due to the lower Ekman layer via the Ekman pumping condition.

5. THE THERMAL SIDE WALL BOUNDARY LAYERS

It is illustrative to examine the thermal boundary layers at the side wall in somewhat greater detail than was done in Section 7.1 above. The governing equations are still (7.3.2) to (7.3.8) . Equation (7.3.9) also arises and requires an extension of the critical layer scaling into an $E^{1/8}$ square corner region. If this is done it can be shown that the lowest order boundary condition, for the side layer , at $z = 0$ is still the Ekman pumping condition and therefore we shall bypass the corner region analysis.

We consider here the side $x = -1/2$. The appropriate stretched variable is $\rho = (x + 1/2) E^{-1/8}$, and the following rescaling of the dependent variables in (7.3.2) to (7.3.8) ensures matching to the interior:

$$(\hat{u}, \hat{w}, \hat{p}, \hat{T}) = E^{1/8} (\tilde{u}, \tilde{w}, \tilde{p}, \tilde{T}) \qquad (7.5.1)$$

The governing equations are, with errors which are $O (E^{1/8})$ or less,

$$\hat{v} = \frac{\partial \tilde{p}}{\partial \rho} \tag{7.5.2}$$

$$\tilde{\omega} = -i\tilde{p} \tag{7.5.3}$$

$$\frac{\partial \tilde{\omega}}{\partial z} = -i\mu\tilde{T} + i\frac{\delta^2}{\sigma}\gamma z\left[\frac{1}{\delta^2}\frac{\partial^2 \tilde{p}}{\partial \rho^2} - \tilde{p}\right] \tag{7.5.4}$$

$$\frac{\partial \tilde{p}}{\partial z} = \tilde{T} \tag{7.5.5}$$

$$i\gamma\left[z\frac{\partial \tilde{p}}{\partial z} - \tilde{p}\right] = \delta E^{1/8}\left[\frac{1}{\delta^2}\frac{\partial^2}{\partial \rho^2} - 1\right]\frac{\partial \tilde{p}}{\partial z} \tag{7.5.6}$$

$$\tilde{\omega}(0,\rho) = \frac{\delta}{\sqrt{2}E^{1/8}}\left[\frac{1}{\delta^2}\frac{\partial^2}{\partial \rho^2} - 1\right]\tilde{p}(0,\rho) \tag{7.5.7}$$

$$\tilde{\omega}(D,\rho) = -i\mu\,\tilde{p}(D,\rho) \tag{7.5.8}$$

Equation (7.5.6) has a solution of the form

$$\tilde{p} = z\left[B_0(\rho) + E^{1/8}B_1(\rho)\right] + \frac{i\delta}{\gamma}E^{1/8}\left[\frac{1}{\delta^2}\frac{d^2B_0}{d\rho^2} - B_0\right] \tag{7.5.9}$$

Applying (7.5.4) and the boundary conditions (7.5.7) and (7.5.8) then shows that

$$\left[\frac{1}{\delta^2}\frac{d^2}{d\rho^2} - 1\right]\left[\frac{1}{\delta^2}\frac{d^2 B_0}{d\rho^2} + \left(\frac{\sqrt{2}\,\gamma_0^2 D^3}{3\sigma} - 1\right)B_0\right] = 0 + O(E^{1/8}) \qquad (7.5.10)$$

Since $(\sqrt{2}\ \gamma_0^2\ D^3 / 3\sigma) - 1 = 0$ the solution of this is of the form

$$B_0 = a_0 + b_0\rho + K_0 e^{-\delta\rho} \qquad (7.5.11)$$

Now, as mentioned in Section 7.1, matching to the outer Stewartson-Proudman layer is ensured if

$$B_0(0) = 0 \qquad (7.5.12)$$

$$\frac{d^2 B_0(0)}{d\rho^2} = \frac{i\delta\gamma_0 D^{3/2}}{2^{3/4}}\frac{d B_0(0)}{d\rho} \qquad (7.5.13)$$

These conditions are satisfied if B_0 is of the form:

$$B_0 = b_0\left\{\rho - \frac{i}{\delta}\left[\frac{\gamma_0 D^{3/2}}{2^{3/4} + i\gamma_0 D^{3/2}}\right]\right]\left[1 - e^{-\delta\rho}\right] \qquad (7.5.14)$$

This matches to the interior if the boundary conditions (7.4.6) and (7.4.7) are satisfied at $x = -1/2$.

6. CALCULATION OF THE TRANSITION CURVES AND COMPARISON WITH EXPERIMENTS

One of the more important results of this chapter is the expression (7.4.23) for γ_c since this now provides the information required to compute the transition Rossby number.

Calculation of the right hand side of (7.4.23) complicated slightly by the necessity of evaluating $\chi(0)/\chi''(0)$. This quantity can be evaluated from (7.3.19). It is easily shown, using some recurrence relations for the Hankel functions, that :

$$\frac{\chi(0)}{\chi''(0)} = \frac{i}{\gamma_0} e^{i\pi/6} \frac{\int_0^\infty \frac{1}{\eta - i\delta/\gamma_0} H^{(1)}_{2/3}(y)\,d\eta}{H^{(1)}_{1/3}(2\delta^2/3\gamma_0)} \qquad (7.6.1)$$

where y is as defined in (7.3.20). This expression is somewhat cumbersome since y is a complex valued function of η.

However, we note that the integrand in (7.6.1) is analytic and decreases with increasing η everywhere in the lower right hand quadrant of the complex η plane including the negative

imaginary axis *. Thus we can transform (7.6.1) into an integral along the negative imaginary axis. If we take $\arg(\eta - i\delta/\gamma_0) = -\pi/2$ along this axis then our choice for $\arg y$ is zero and it is not difficult to show that

$$\frac{\chi(0)}{\chi''(0)} = -\frac{2i}{3\gamma_0} e^{i\pi/6} \mathcal{F}\left(\frac{2}{3}\frac{\delta^2}{\gamma_0}\right) \qquad (7.6.2)$$

where

$$\mathcal{F}(a) = \frac{\int_a^\infty \frac{1}{y} H_{2/3}^{(1)}(y)\,dy}{H_{1/3}^{(1)}(a)} \qquad (7.6.3)$$

---

* We define $H_{2/3}^{(1)}(y)$ in the usual manner, i.e., using a branch cut along the negative real y axis with $-\pi < \arg y \leq \pi$ so that $-7\pi/6 < \arg(\eta - i\delta/\gamma_0) \leq \pi/6$.

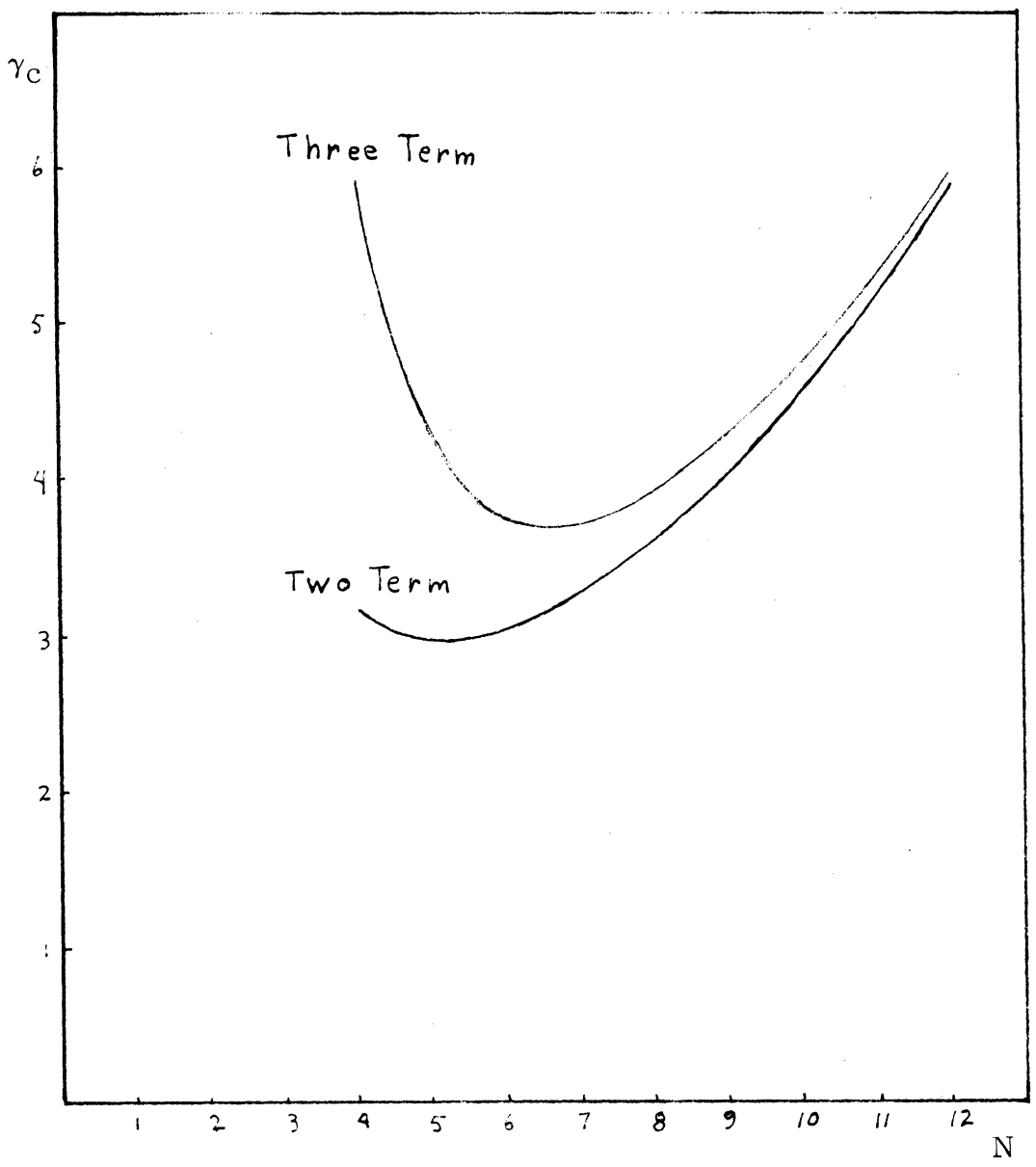

Figure 7. 2. Comparison of the two and three term intermediate expansions. Other data as in Figure 6. 1.

The advantage of (7.6.2) is now that (7.6.3) involves evaluation of the Hankel functions on the real axis only. Also, there is the added convenience of having the parameters δ and γ_o combined into the single parameter, a, in (7.6.3).

In practice the integral in (7.6.3) must still be evaluated numerically. We have chosen to do this by means of a thirty two point Gaussian-Laguerre quadrature formula.

Figure 7.2 illustrates the behavior of both the two-term and the three-term expansions (7.4.11) and (7.4.23), as a function of the wave number, for a typical case. The minimum value of γ_c is the one from which a transition Rossby number can be computed and compared with experiments.

Figure 7.3 illustrates the behavior of the transition curve for the same annular geometry as that used in Figure 7.2. In this figure we have used $R_o D$ as the ordinate since this facilitates comparison with experimental data which is usually plotted in the same way. A cursory comparison with the experimental results of Fowlis and Hide (1965) shows good agreement as to the slope of the transition curve and the value of the transition wave number.

The actual values of the theoretical transition Rossby numbers are somewhat lower than the experimental values. This is in contrast to the previous theoretical results of Kuo (1956), Barcilon (1964), O'Neill (1968), and Warn (1973) all of which predict values of the transition Rossby number which are too large. This is without doubt due in part to the fact that, in contrast to these studies, the vertical stratification of the symmetric state plays no role in our anal-

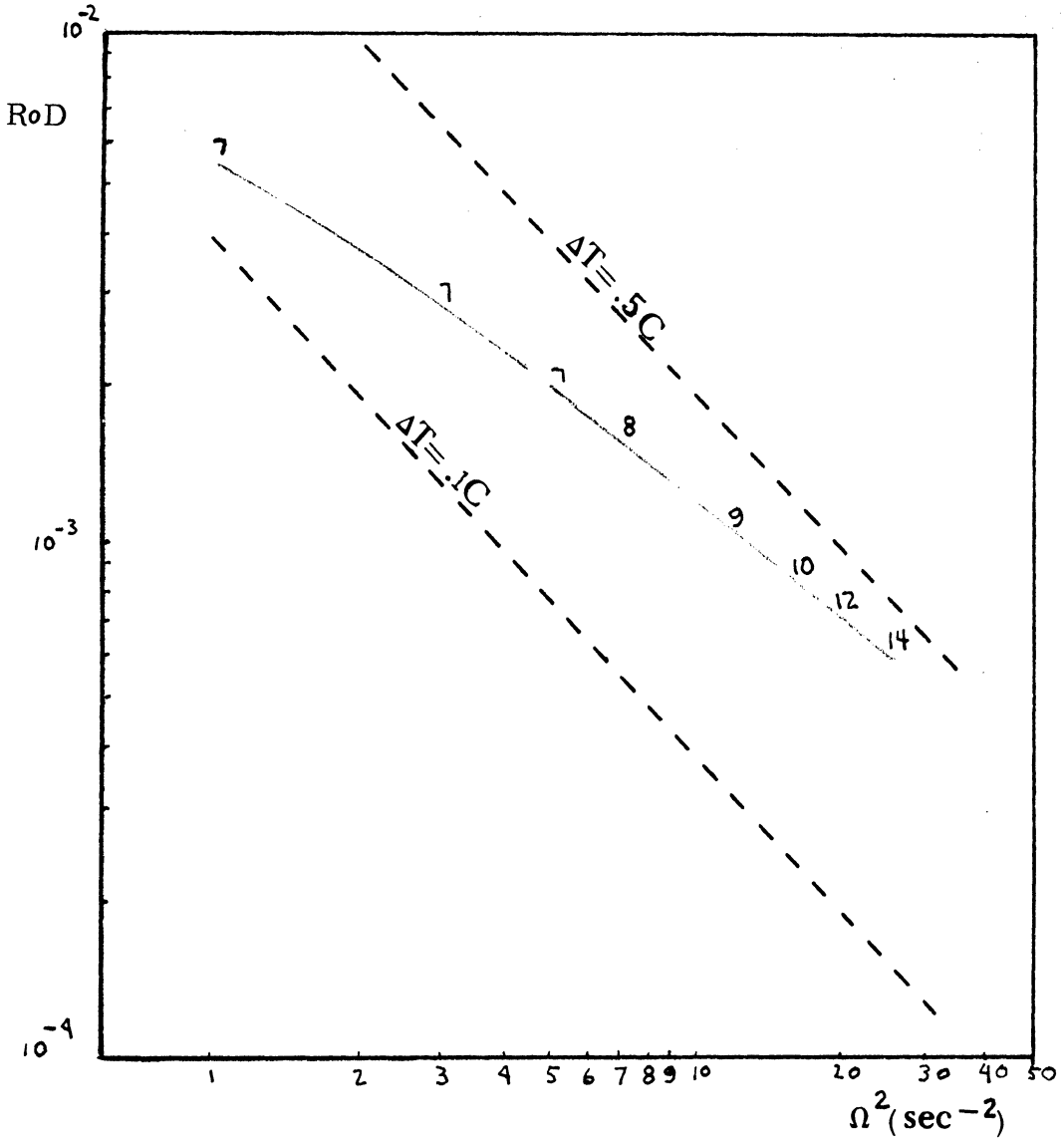

Figure 7.3. A typical transition curve as obtained from the intermediate wave number three term expansion for γ_c. Other data as in Figure 6.1. Numbers appearing along the curve are transition wave numbers. (N_T is the integer closest to $r_o\delta_T / LE^{1/8}$)

ysis . There is indication in Kaiser's (1972) paper that the ideal of truly isothermal side walls is difficult to achieve in an experimental configuration of the type which has usually been employed. In fact it is probable that the fluid is somewhat more stably stratified than our axisymmetric solutions would indicate. Also it must be kept in mind that , in addition to the approximations which were made at the outset (e. g. the narrow gap approximation), we have only determined γ_c correct to $O(E^{3/8})$. Higher order approximations would result in small quantitative changes in the predicted position of the transition curve.

In this regard it should be noted that in many of the experiments (e. g. those of Fowlis and Hide) the transition criteria have been determined visually by observation of the motion of tracer particles on the free surface of the fluid. When this is the case surface tension would certainly affect the results due to the fact that both normal and tangential stresses can exist at the free surface due to its presence and the fact that it varies with temperature. Experimental evidence (Kaiser (1971)) indicates that surface tension effects tend to inhibit radial motions on the free surface of the fluid when the flow is axisymmetric (See also Hide (1965)) . Also it is to be remembered that the deviation of the free surface from its reference position is very small compared to the magnitude of the tangential motions at the reference position. Thus significant motion normal to the reference position would not be observed until the tangential motions and the motions in the fluid interior had achieved sizeable amplitudes. These considerations suggest that wave motion may not be observed at the

free surface until it had become established in the interior of the fluid.

The most encouraging feature of our results is that the slope of the lower transition curve appears to be in substantial agreement with the experimental results. This is due mainly to the fact that we have included the effects of the centrifugal force explicitly. This is illustrated in Figure 7.4 where we have plotted the transition curve which would be obtained if the centrifugal effects had been neglected completely ($\mu \equiv 0$). Comparison of the $\mu = 0$ with the $\mu \neq 0$ curves shows very clearly that the centrifugal force is of importance in determining the slope of the lower transition curve.

However this result must be stated with some caution. The difference between the two curves in Figure 7.4 is most pronounced at higher rotation rates. It should be born in mind , however, that at sufficiently high rotation rates μ becomes significantly larger than unity. In fact, if $\Omega \gtrsim 3 \text{ sec}^{-1}$, then $\mu \gtrsim O(E^{-1/8})$ for the situation of Figure 7.4 . It is then clear that in such a case the asymptotic ordering which led to (7.4.23) is considerably lacking in accuracy due to the largeness of the centrifugal terms in the governing equations. This inaccuracy also affects the value of the transition wave number as is illustrated by the rather rapid increase in that quantity as Ω^2 increases above 10 sec^{-2} (Figure 7.3) . Note that , as illustrated in Figure 7.4 , the increase in the transition wave number is not as rapid when μ is explicitly set to zero.

These considerations suggest that the result illustrated in Figure 7.4 should be regarded as indicative only owing to the difficulties which arise with the present analysis when μ becomes too

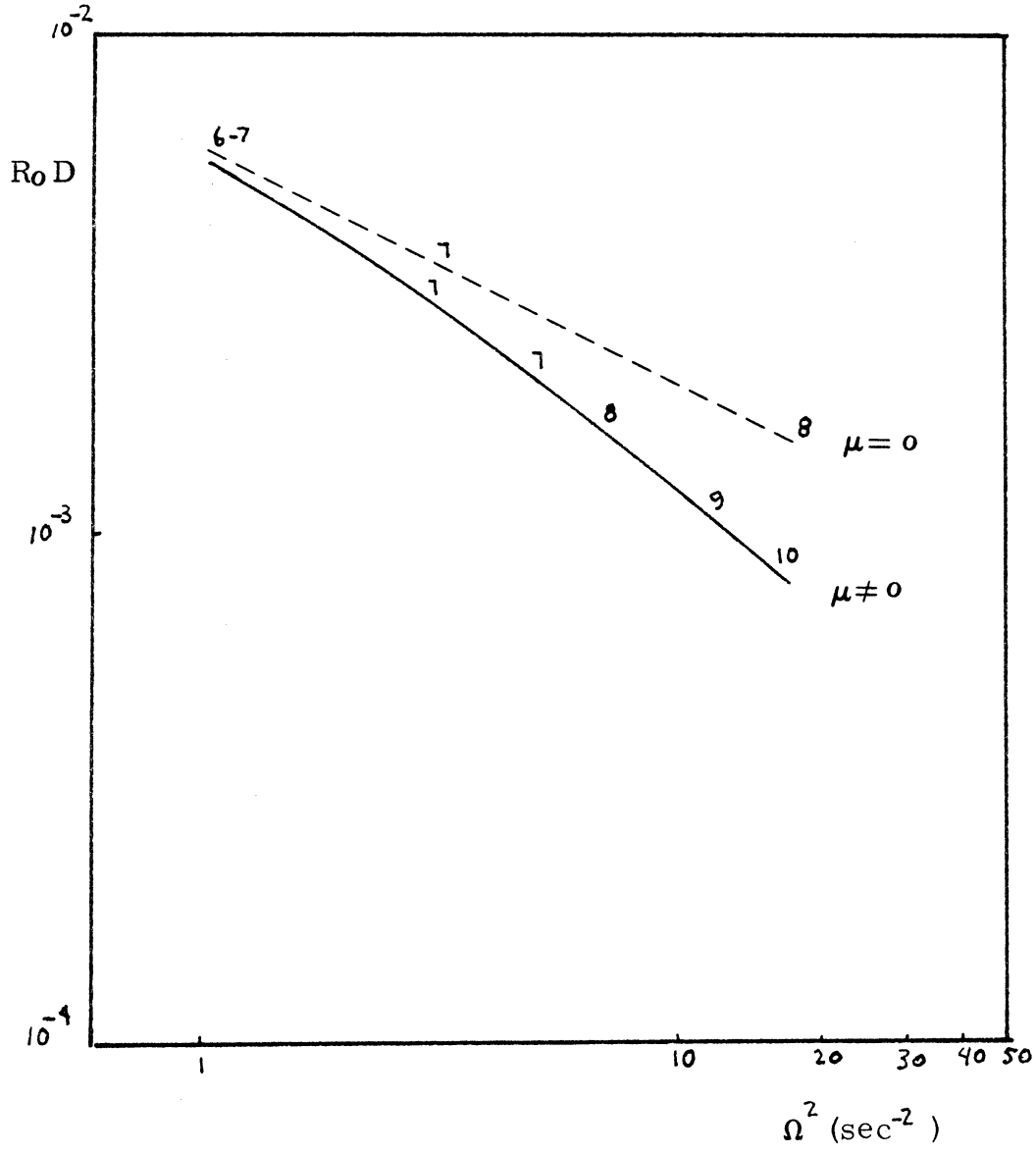

Figure 7.4. Comparison of the transition curve for $\mu = 0$ with that for $\mu \neq 0$. Other data as in Figure 6.1.

large. These can only be removed by considering explicitly the circumstance in which μ is significantly larger than unity. However this requires a new analysis for the axisymmetric state as well as for the stability problem. (As an illustration of this point see Barcilon and Pedlosky (1967) for the analysis of a problem in which the centrifugal terms are not small).

Most of the experiments have been carried out with deep annuli. Typically D is 4 or 5 . Figure 7.5 compares the transition curves for $D = 4$ and $D = 2$. There is , again , reasonably good agreement with the experimental results as to the slope of the transition curve and the values of the transition wave numbers. It should be born in mind, however , that our results will not be valid if D is too large since we have assumed it to be O (1) throughout the present study .

Figure 7.5 also suggests some steepening of the transition curve slope as D increases. The experimental results of Fowlis and Hide (1965) seem to indicate that the position of the lower transition curve is almost independent of D although this conclusion is uncertain to some degree due to the fact that there is a certain amount of error in their determination of the lower transition curve (e.g. see their Fig. 7) .

Finally , we can note that, for the external parameter settings corresponding to the figures we have just discussed actual calculation shows that the contribution of the critical layer term $\chi(0)/\chi''(0)$ is small compared to the other terms in equation (7.4.22) . This is due to the fact that this quantity has a very

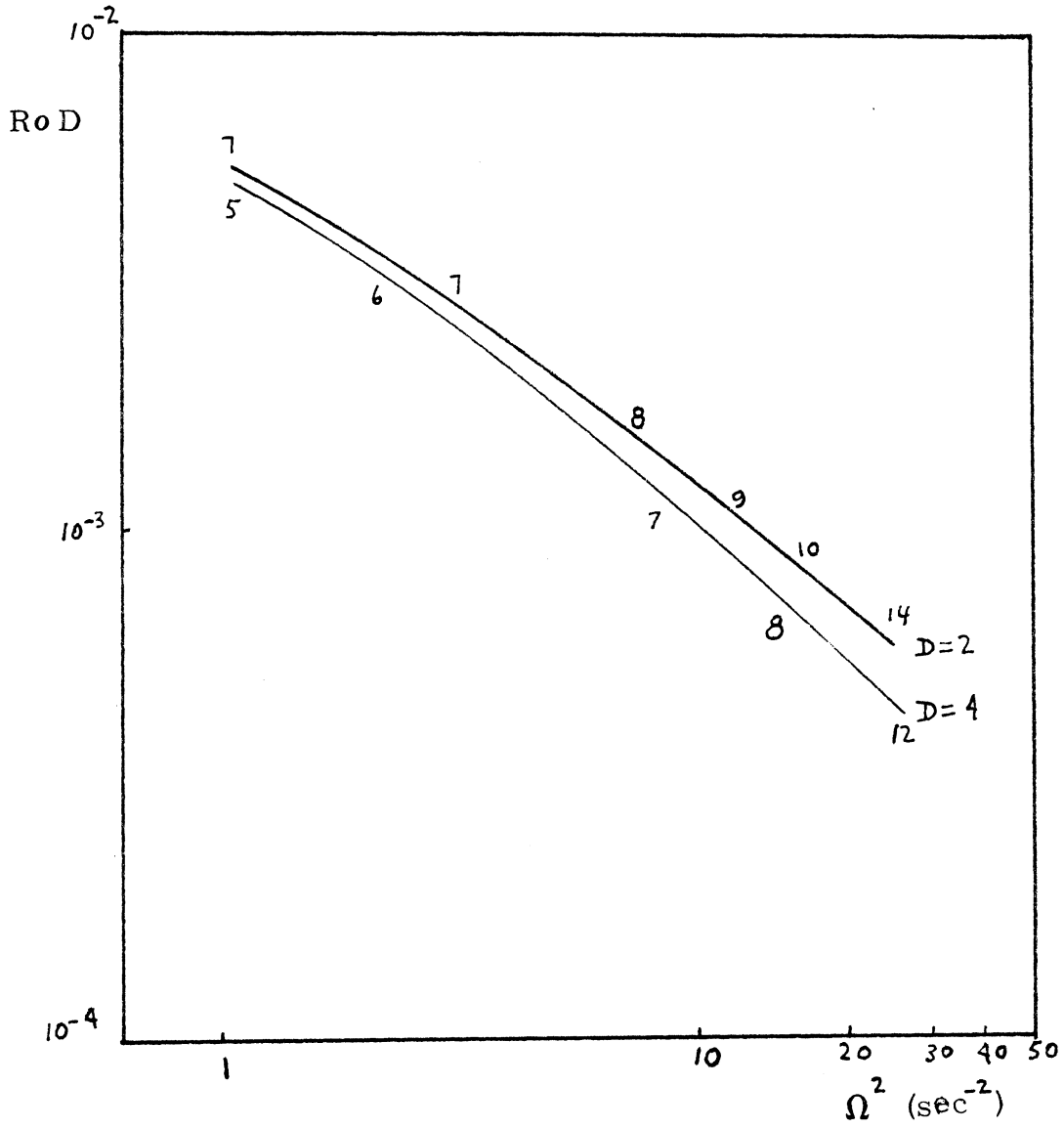

Figure 7.5. Comparison of transition curves for different aspect ratios. Other data as in Figure 6.1.

small imaginary part for these cases. To illustrate this point we take the case $D = 4$, $L = 2.54$, $r_o = 5$. Then if water is the working fluid the quantity $2\delta^2 / 3\gamma_o$ varies from a value of 1.5 for the $\Omega^2 = 1$ transition wave number to a value of 2.16 at $\Omega^2 = 10$. Since these quantities are both larger than unity some insight into the behavior of $\chi(0)/\chi''(0)$ can be obtained by using the asymptotic expansions of the Hankel functions. These are :

$$H^{(1)}_{2/3}(x) \sim \sqrt{\frac{2}{\pi x}}\, e^{i[x - 7\pi/12]}\left[1 + i\cdot O(x^{-1})\right]$$

$$H^{(1)}_{1/3}(x) \sim \sqrt{\frac{2}{\pi x}}\, e^{i[x - 5\pi/12]}\left[1 + i\cdot O(x^{-1})\right]$$

as x becomes large and positive. Thus the quantity $\mathcal{J}(a)$ of equation (7.6.3) can be written, for large a, as follows :

$$\mathcal{J}(a) \sim e^{-i\pi/6} a^{1/2}\left[1 + O(a^{-1})\right] \int_a^\infty \frac{e^{ix}}{x^{3/2}}\left[1 + O(x^{-1})\right] dx$$

$$\sim \frac{i e^{-i\pi/6}}{a} + O(a^{-2})$$

where the latter result is obtained by expanding the integral in inverse powers of $a^{1/2}$ through integration by parts. This result, in combination with (7.6.2) shows that $\mathrm{Im}\left(\chi(0)/\chi''(0)\right)$ is $O(\gamma_o \delta^{-4})$

if $a = 2\delta^2 / 3\gamma_0$ is sufficiently large . In practice the asymptotic estimates are accurate enough for our purpose if a is greater than unity .

CHAPTER VIII

CONCLUSIONS

The main intent of this study was to reexamine the problem of theoretically determining the lower symmetry transition criteria. The program for accomplishing this involved first the determination of an approximate steady axisymmetric solution of the governing equations and boundary conditions. Then an investigation of the circumstances under which this symmetric state becomes unstable to small wave-like disturbances determines the criteria for instability.

Since we have restricted our attention to the situation in which $R_o \lesssim E^{1/2}$ our analysis has shown that the symmetric state is, in the lowest approximation, exactly as found by Hunter (1967). However, there are higher order corrections to this due to convection in the side wall boundary layers and also to the fact that the free upper surface has a small quasi-static deviation from the horizontal. This deviation was taken to be $O(E^{1/2})$ and that is the magnitude of the corrections due to it. Convection in the side wall layers produces a weak stable vertical stratification which is formally $O(E^{1/2})$ or less if $R_o \lesssim O(E^{1/2})$.

The major part of this study has been the analysis of the stability of the above axisymmetric state. This investigation has shown first of all that if the thermal Rossby number is sufficiently large (but still $\lesssim O(E^{1/2})$) the axisymmetric state is unstable. However, when $R_o = O(E^{3/4})$ stabilization of low wave numbers can result from heat conduction in the interior of the fluid.

However, heat conduction alone does not explain the position and shape of the lower transition curve. As the disturbance wave number increases viscous effects become important in the interior and these, in conjunction with heat conduction, are of major importance in determining the critical wave number for the lower transition . In addition , the centrifugal forces play a role in the stability of the lower symmetry regime. Our analysis has shown that these affect not only the value of the transition wave number but also the slope of the lower transition curve. In this regard we have shown that centrifugal effects can account , in part at least , for the observed slope of the lower transition curve.

Finally , we have determined the lowest order effect of the side wall boundary layers in determining the position and slope of the lower transition curve. Our results show that, mainly at lower rotation rates, both the transition Rossby number and the corresponding wave number are under-estimated if the effect of the side wall boundary layers is ignored.

APPENDIX

THE SIDE WALL BOUNDARY LAYERS FOR THE STABILITY PROBLEM

1. THE INNER STEWARTSON LAYER:

The analysis of the axi-symmetric state for isothermal side walls shows that in the inner Stewartson boundary layer the basic flow is characterize by zonal and vertical velocities which are $O(1)$ while u, T, and p are $O(E^{1/3})$. The lowest approximation to T is conductive.

We begin with the boundary layer adjacent to the cold wall and take $\xi = (x+1/2)/E^{1/3}$. Then the basic state is characterized by

$$v = V(\xi,z) + O(E^{1/6}) \tag{1.1}$$

$$T = E^{1/3}\xi + O(E^{1/2}) \tag{1.2}$$

$$u = E^{1/3}\bar{u}(\xi,z) + O(E^{1/2}) \tag{1.3}$$

$$w = W(\xi,z) + O(E^{1/6}) \tag{1.4}$$

The expressions for V, $\bar{u}$ and W are given in Chapter IV above but are not needed at the moment. As for the axi-symmetric case we scale the perturbation temperature, pressure, and radial velocity by the non-dimensional boundary layer thickness, i.e.,

$$p, T, u = E^{1/3}\{\hat{p}, \hat{T}, \hat{u}\} \tag{1.5}$$

With this scaling the perturbation equations are the following:

$$v = \hat{p}_\xi + \mu E^{5/12} \hat{T} + E^{2/3} \hat{u}_{\xi\xi} + O\left(\frac{\lambda k}{\sigma} E^{5/6}\right) \tag{1.6}$$

$$\hat{u} = -ik\hat{p} + v_{\xi\xi} - \frac{\lambda}{\sigma} E^{1/6} \left\{ ik(V-c)v + \bar{U} v_\xi + \hat{u} V_\xi + w \bar{U}_z + W v_\xi \right\} + O(E^{2/3}) \tag{1.7}$$

$$\hat{p}_z = \hat{T} + w_{\xi\xi} + O\left(\frac{\lambda}{\sigma} E^{1/6}\right) \tag{1.8}$$

$$\hat{u}_\xi + ikv + w_z = 0 \tag{1.9}$$

$$\hat{T}_{\xi\xi} = \lambda E^{1/6} \left[ik(V-c)\hat{T} + \bar{U}\hat{T}_\xi + \hat{U} + W\hat{T}_z \right] + O(E^{2/3}) \tag{1.10}$$

The boundary conditions at $z = 0, D$ must be established by analysis of the corner regions in a manner similar to that carried out for the symmetric state. The result of that analysis will show that the appropriate lowest order boundary conditions are the following:

$$w(0,\xi) = \frac{E^{1/6}}{\sqrt{2}} \hat{p}_{\xi\xi}(0,\xi) \tag{1.11}$$

$$w(D,\xi) = 0 \tag{1.12}$$

The boundary conditions at $\xi = 0$ are no-slip for the velocity components and vanishing of $\hat{T}$.

The lowest order approximations for small E are, from 1.6 through 1.12, given by the following:

$$v_0 = \hat{p}_{0\xi} \tag{1.13}$$

$$\hat{u}_0 = -ik\hat{p}_0 + v_{0\xi\xi} \tag{1.14}$$

$$\hat{p}_0 = \hat{T}_0 + w_{0\xi\xi} \tag{1.15}$$

$$T_{0\xi\xi} = 0 \tag{1.16}$$

$$\hat{u}_{0\xi} + ikv_0 + w_{0z} = 0 \tag{1.17}$$

with boundary conditions:

$$(\hat{u}_0, v_0, w_0, \hat{T}_0) = 0 \; ; \; \xi = 0 \tag{1.18}$$

$$w_0(0,\xi) = w_0(D,\xi) = 0 \tag{1.19}$$

Equation 1.16 and the boundary condition (1.18) on implies that:

$$\hat{T}_0 = \beta_0(z)\,\xi \tag{1.20}$$

Then $\hat{p}_0$ is of the form:

$$\hat{p}_0 = H_0(\xi) + \xi \int_0^z \beta_0(z')dz' + \int_0^z \omega_{0\xi\xi}\, dz' \tag{1.21}$$

Equations 1.14 and 1.15 then show that

$$v_0 = \frac{dH_0}{d\xi} + \int_0^z \beta_0 dz' + \int_0^z \omega_{0\xi\xi\xi}\, dz' \tag{1.22}$$

$$\hat{u}_0 = -ik\hat{p}_0 + \frac{d^3H_0}{d\xi^3} + \int_0^z \frac{\partial^5 \omega_0}{\partial \xi^5}\, dz' \tag{1.23}$$

The continuity equation 1.17 then requires that

$$\frac{d^4H_0}{d\xi^4} + \int_0^z \frac{\partial^6 \omega_0}{\partial \xi^6}\, dz' + \frac{\partial \omega_0}{\partial z} = 0 \tag{1.24}$$

Since H_0 is independent of ξ we must therefore have that

$$\frac{\partial^6 \omega_0}{\partial \xi^6} + \frac{\partial^2 \omega_0}{\partial z^2} = 0 \tag{1.25}$$

and this is the governing equation for ω_0.

Integrating 1.24 with respect to z and making use of the boundary conditions 1.19 shows that

$$\frac{d^4H_0}{d\xi^4} + \frac{1}{D}\int_0^D \int_0^z \frac{\partial^6 \omega_0}{\partial \xi^6}\, dz'dz = 0 \tag{1.26}$$

Consequently:

$$H = a_0 + b_0 \xi + \tilde{c}_0 \xi^2 + d_0 \xi^3 - \frac{1}{D} \int_0^D \int_0^z \frac{\partial^2 \omega_0}{\partial \xi^2} \, dz' \, dz \tag{1.27}$$

The constants a_0, b_0, $\tilde{c}_0$, d_0 have yet to be determined.

If we now use 1.22 and 1.23 and apply the boundary conditions at $\xi = 0$ for $\hat{u}_0$ and v_0 we find that

$$\left. \frac{dH_0}{d\xi} \right|_{\xi=0} = - \int_0^z \beta_0 \, dz' - \left[\int_0^z \omega_0 \xi \xi \, dz' \right]_{\xi=0} \tag{1.28}$$

$$\left[\frac{d^3 H_0}{d\xi^3} - ikH_0 \right]_{\xi=0} = - \int_0^z \left[\frac{\partial^5 \omega_0}{\partial \xi^5} - ik \frac{\partial^2 \omega_0}{\partial \xi^2} \right]_{\xi=0} dz' \tag{1.29}$$

We can now use (1.27), (1.28), and (1.29) to show that

$$b_0 = - \frac{1}{D} \int_0^D \int_0^z \beta_0 \, dz' dz \tag{1.30}$$

$$6d_0 - ika_0 = 0 \tag{1.31}$$

$$\left[\frac{\partial^5 \omega_0}{\partial \xi^5} - ik \frac{\partial^2 \omega_0}{\partial \xi^2} \right]_{\xi=0} = 0 \tag{1.32}$$

$$\left\{ \int_0^z \frac{\partial^3 \omega_0}{\partial \xi^3} \, dz' - \frac{1}{D} \int_0^D \int_0^z \frac{\partial^3 \omega_0}{\partial \xi^3} \, dz' dz \right\}_{\xi=0} = \frac{1}{D} \int_0^D \int_0^z \beta_0 \, dz' dz - \int_0^z \beta_0 \, dz' \tag{1.33}$$

Equations 1.32 and 1.33, in addition to the requirements that ω_0 shall vanish at $\xi = 0$ and shall be exponentially small

for large ξ , provide sufficient boundary conditions to complete the determination of ω_0 in terms of $\beta_0(z)$.

The solution of 1.25 which satisfies the boundary conditions 1.19, 1.32, 1.33 and is such that $\omega_0(z,0) = 0$ is of the form:

$$\omega_0 = \sum_{j=1}^{\infty} f_{0j}(\xi) \sin j\pi z/D \tag{1.34}$$

$$f_{0j}(\xi) = -\alpha_{0j}\left\{e^{-\nu_j \xi} - e^{-\nu_j \xi/2}\left[\cos\frac{\sqrt{3}}{2}\nu_j\xi + \frac{(j\pi + 3ikD)}{\sqrt{3}(j\pi - ikD)}\sin\frac{\sqrt{3}}{2}\nu_j\xi\right]\right\} \tag{1.35}$$

and $\nu_j = (j\pi/D)^{1/3}$ while

$$\alpha_{0j} = \frac{1}{D}\int_0^D \cos j\frac{\pi z}{D}\, dz \left\{\int_0^z \beta_0\, dz' - \frac{1}{D}\int_0^D\int_0^z \beta_0\, dz'dz\right\} \tag{1.36}$$

We now have , at lowest order,

$$p \sim E^{1/3}\left\{a_0\left[1 + \frac{ik}{c}\xi^3\right] + \xi\left[\int_0^z \beta_0\, dz' - \frac{1}{D}\int_0^D\int_0^z \beta_0\, dz'dz\right]\right.$$

$$\left. + \tilde{c}_0\xi^2 + \int_0^z \frac{\partial^2\omega_0}{\partial\xi^2}\, dz' - \frac{1}{D}\int_0^D\int_0^z \frac{\partial^2\omega_0}{\partial\xi^2}\, dz'dz\right\} \tag{1.37}$$

The quantities a_0, β_0, and $\tilde{c}_0$ must be determined from matching to the outer Stewartson layer. The error in (1.37) is formally $O(E^{1/4})$.

2. THE OUTER STEWARTSON LAYER:

2.1 $\lambda = O(1)$

The lowest order basic state in the outer Stewartson layer has been shown to be of the form:

$$v = z - \frac{D}{2} e^{-z/2^{1/4}\sqrt{D}} = z - \bar{V} \qquad (2.1.1a)$$

$$u = E^{1/2} \bar{V}_z z \qquad (2.1.1b)$$

$$T = E^{1/4} z \qquad (2.1.1c)$$

$$w = \frac{E^{1/4}}{2^{7/4}\sqrt{D}} (D-z) e^{-z/2^{1/4}\sqrt{D}} \qquad (2.1.1d)$$

where, near the cold wall, $z = (x+1/2) E^{-1/4}$.

It is convenient to scale the perturbation pressure, temperature, radial and vertical velocities by the boundary layer thickness, i.e.,

$$p, T, u, w = E^{1/4} (\hat{p}, \hat{T}, \hat{u}, \hat{w})$$

With this choice of scaling the perturbation equations assume the following form:

$$v = \hat{p}_z - E^{3/4} \left[\hat{u}_{zz} - ik\frac{\lambda}{\sigma}(z-c-\bar{V})\hat{u} - \mu\hat{T} \right] + O(E^{5/4}) \qquad (2.1.2)$$

$$\hat{u} = -ik\hat{p} + E^{1/4} \left\{ \hat{v}_{zz} - \frac{\Lambda}{\sigma} \left[ik(z-c-\bar{V})\hat{v} + \hat{u}\bar{V}_z \right] \right\} + O(E^{1/2}) \qquad (2.1.3)$$

$$\hat{u}_z + ik\sigma + E^{1/4}\hat{w}_z = 0 \tag{2.1.4}$$

$$\hat{p}_z = \hat{T} + O(E^{1/2}) \tag{2.1.5}$$

$$\hat{T}_{zz} = \lambda\left[ik(z-c-\bar{V})\hat{T} + \hat{u}\right] + O(E^{1/4}) \tag{2.1.6}$$

The lowest order boundary conditions can be shown, via analysis of the corner regions, to be the following:

$$\hat{w}(0,z) = \frac{1}{\sqrt{2}}\hat{p}_{zz} \tag{2.1.7}$$

$$\hat{w}(D,z) = 0 \tag{2.1.8}$$

It is convenient to combine 2.1.2 and 2.1.4 in the following form:

$$\hat{w}_z = -\left\{\sigma_{zzz} - \frac{\lambda}{\sigma}\left[ik(z-c-\bar{V})\sigma_z - \hat{u}\bar{V}_{zz}\right]\right\} + O(E^{1/4}) \tag{2.1.9}$$

The zero-order approximate solutions to 2.1.3 through (2.1.9) satisfy the following equations:

$$\sigma_0 = \hat{p}_{0z} \tag{2.1.10}$$

$$u_0 = -ik\hat{p}_0 \tag{2.1.11}$$

$$\hat{p}_{0z} = \hat{T}_0 \tag{2.1.12}$$

$$\hat{p}_{0zzz} = ik\lambda\left[(z-c-\bar{V})\hat{p}_{0z} - \hat{p}_0\right] \tag{2.1.13}$$

$$\hat{\omega}_{0z} = -\frac{\partial^4 \hat{p}_0}{\partial z^4} + \frac{ik\lambda}{\sigma}\left[(z-c-\bar{V})\hat{p}_{0zz} + \hat{p}_0 \bar{V}_{zz}\right] \tag{2.1.14}$$

$$\hat{\omega}_0(0,z) = \frac{1}{\sqrt{2}} \frac{\partial^2 \hat{p}_0}{\partial z^2}(0,z) \tag{2.1.15}$$

$$\hat{\omega}_0(0,z) = 0 \tag{2.1.16}$$

We will look for solutions in which $\hat{p}_0$ is of the form:

$$\hat{p}_0 = (z-c)\,M_0(z) + H_0(z) \tag{2.1.17}$$

Such a solution will match, for large z to an interior solution of the form $p = A_0(x)(z-c) + O(\epsilon^{1/4})$ provided:

$$A_0(-1/2) = 0 \tag{2.1.18}$$

$$\left.\begin{aligned} H_0 &\longrightarrow 0 \\ M_0 &\longrightarrow a + bz \end{aligned}\right\}\ ;\ z \longrightarrow \infty \qquad \begin{matrix} \text{(2.1.19a)} \\ \text{(2.1.19b)} \end{matrix}$$

with matching accomplished if $b = dA_0(-1/2)/dx$ and $A_1(-1/2) = a$.

If M_0 and H_0 can be determined so as to have the above behavior then equation 2.1.18 provides one of the boundary conditions

required for solution of zero-order interior problem.

Matching to the inner Stewartson layer in accomplished if 2.1.17 matches, as $\zeta \to 0$, to 1.37 (as ξ becomes large). This is accomplished if:

$$M_0(0) = H_0(0) = 0 \tag{2.1.20}$$

$$(z-c)\frac{dM_0}{dz}(0) + \frac{dH_0}{dz}(0) = \int_0^z \beta_0 dz' - \frac{1}{D}\int_0^D\int_0^z \beta_0 dz'dz \tag{2.1.21}$$

$$\tilde{c}_0 = \frac{E^{1/12}}{2}\left\{(z-c)\frac{d^2M_0}{dz^2}(0) + \frac{d^2H_0}{dz^2}(0)\right\} \tag{2.1.22}$$

$$a_0 = 0 \tag{2.1.23}$$

Condition 2.1.23 is due to the fact that the term $E^{1/3} i k a_0 \xi^3/6$ is formally too large to match to the ζ^3 term in the expansion, for small ζ, of 2.1.17.

Equation 2.1.22 shows that $\tilde{c}_0 = O(E^{1/12})$ and also, since H_0 and $\tilde{c}_0$ are independent of z, that

$$\frac{d^2M_0}{dz^2}(0) = 0 \tag{2.1.24}$$

Equation 2.1.21 shows that β_0 is constant and therefore:

$$\frac{dM_0}{dz}(0) = \beta_0 \tag{2.1.25}$$

$$\frac{dH_0}{dz}(0) = \beta_0\left(c - \frac{D}{2}\right) \tag{2.1.26}$$

Equations 2.1.20, 2.1.24, 2.1.25, and 2.1.26 are the additional boundary conditions required for determination of M_0 and H_0. The quantity β_0 must eventually be determined from matching to the interior, i.e., $a = a(\beta_0)$, $b = b(\beta_0)$ in 2.1.19.

Substituting 2.1.17 into 2.1.13 shows that

$$H_0(z) = \frac{i}{k\lambda}\left[\frac{d^2M_0}{dz^2} + ik\lambda\bar{V}M_0\right] \tag{2.1.27}$$

This expresses H_0 in terms of M_0 and therefore 2.1.20 and 2.1.26 become

$$M_0(0) = \frac{d^2M_0}{dz^2}(0) = 0 \tag{2.1.28}$$

$$\frac{d^3M_0}{dz^3}(0) = -ik\lambda C\beta_0 \tag{2.1.29}$$

where 2.1.29 follows from 2.1.27 and the fact that $\bar{V}(0) = D/2$.

Equation (2.1.14) can be integrated from $z = 0$ to $z = D$ and the result, on making use of 2.1.15 and 2.1.16, is: (primes denote differentiation)

$$\frac{1}{\sqrt{2}}\left[cM_0'' - H_0''\right] = -\left[D\left(\frac{D}{2}-c\right)M_0^{(IV)} + DH_0^{(IV)}\right]$$

$$+ i\frac{k\lambda}{\sigma}\left\{\left(\frac{D^3}{3} - cD^2 + c^2D\right)M_0'' + D\left(\frac{D}{2}-c\right)\left[H_0'' + \bar{V}''M_0 - \bar{V}M_0''\right]\right.$$

$$\left. + D\left[\bar{V}''H_0 - \bar{V}H_0''\right]\right\} \tag{2.1.30}$$

Substituting for $\bar{V}$ and H_0 leads, after some algebra, to the following sixth order equation for M_0 :

$$M_0^{(VI)} - \left\{1 - i k\Lambda \sqrt{2} D \left(\frac{\sigma+1}{\sigma}\right)\left[c - \frac{D}{2}(1-e^{-s})\right]\right\} M_0^{(IV)} - 2\sqrt{2} i k\Lambda D^2 e^{-s} M_0'''$$

$$- 2 i k\Lambda D^2 \left\{ \mathcal{F}(c) - \frac{1}{2\sqrt{2}} \left(s + \frac{1}{\sigma}\right) e^{-s} - i\frac{k\Lambda}{\sigma} D\left[c - \frac{D}{2}(1-e^{-s})\right] e^{-s} \right\} M_0''$$

$$- \sqrt{2}\, D^2 i k\Lambda \left[1 + \sqrt{2}\, i\frac{k\Lambda}{\sigma}\left[c - \frac{D}{2}(1-e^{-s})\right]\right] e^{-s} M_0' = 0$$

(2.1.31)

where

$$\mathcal{F}(c) = \frac{1}{D}\left[\frac{c}{\sqrt{2}} - i\frac{k\Lambda}{\sigma}\left(\frac{D^3}{3} - cD^2 + c^2 D\right)\right] \qquad (2.1.32)$$

and the independent variable has been changed to $s = \tau / 2^{1/4}\sqrt{D}$.

The complexity of 2.1.31 renders the problem of finding solutions in closed form difficult. One solution is clearly of the form $M_0 =$ constant. The remaining solutions can be found formally in series form by taking

$$\frac{dM_0}{ds} = e^{rs} \sum_{j=0}^{\infty} a_j e^{-js} \qquad (2.1.32)$$

where r is a root of the indicial equation

$$F(r) = r^5 - \left[1 - i k\Lambda \sqrt{2} D \left(\frac{\sigma+1}{\sigma}\right)\left(c - \frac{D}{2}\right)\right] r^3 - 2 i k\Lambda D^3 \mathcal{F}(c)\, r = 0 \qquad (2.1.33)$$

and the coefficients a_j are determined by the recurrence relations:

$$F(r-1)a_1 + G(r)a_0 = 0 \tag{2.1.34}$$

$$F(r-j)a_j + G(r-j+1)a_{j-1} + \chi(r-j+2)a_{j-2} = 0 \; ; \; j \geq 2 \tag{2.1.35}$$

where

$$\begin{aligned} G(r) = {} & \frac{ik\Lambda D^2}{\sqrt{2}}\left(\frac{\sigma+1}{\sigma}\right)r^3 - 2\sqrt{2}ik\Lambda D^2 r^2 \\ & + \left[ik\Lambda D^2 - 2k^2\Lambda^2 D^3\left(c-\frac{D}{2}\right)\right]r \\ & - \sqrt{2}D^2 ik\Lambda\left[1 + \sqrt{2}\frac{ik\Lambda}{\sigma}\left(c-\frac{D}{2}\right)\right] \end{aligned} \tag{2.1.36}$$

$$\chi(r) = -\frac{k^2\Lambda^2 D^4}{2\sigma}r + \frac{k^2\Lambda^2}{\sigma}D \tag{2.1.37}$$

One of the roots of 2.1.33 is $r = 0$. The remaining four are given by:

$$\begin{aligned} r = {} & \pm \text{P.V.}\left\{\frac{1}{2}\left[1 - ik\Lambda\sqrt{2}D\left(\frac{\sigma+1}{\sigma}\right)\left(c-\frac{D}{2}\right)\right]\right. \\ & \left. \pm \frac{1}{2}\text{P.V.}\left[\left[1 - ik\Lambda\sqrt{2}D\left(\frac{\sigma+1}{\sigma}\right)\left(c-\frac{D}{2}\right)\right]^2 + 8ik\Lambda D^3 f(c)\right]^{1/2}\right\}^{1/2} \end{aligned} \tag{2.1.38}$$

where P. V. denotes the principle value of the complex square roots.

In general only two of the roots 2.1.38 will have negative real parts. The other two must be rejected because the solutions corresponding to them are not of boundary layer type. Let r_2 and r_3 be those roots which have negative real parts. Then M_0 is of the general form:

$$M_0 = \alpha_0 + \alpha_1 \left[s + \sum_{j=1}^{\infty} b_{1j} e^{-js} \right]$$

$$+ \alpha_2 e^{\kappa_2 s} \left[1 + \sum_{j=1}^{\infty} b_{2j} e^{-js} \right]$$

$$+ \alpha_3 e^{\kappa_3 s} \left[1 + \sum_{j=1}^{\infty} b_{3j} e^{-js} \right] \qquad (2.1.39)$$

The outer expansion (for large s) of this is of the form

$$M_0 \sim \alpha_0 + \alpha_1 s \qquad (2.1.40)$$

while 2.1.27 shows that H_0 becomes exponentially small as s becomes large. Thus the formal solution (2.1.39) has the required behavior for matching to the interior. The constants α_0, α_1, α_2, and α_3 must be obtained by application of the boundary conditions 2.1.25, 2.1.28 and 2.1.29.

Although 2.1.39 is a formal solution of 2.1.31 it is of limited practical use by virtue of its series form. In fact, in order that the boundary conditions $\tau = s = 0$ can be satisfied it is necessary that the series be convergent there. The recurrence relation (2.1.35) implies that this is probable because, for large values of j,

$$\frac{G(\kappa - j + 1)}{F(\kappa - j)} = O(j^{-2})$$

$$\frac{X(\kappa - j + 2)}{F(\kappa - j)} = O(j^{-4})$$

so that successive coefficients have decreasing absolute values if j is sufficiently large.

Fortunately it is sufficient for our purpose to simply establish 2.1.19 and therefore the validity of 2.1.18 and we have done this. An analysis which is entirely similar to the above near $x = 1/2$ shows that a boundary condition of the form 2.1.18 applies there also.

2.2 $\lambda = \gamma \epsilon^{1/4}$; $\gamma = O(1)$.

When λ is small reference to the analysis in Chapter 6 shows that $\mathcal{F}(c) = O(\lambda)$ and therefore one of the roots r_2, r_3 becomes $O(1)$ while the other becomes $O(\lambda)$. When $\lambda = O(\epsilon^{1/4})$ the solution corresponding to this smaller root merges with the interior and the boundary layer analysis is then considerably simplified.

In this case 2.1.13 and 2.1.14 simplify to the following:

$$\hat{p}_{0zzz} = 0 \tag{2.2.1}$$

$$\hat{w}_{0z} = -\frac{\partial^4 \hat{p}_0}{\partial z^4} \tag{2.2.2}$$

Thus we look for simple solutions of the form

$$\hat{T}_0 = \beta_0(z)z \tag{2.2.3}$$

$$\hat{p}_0 = H_0(z) + z\int_0^z \beta_0 \, dz' \tag{2.2.4}$$

It is evident that these will match to 1.37 provided

$$H_0(0) = 0 \tag{2.2.5}$$

$$\frac{dH_0}{d\zeta}(0) = -\frac{1}{D}\int_0^D\int_0^\zeta \beta_0\, d\zeta' d\zeta \tag{2.2.6}$$

while, as before, a_0 and $\tilde{c}_0$ are given by:

$$a_0 = 0$$
$$\tilde{c}_0 = \frac{E^{1/12}}{2}\frac{d^2H_0}{d\zeta^2}(0)$$

Equations 2.2.2 , 2.2.4 and the boundary conditions 2.1.15 and 2.1.16 may be combined to show that

$$\frac{d^4H_0}{d\zeta^4} - \frac{1}{\sqrt{2}D}\frac{d^2H_0}{d\zeta^2} = 0 \tag{2.2.7}$$

The solution of this which satisfies 2.2.5 and 2.2.6 and has the appropriate boundary layer behavior for large ζ is as follows:

$$H_0 = \delta_0\zeta - 2^{1/4}\sqrt{D}\left[\delta_0 + \frac{1}{D}\int_0^D\int_0^\zeta \beta_0\, d\zeta' d\zeta\right]\left[1 - e^{-\zeta/2^{1/4}\sqrt{D}}\right] \tag{2.2.8}$$

and , therefore, for large ζ ,

$$\hat{\rho}_0 \sim \zeta\left[\delta_0 + \int_0^\zeta \beta_0\, d\zeta'\right] - 2^{1/4}\sqrt{D}\left[\delta_0 + \frac{1}{D}\int_0^D\int_0^\zeta \beta_0\, d\zeta' d\zeta\right] \tag{2.2.9}$$

This must match to the interior pressure field near $X = -1/2$. This was shown to be of the form

$$p \sim A(x)\,(z - E^{1/4}\hat{c}) + \frac{iE^{1/4}}{kY}\,\mathcal{L}A(x)$$

where $\mathcal{L}A = d^2A/dx^2 - k^2A$. Thus, matching is accomplished if $A \sim A_0(x) + E^{1/4}\,A_1(x)$, and:

$$A_0(-1/2) = A_1(-1/2) = 0 \qquad (2.2.10)$$

$$\beta_0 = \frac{dA_0}{dx}(-1/2) \qquad (2.2.11)$$

$$\delta_0 = 0 \qquad (2.2.12)$$

$$\frac{i}{kY}\frac{d^2A_0}{dx^2}(-1/2) = \frac{2^{1/4}}{\sqrt{D}}\int_0^0\int_0^z \beta_0\,dz'\,dz = -\frac{D^{3/2}}{2^{3/4}}\frac{dA_0}{dx}(-1/2) \qquad (2.2.13)$$

Equations 2.2.9 and 2.2.12 are the boundary conditions which were used to determine the interior temperature field in Chapter VI. This analysis has established the validity of those conditions. The same kind of analysis for the boundary layers near $X = 1/2$ established the hot wall conditions:

$$A_0(1/2) = 0 \qquad (2.2.14)$$

$$\frac{d^2A_0}{dx^2}(1/2) = -\frac{ikYD^{3/2}}{2^{3/4}}\frac{dA_0}{dx}(1/2) \qquad (2.2.15)$$

where the change in sign in (2. 2. 14) is due to the fact that the inward normal to the wall has the opposite sign to that at $X = -1/2$.

3. MODIFICATIONS FOR HIGH WAVE NUMBERS

When k is large some modification of the above boundary layer analyses is required. We shall restrict our attention to the situation which is discussed in the analyses for the fluid interior as carried out in Chapters VI and VII. Thus we take $\lambda = \gamma E^{1/4}$ with $\gamma = O(1)$. Also, we must scale p , T , v , and w by k^{-1} to make the analyses consistent with that for the fluid interior. We shall consider each of the Stewartson layers in turn.

3.1 THE INNER STEWARTSON LAYER

Here we take the scaling (1. 5) and modify it as follows:

$$\hat{p}, \hat{T}, v, w = k^{-1}(\tilde{p}, \tilde{T}, \tilde{v}, \tilde{w}) \qquad (3.1.1)$$

We shall assume that $k \leq O(E^{-1/4})$. In this case the zero order governing equations are essentially unchanged, the only modification for large k being in equations 1. 14 and 1. 17 which now take the form:

$$\hat{u}_0 = -i\tilde{p}_0 + O(k^{-1}) + O(E^{5/12}) \qquad (3.1.2)$$

$$\hat{u}_{0\xi} + i\tilde{v}_0 = 0 + O(k^{-1}) \qquad (3.1.3)$$

However, 1. 13, 1. 14 and 1. 17 can be combined to show that

$$\tilde{w}_{0z} = -\tilde{v}_{0\xi\xi\xi} \qquad (3.14)$$

The remaining of equations 1.13 to 1.19 are unchanged and the analysis in entirely similar to that carried out in Section 1 above. The boundary condition 1.32 becomes modified to

$$\left(\frac{\partial^2 \tilde{\omega}_0}{\partial \xi^2}\right)_{\xi=0} = 0 \tag{3.15}$$

The solution $\tilde{\omega}_0$ which satisfies all the boundary conditions is obtainable from 1.34 and 1.35 by taking the limit of large k . The final expression for $\tilde{p}_0$ is analogous to 1.37 , i.e.

$$p \sim k^{-1} E^{1/3} \left\{ \xi \left[\int_0^z \beta_0 \, dz' - \frac{1}{D} \int_0^D \int_0^z \beta_0 \, dz' dz \right] + EXP \right\} \tag{3.1.6}$$

where EXP denotes terms which are exponentially small for large ξ. Thus, the conditions for matching to the outer Stewartson layer are exactly as before.

3.2 THE OUTER STEWARTSON LAYER

The modified scaling of dependent variables for the outer layer is the similar to that for the inner layer, i.e.

$$(v, \hat{p}, \hat{T}, \hat{\omega}) = k^{-1} (\tilde{v}, \tilde{p}, \tilde{T}, \tilde{\omega}) \tag{3.2.1}$$

With this modification the lowest order governing equations become:

$$\tilde{v} = \tilde{p}_z + o(k E^{3/4}) \tag{3.2.2}$$

$$\hat{u} = -i \tilde{p} + o(E^{1/4} k^{-1}) \tag{3.2.3}$$

$$\tilde{\omega}_{zz} = -L^2\tilde{p} + i\frac{\gamma}{\sigma} kE^{1/4}\left[(z-c-\bar{V})L\tilde{p} + \tilde{p}\,\bar{V}_{zz}\right] \qquad (3.2.4)$$

$$\tilde{p}_z = \tilde{T} + O(E^{1/2}) \qquad (3.2.5)$$

$$L\tilde{p}_z = ik\gamma E^{1/4}\left[(z-c-\bar{V})\tilde{p}_z - \tilde{p}\right] \qquad (3.2.6)$$

$$\tilde{w}(0,t) = 0 \qquad (3.2.7)$$

$$\tilde{w}(0,z) = \frac{1}{\sqrt{2}} L\,\tilde{p}(0,z) \qquad (3.2.8)$$

where $L = \partial^2/\partial z^2 - k^2E^{1/2}$.

If $k = O(E^{-1/4})$ all terms involving the product $kE^{1/4}$ alone are $O(1)$ and solutions to 3.2.2. through 3.2.8 must be obtained in a manner similar to that used in Section 2.1 above. We shall not go into the details of this solution except to say that the indicial equation for the series solutions becomes:

$$(r^2 - k_*^2)\left\{r^4 - \left[2k_*^2 + \frac{1}{\sqrt{2}D}\left[1 - \sqrt{2}\,ik_*\gamma\left(\frac{\sigma+1}{\sigma}\right)D\left(c-\frac{D}{2}\right)\right]\right]r^2 - \frac{k_*^2\gamma^2}{\sigma}\mathcal{H}(c)\right\} = 0 \qquad (3.2.9)$$

where $k_* = kE^{+1/4}$ and

$$\mathcal{H}(c) = c^2 - \left[D - \frac{ik_*}{\gamma}(\sigma+1) - \frac{i\sigma}{\sqrt{2}D\gamma k_*}\right]c$$

$$- \left[\frac{\sigma\gamma^2}{\sqrt{2}D}\left(1 - \frac{\sqrt{2}\gamma^2D^3}{3\sigma}\right) + \frac{iD}{2}\frac{k_*}{\gamma}(\sigma+1) + \sigma\frac{k_*^2}{\gamma^2}\right] \qquad (3.2.10)$$

However, when $k_* = O(1)$ the high wave number analysis in Chapter VII showed that $\mathcal{H}(c) = 0$ in the lowest approximation. Thus 3.2.9 has the double root $r = 0$ in addition to

$$r = \pm k_*, \quad r = \pm \text{P.V.} \left\{ 2k_*^2 + \frac{1}{\sqrt{2}D} \left[1 - \sqrt{2}\, i k_* \gamma \left(\frac{\sigma+1}{\sigma} \right) D\left(c - \frac{D}{2}\right) \right] \right\}^{1/2}$$

Thus, near the outer edge of the boundary layer the pressure field will be of the form $\left(z - c - \frac{i k_*}{\gamma}\right) M_0(z)$ with

$$M_0 \sim a + bz + \alpha_1 e^{-k_* z} + \alpha_2 e^{-r_1 z} \qquad (3.2.11)$$

This will match to the interior solutions for the pressure field.

The case $1 < k < E^{-1/4}$ is relevant to the intermediate wave number analysis of Chapter VII and is therfore of more practical interest. Equations 3.2.2 through 3.2.8 show that, in this case, the lowest approximations have the same form as in Section 2.2 above and therefore the conditions for matching to the interior solutions are unchanged. However the error in the lowest order boundary layer analysis is now formally $O(kE^{1/4}) > O(E^{1/4})$.

BIBLIOGRAPHY

Barcilon, V., 1964 : Role of Ekman layers in the stability of the symmetric regime obtained in a rotating annulus, J. Atmos. Sci., 21, 291-299.

_____ and J. Pedlosky, 1967 : On steady motions produced by a stable stratification in a rapidly rotating fluid, J. Fluid Mech., 29, 673-690.

Batchelor, G. K., 1967 : An introduction to fluid mechnics, Cambridge University Press, 615 p.

Brindley, J., 1960 : Stability of flow in a rotating viscous incompressible fluid subjected to differential heating, Phil. Trans. Roy. Soc., London, A 253, 1-25.

Charney, J. G. and A. Eliassen, 1949 : A numerical method for predicting perturbations of the middle latitude westerlies, Tellus, 1, 38-54.

Davies, T. V., 1956 : The forced motion due to heating of a rotating liquid in an annulus, J. Fluid Mech., 5, 593-631.

_____, 1959 : On the forced motion due to heating of a rotating liquid in an annulus, J. Fluid Mech., 5, 593-621.

Eady, E. T., 1949 : Long waves and cyclone waves, Tellus, 13, 33-52.

Fjortoft, R., 1951 : Stability properties of large scale atmospheric disturbances, Compedium of Meteorology, Amer. Meteor. Soc., Boston, 454-463.

Fowlis, W. W. and R. Hide, 1965 : Thermal convection in a rotating fluid annulus : effect of viscosity on the transition between axisymmetric and non axisymmetric flow regimes, J. Atmos. Sci., 22, 541-558.

Fultz, D., 1951 : Experimental analysis to atmospheric motions, Compendium of Meteorology, Amer. Meteor. Soc., Boston, 1235-1248.

_____, 1966 : Spectrum of thermal convection in a rotating annulus, A Report to the International Union of Theoretical and Applied Mechanics, Symposium on Rotating Fluid Systems, La Jolla.

Greenspan, H. P., 1968 : The theory of rotating fluids, Cambridge University Press, 327 p.

Hide, R., 1953 : Some experiments on thermal convection in a rotating liquid, Quart. J. Roy. Meteor. Soc., 79, 161.

BIBLIOGRAPHY (continued)

Hide, R., 1964 : The viscous boundary layer at the free surface of a rotating baroclinic fluid, Tellus, 16, 523-529.

_____, 1965 : The viscous boundary layer at the free surface of a rotating baroclinic fluid : effects due to temperature dependence of surface tension, Ibid, 17, 440-442.

_____, 1970 : Some laboratory experiments on free thermal convection in a rotating fluid subject to a horizontal temperature gradient and their relation to the theory of the global atmospheric circulations, The Global Circulation of the Atmosphere (ed. G. A. Corby), Roy. Meteor. Soc.

Holopainen, E. O., 1961 : On the effects of friction in baroclinic waves, Tellus, 13, 363-367.

Hunter, C., 1967 : The axisymmetric flow in a rotating annulus due to a horizontally applied temperature gradient, J. Fluid Mech. 27, 753-778.

Jacobs, S. J., 1964 : The Taylor column problem, J. Fluid Mech., 20, 581-591.

Kaiser, J. A. C., 1969 : Rotating deep annulus convection I , Thermal properties of the upper symmetric regime, Tellus, 21, 789-805.

_____, 1970 : Rotating deep annulus convection, Part 2, Wave instabilities, vertical stratification and associated theories, Tellus, 22, 275-287.

_____, 1971 : Heat transfer by symmetrical rotating annulus convection, J. Atmos. Sci. , 28, 929-932.

_____, 1972 : Rotating deep annulus convection : the steady high amplitude wave regime-internal thermal fields, Geophysical Fluid Dynamics, 4, 159-186.

Kuo, H. L., 1956 : Energy-releasing processes and stability of thermally driven motions in a rotating fluid, J. Meteor. 13, 82-101.

_____, 1957 : Further studies of thermally driven motions in a rotating fluid, J. Meteor. 14 , 553-558.

Lin, C. C. , 1955 : The theory of hydrodynamic stability , Cambridge University Press, 155 p.

BIBLIOGRAPHY (continued)

Lorenz, E. N., 1953 : A proposed explanation for the existence of two regimes of flow in a symmetrically heated cylindrical vessel, Fluid Models in Geophysics, Proc. 1st Symposium on the Use of Models in Geophysical Fluid Dynamics, Baltimore, Md. 73-80.

_____, 1960 : Energy and numerical weather prediction, Tellus, 12, 364-373.

_____, 1962 : Simplified dynamic equations applied to rotating basic experiments, J. Atmos. Sci., 19, 39-51.

McIntyre, M., 1968 : The axisymmetric convective regime for a rigidly bounded rotating annulus, J. Fluid Mech., 32, 625-655.

Merilees, P., 1968 : On the transition from axisymmetric to non - symmetric flow in a rotating annulus, J. Atmos. Sci., 25 , 1003-1014.

O'Neil, E., 1969 : The stability of flows in a differentially heated rotating fluid system with a rigid bottom and a free top, Studies in Applied Mathematics, 48, 227-256.

Robinson, A. R. , 1959 : The symmetric state of a rotating fluid differentially heated in the horizontal, J. Fluid Mech., 6, 599-620.

Warn, T., 1973 : On the stability of quasi-geostrophic waves in a rotating annulus, Ph. D. Thesis, McGill University, 93 p.

Wiin-Nielsen, A., 1967 : On baroclinic instability as a function of the vertical profile of the zonal wind, Mon. Wea. Rev., 95, 733-739.

Williams, G., 1967 : Thermal convection in a rotating fluid annulus, Parts I and II, J. Atmos. Sci., 24, 144-174.